DEPT LANGLEY

DEPARTMENT REPORT UWME-DR-401-103-1

VERIFICATION AND APPLICATION OF THE IOSIPESCU SHEAR TEST METHOD

David E. Walrath
Donald F. Adams

June 1984

TECHNICAL REPORT
NASA-Langley Research Center
Hampton, Virginia 23665
Grant No. NAG-1-272

Approved for Public Release: Distribution Unlimited

COMPOSITE MATERIALS RESEARCH GROUP
DEPARTMENT of MECHANICAL ENGINEERING
University of Wyoming Laramie, Wyoming 82071

DEPARTMENT REPORT
UWME-DR-401-103-1

VERIFICATION AND APPLICATION OF THE IOSIPESCU SHEAR TEST METHOD

DAVID E. WALRATH
DONALD F. ADAMS

JUNE 1984

TECHNICAL REPORT
NASA-LANGLEY RESEARCH CENTER
HAMPTON, VIRGINIA 23665
GRANT NO. NAG-1-272

COMPOSITE MATERIALS RESEARCH GROUP
MECHANICAL ENGINEERING DEPARTMENT
UNIVERSITY OF WYOMING
LARAMIE, WYOMING 82071

1 Report No.	2. Government Accession No.	3. Recipient's Catalog No.

4 Title and Subtitle	5 Report Date
Verification and Application of the Iosipescu Shear Test Method	June 1984
	6 Performing Organization Code
7 Author(s)	8 Performing Organization Report No
David E. Walrath and Donald F. Adams	UWME-DR-401-103-1
	10 Work Unit No
9 Performing Organization Name and Address	11 Contract or Grant No
Department of Mechanical Engineering University of Wyoming Laramie, Wyoming 82071	NAG-1-272
	13 Type of Report and Period Covered
12 Sponsoring Agency Name and Address	Technical Report 6/83-5/84
NASA-Langley Research Center Hampton, VA 23665	14. Sponsoring Agency Code

15 Supplementary Notes

16 Abstract

Finite element models were used to study the effects of notch angle variations on the stress state within an Iosipescu shear test specimen. These analytical results were also studied to determine the feasibility of using strain gage rosettes and a modified extensometer to measure shear strains in this test specimen. Analytical results indicated that notch angle variations produced only small differences in simulated shear properties. Both strain gage rosettes and the modified extensometer were shown to be feasible shear strain tranducers for the test method. Correlations of the analytical results with experimental results from shear tests of isotropic (aluminum) as well as orthotropic ($[0]_{8T}$ AS4/3501-6) materials were also performed.

The Iosipescu shear test fixture was redesigned to incorporate several improvements. These improvements include accommodation of a 50 percent larger specimen for easier measurement of shear strain, a clamping mechanism to relax strict tolerances on specimen width, and a self contained alignment tool for use during specimen installation. The inner loading surfaces were also moved further from the test region. Drawings of this new fixture are included in the report.

A set of in-plane and interlaminar shear properties were measured for three graphite fabric/epoxy composites of T300/934 composite material. The three weave patterns were Oxford, 5-harness satin, and 8-harness satin. These tests were performed for room temperature/dry conditions.

17. Key Words (Suggested by Author(s))	18. Distribution Statement
Composites, shear test methods, Iosipescu shear	Unclassified, Unlimited

19. Security Classif. (of this report)	20. Security Classif. (of this page)	21. No. of Pages	22. Price*
Unclassified	Unclassified	112	

* For sale by the National Technical Information Service, Springfield, Virginia 22161

NASA-C-168 (Rev. 10-75)

PREFACE

This technical report summarizes results of a combined analytical and experimental study performed for the National Aeronautics and Space Administration-Langley Research Center under Grant Number NAG-1-272, University of Wyoming Project Number 43-8315. Mr. Jerry W. Deaton served as the NASA Technical Monitor.

Work conducted as part of this research program was performed by members of the Composite Materials Research Group (CMRG) within the Mechanical Engineering Department at the University of Wyoming. The CMRG is led by Dr. Donald F. Adams, Professor of Mechanical Engineering. Mr. David E. Walrath, CMRG Staff Engineer, served as Principal Investigator for this program. Also participating in this program were Messers. Edwin M. Odom and Richard S. Zimmerman, CMRG Staff Engineers; Mr. Russ Porter and Mr. John Miller, Mechanical Engineering Machine Shop; and Messrs. Dennis McCarthy, Greg Morrison, Robert Wakelee, and Jeff Kessler, undergraduate students in Mechanical Engineering.

TABLE OF CONTENTS

SECTION 1

INTRODUCTION

Various shear test methods employing some version of a double edge-notched test specimen have been in use for many years. These test techniques include methods first suggested by Arcan [1-3], Iosipescu [4], and Slepetz et. al. [5]. All three of these test methods employ the same basic principle. Pure shear loading is applied to a test specimen via force couples producing bending moments, as shown in Figure 1a for the Iosipescu shear test method. This type of loading produces pure shear loading in the gage section of the test specimen, the bending moment being zero in this region as shown in Figures 1b and 1c. The notches machined in the edges of the test specimen produce a uniform shear stress distribution as opposed to the parabolic shear stress distribution which would be produced in a specimen without edge notches.

The present authors have been studying and using the Iosipescu shear test method for a number of years, particularly for measuring shear properties of composite materials [6-11]. A summary of that work prior to initiation of the present research program is contained in Reference [6].

For the past two years, the Composite Materials Research Group (CMRG) at the University of Wyoming has been studying the Iosipescu shear test method under grant funding provided by the NASA-Langley Research Center. During the first year of this grant, the Iosipescu shear test specimen was modeled using finite element techniques [7].

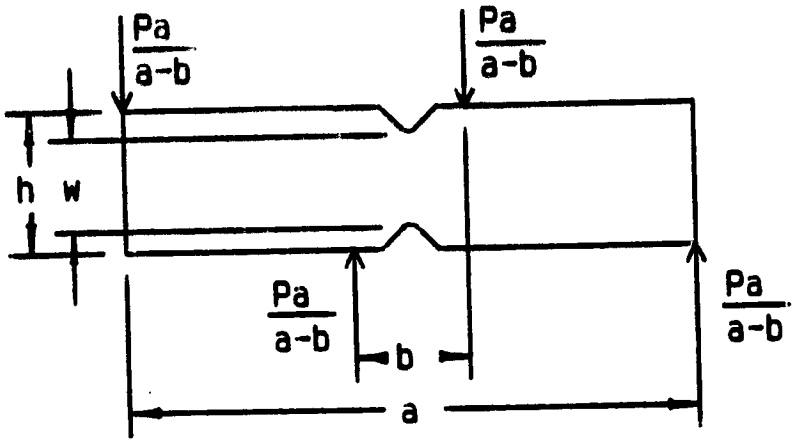

a. Force Diagram

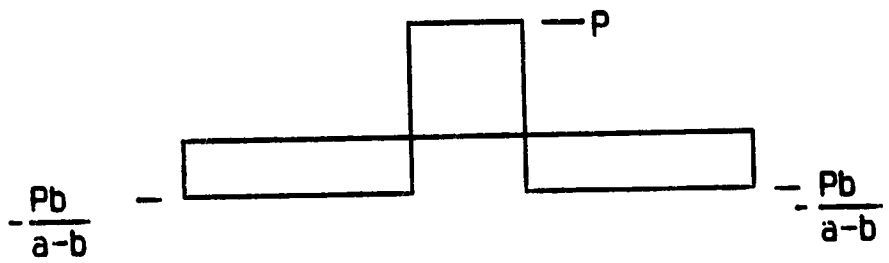

b. Shear Diagram

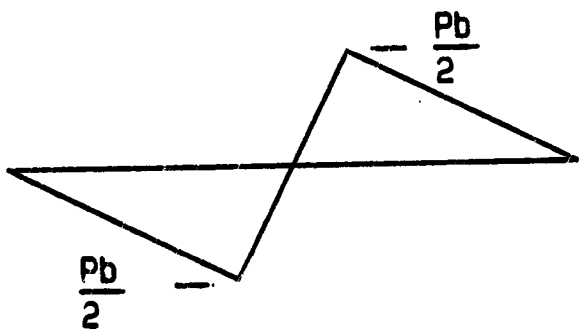

c. Moment Diagram

Figure 1. Force, Shear, and Moment Diagrams for the Iosipescu Shear Test Method.

Various specimen geometry parameters were studied for their influence on test results. These geometric parameters included notch depth, notch root radius, notch angle, and loading point placement. It was found that notch root radius plays an important role in determining the shear stress distribution between the notches. A sharp notch root radius results in shear stress concentrations in orthotropic Iosipescu shear test specimens. It was also found that the inner loading points of the Iosipescu shear fixture used at that time were too near the center of the test specimen. Compressive stresses induced by the loading fixture extended into the test region of the specimen.

The purpose of the second-year study presented in this report was four-fold. First, the test fixture was to be redesigned and rebuilt to correct various deficiencies detected during prior studies, particularly those involving loading point placement. Since a new fixture was to be built, other features contributing to convenience of use were also incorporated. Second, the analytical modeling of the test specimen was to continue in an effort to further understand the influence of test specimen geometry on test results. Third, various shear strain measurement techniques were to be studied, including strain gages and the modified extensometer discussed in Reference [6]. Finally, a series of tests were to be performed on woven fabric graphite/epoxy composite materials to measure both in-plane and through-the-thickness (interlaminar) shear strengths and shear moduli.

Finite element models were constructed to analyze 90-degree and 110-degree included angle notch geometry Iosipescu test specimens. Properties for an isotropic (aluminum) as well as an orthotropic (AS4/3501-6 graphite/epoxy) material were used.

Analytically, notch angle was shown to have some effect on the simulated measurement of shear modulus. However, experimental shear property measurements on aluminum specimens showed that the difference in measured properties was small.

A new Iosipescu shear test fixture was designed and built to incorporate two major changes in the test method. First, the inner loading points (surfaces) were moved further from the specimen center, increasing that distance from 2.5 mm (0.10 in) to 6.3 mm (0.25 in). This was done to minimize the intrusion of loading point-induced transverse normal compressive stresses into the test region. The second major change was to incorporate adjustable clamping mechanisms into the fixture halves. These were designed to minimize rotation of the specimen during testing due to a loose fit between the test specimen and the fixture. Other changes included increasing the specimen size to provide greater area for shear strain instrumentation, and building an alignment tool into the fixture for centering specimens during specimen installation.

Experiments on the unidirectional $[0]_{8T}$ AS4/3501-6 graphite/epoxy composite indicated axial cracks developing at the notch roots. Simple finite element models including these cracks were analyzed to study the effect of the cracks on the internal stress state. The cracks were shown to not significantly alter the stress state in the test region of the specimen. In fact, by relieving some of the shear stress concentration at the notch root, the shear stress distribution was improved.

A major portion of the analytical effort was devoted to predicting the possible measurement errors when measuring shear strains with strain gage rosettes or a modified extensometer. Both strain rosettes and the

modified extensometer were shown to be feasible strain measurement techniques. Shear modulus determinations using strain rosettes on aluminum specimens agreed very well with handbook values of shear modulus. Similar measurements on undirectional composite specimens also provided consistent data, which agreed with available shear properties data in the literature. The modified extensometer was shown to be a very feasible method for measuring shear strains, but the exact method of attachment of the extensometer to the specimen must still be designed. This work is continuing.

Finally, in-plane and interlaminar shear tests using the redesigned Iosipescu shear test fixture were performed on three T300/934 graphite fabric/epoxy composite materials. Consistent in-plane shear strength and shear modulus values were measured, with only slight differences between the three materials. Interlaminar shear strength and shear moduli data were somewhat more scattered but still provided useful comparisons of the three woven composite materials.

Analytical and experimental studies of the Iosipescu shear test method itself are presented in Section 2 of this report. Section 3 contains the shear test results for the three T300/934 graphite fabric/epoxy composites. Conclusions of this research program are summarized in Section 4. Test fixture plans, test procedures, and individual test specimen results are included in the Appendices.

SECTION 2

TEST SPECIMEN AND FIXTURE DESIGN

2.1 Background

A major thrust of the present study was to complete the analytical investigation initiated during the previous year, in order to better understand the influence of test specimen design and specimen-fixture interaction on Iosipescu shear test measurements. Results to be presented in this section reflect analytical and experimental efforts to understand the influence of notch geometry and loading point placement on the measured shear properties. Two potential methods of shear strain measurement were also examined.

An effort was made to interpret the finite element analytical results in terms of what could be measured in the laboratory. Five basic questions were posed:

1) Is the shear stress state in the test region of the specimen uniform pure shear, and does it reflect the applied shear stress as determined by the testing machine?
2) What is the effect of inelastic material behavior on test results?
3) What are the load distributions at the inner loading points, and do the induced normal stresses intrude into the test region?
4) What is the strain distribution in the test region and can this strain be accurately measured with strain gages or a modified

extensometer?

5) What are the differences in overall test response between 90-degree and 110-degree included angle edge-notched specimens?

These questions will be addressed in this section.

2.2 Description of the Analysis

The finite element analysis used during this research effort was a 3-D, orthotropic, inelastic analysis developed by the CMRG at the University of Wyoming. This analysis and associated computer program allows for temperature- and/or moisture-dependent orthotropic material behavior. As this analysis has been described elsewhere [12-15], a detailed description will not be repeated here. Briefly however, elastoplastic material behavior is modeled by use of the tangent modulus method and incremental loading. The onset of plastic deformation is determined by a yield surface in three-dimensional space. The analysis is based on a displacement formulation and employs linear isoparametric finite elements.

2.3 Material Properties

Because the stress-strain response of many composites when subjected to shear loading is nonlinear (irregardless of the test method) it was important to include nonlinear shear behavior in this analytical effort. As part of another research program performed for the Naval Air Systems Command [15], the unidirectional material properties of Hercules AS4/3501-6 graphite/epoxy had been modeled using numerical micromechanics techniques. As part of the Navy study a complete set of three-dimensional material properties, including stiffnesses, yield strengths, and thermal and moisture expansion coefficients as functions of temperature, was developed. The elastic coefficients associated with

this data base are listed in Table 1 for three temperatures and two moisture conditions. A subset of these data, i.e., the room temperature stiffness and yield behavior for this composite material, was used in the present study. Input shear stress-shear strain material behavior for the orthotropic analyses to be presented in this report is plotted in Figure 2. Although the data plotted in Figure 2 were generated using a micromechanics analysis (predicted knowing only the properties of the constituents, i.e., the fiber and the matrix), this stress-strain behavior is consistent with actual composite material measurements. A typical set of shear test data generated by the CMRG, for a unidirectional AS4/3501-6 graphite/epoxy composite, is shown in Figure 3. As can be seen by comparing Figures 2 and 3, the input material properties which were used in the present analytical effort are consistent with actual measured values. The apparent failure strains indicated in Figure 3, at approximately 7.5 percent were due to failure of the strain gage rosettes, not actual failure in the material.

Limited calculations in the linear elastic range of material response were also conducted for an unreinforced aluminum specimen using known properties of an aluminum alloy taken from Reference[20]. These properties are listed in Table 2.

TABLE 1
PREDICTED ELASTIC CONSTANTS FOR AN AS4/3501-6
GRAPHITE/EPOXY UNIDIRECTIONAL COMPOSITE LAMINA

Loading Case	Material Property		21°C, Dry	82°C, Dry	160°C, Dry	21°C, 1% M
Longitudinal Tension	E_{11}	GPa (Msi)	142 (20.6)	141 (20.5)	140 (20.4)	141 (20.5)
	$\nu_{12} = \nu_{13}$		0.25	0.26	0.25	0.25
Transverse Tension	$E_{22} = E_{33}$	GPa (Msi)	9.10 (1.32)	7.79 (1.13)	4.96 (0.72)	8.55 (1.24)
Longitudinal Shear	$G_{12} = G_{13}$	GPa (Msi)	5.17 (0.75)	3.65 (0.53)	1.93 (0.28)	5.03 (0.73)
Transverse Shear	G_{23}	GPa (Msi)	3.38 (0.49)	2.90 (0.42)	1.86 (0.27)	3.10 (0.45)
	$\nu_{23} = \frac{E_{22}}{2G_{23}} - 1$		0.35	0.35	0.33	0.38

Thermal Expansion (dry condition) $(°C)^{-1}$

$$\alpha_{11} = 2.146 \times 10^{-9}T - 2.658 \times 10^{-7}$$

$$\alpha_{22} = \alpha_{33} = 4.634 \times 10^{-8}T + 3.112 \times 10^{-5}$$

Moisture Expansion (room temperature) $(\%M)^{-1}$

$$\beta_{11} = 1.432 \times 10^{-4}$$

$$\beta_{22} = \beta_{33} = 5.120 \times 10^{-3}$$

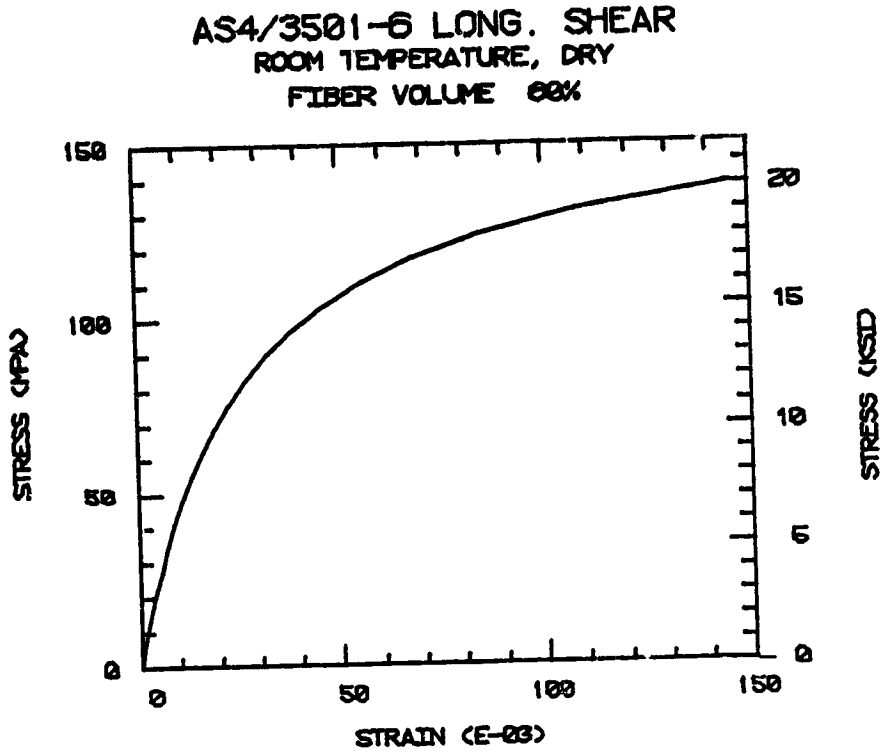

Figure 2. Micromechanics Generated In-plane Shear Stress-Strain Plot Used as Input Material Data for the Iosipescu Finite Element Analysis.

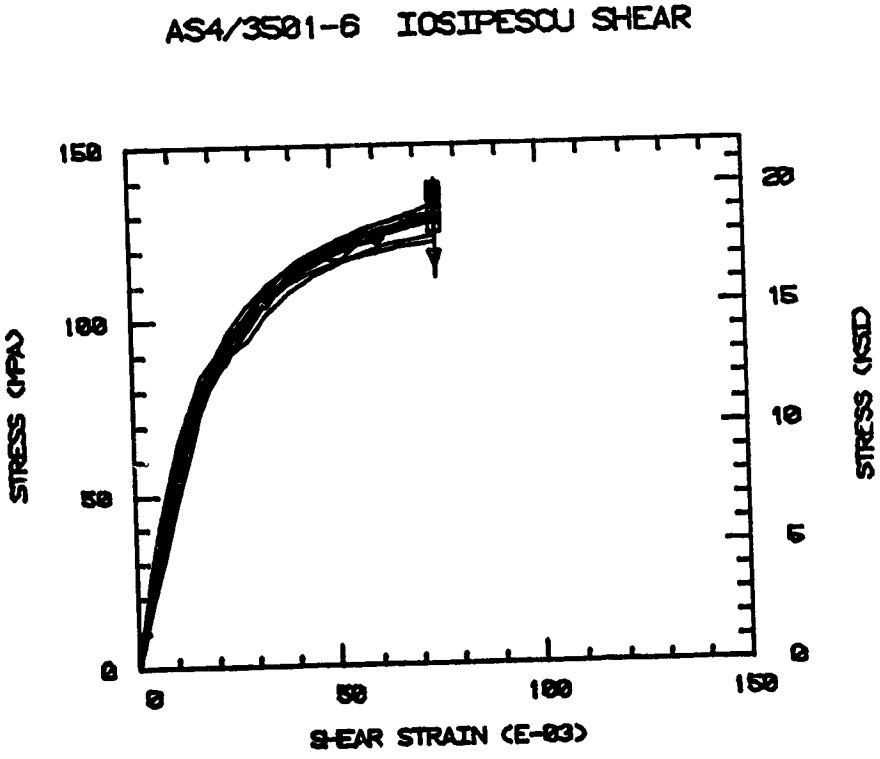

Figure 3. Measured In-plane Iosipescu Shear Stress-Strain Response of $[0]_{8T}$ AS4/3501-6 Graphite/Epoxy.

TABLE 2
MECHANICAL PROPERTIES OF 6061-T651 ALUMINUM ALLOY [20]

Tensile Modulus	
E	68.9 GPa (10.0 Msi)
Poisson's Ratio	
ν	0.33
Shear Modulus*	
$G = \frac{E}{2(1 + \nu)}$	25.9 GPa (3.76 Msi)
Shear Strength	
τ^u	207 MPa (30 ksi)

*Shear modulus was not explicitly listed in Reference [20]. Therefore it was calculated from the given tensile elastic constants E and ν using the well known isotropic relation $G = E/2(1 + \nu)$.

2.4 Finite Element Models

As discussed in the first-year report [7], three geometric variations of the Iosipescu shear specimen were analyzed. These variations included notch depth, notch root radius, and notch angle. Results of this first modeling attempt indicated that a rounded notch root radius produced a more uniform shear stress distribution within an isotropic or an orthotropic material test specimen. A sharp root radius tended to cause a shear stress concentration effect.

Shear behavior in the Iosipescu shear test specimen was found to be relatively insensitive to notch depth. Iosipescu had found, using photoelastic techniques, that notch depths between 20 and 25 percent of the specimen width produced an optimum stress state in isotropic materials [4]. Finite element analyses performed during the previous year [7] tended to verify that conclusion for both isotropic and orthotropic materials.

Variations of notch angle were also analyzed using finite element techniques during the first year [7], for both isotropic and orthotropic materials. As expected, the optimum notch angle for isotropic material specimens was found to be 90-degrees. This result agreed with the analytical and photoelastic results for isotropic materials presented in Reference [4]. However, for orthotropic materials, notch angles greater than 90-degrees appeared to produce a more uniform shear stress state. Finite element meshes used during this previous investigation were too coarse to conclusively demonstrate this notch angle effect.

Investigation of the effect of different notch angles on the stress state within an Iosipescu shear test specimen has been included in this present study. Geometric variations were limited to two different notch

angles. The notch depth was maintained at 20 percent of the specimen width, and the notch root radius was modeled as 1.3 mm (0.050 in). Late in the study, the effect of cracks at the notch root were also examined.

The loading method used in the Iosipescu shear test is asymmetric, as was shown in Figure 1. As such, it was necessary to model the entire test specimen, not a quarter or half of the specimen as can sometimes be done based on symmetry arguments. Plots of the finite element meshes used, including boundary conditions, for the two notch angles modeled in this study are shown in Figures 4 and 5. As can be seen, the meshes near the notch root are very refined in order to produce as accurate a picture of the local stress state as possible. Subregions at the centers of the two models were identified separately, to facilitate a subsequent study of potential strain measurement techniques, including either strain gage rosettes or a modified extensometer. Each finite element mesh contains 1716 nodes forming 778 isoparametric 8-node elements. Although a 3-D finite element analysis was used, these models are actually 2-D in that only one plane of elements was used for each model.

Other investigators have previously analyzed the Iosipescu shear test specimen, typically assuming the model to be symmetric about the midlength and/or midwidth lines [16-18]. The imposed boundary conditions on these specimens included shear loading at the end, as well as the symmetry condition at the center. These were proper assumptions for those particular test fixtures, but are not proper assumptions for the test fixture being studied in the present research effort. Also, the stress state at the loading points was of interest; therefore it was necessary to model the actual loading used. Analytical investigations of other test methods which are very similar to this Iosipescu shear test

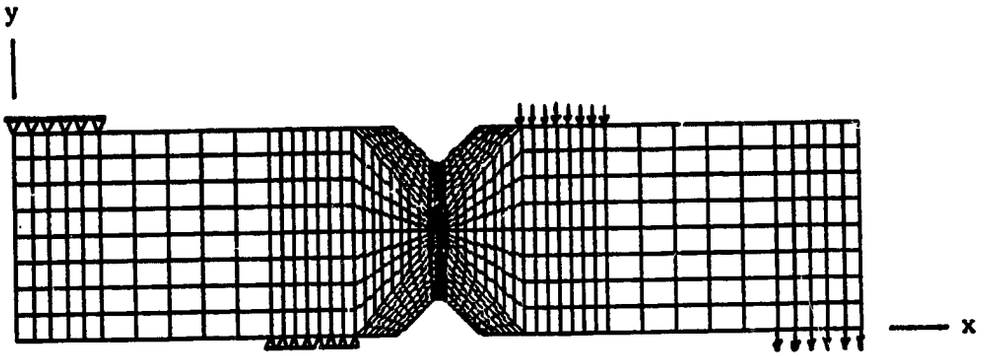

a) Entire Model and Imposed Boundary Conditions.

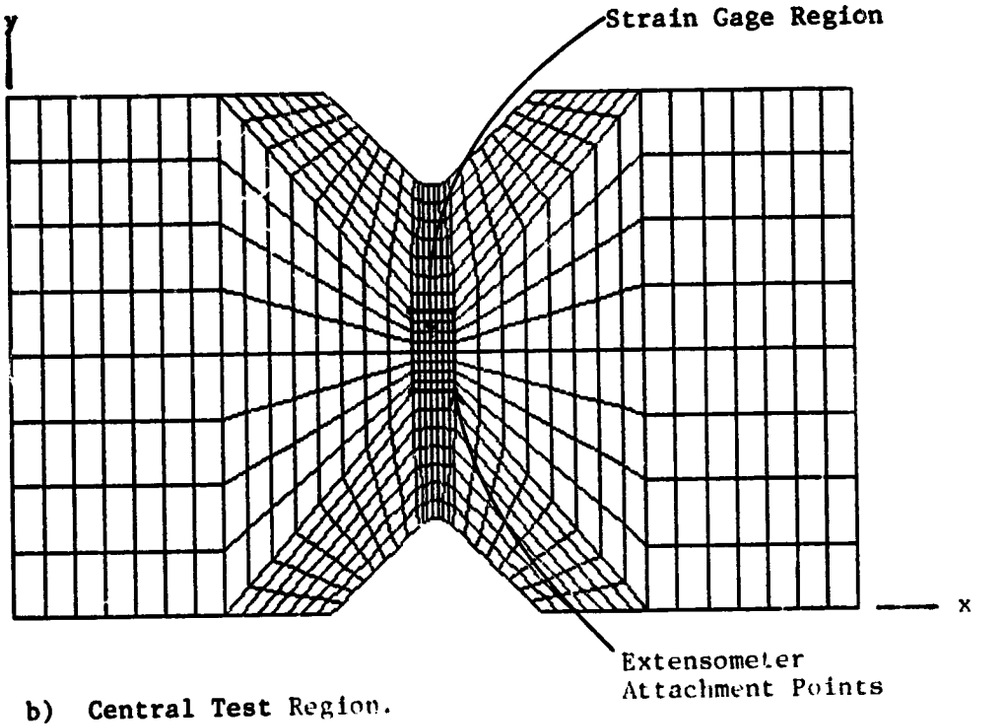

b) Central Test Region.

Figure 4. Finite Element Mesh Used to Model an Iosipescu Shear Specimen Containing 90-Degree Edge Notches.

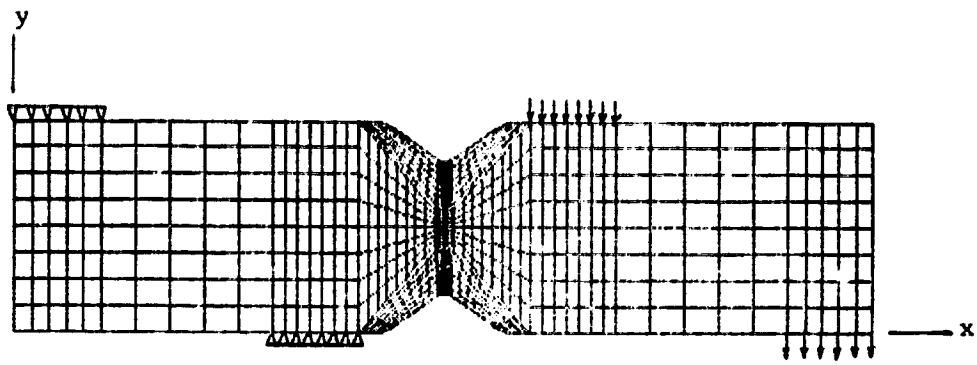

a) Entire Model and Imposed Boundary Conditions.

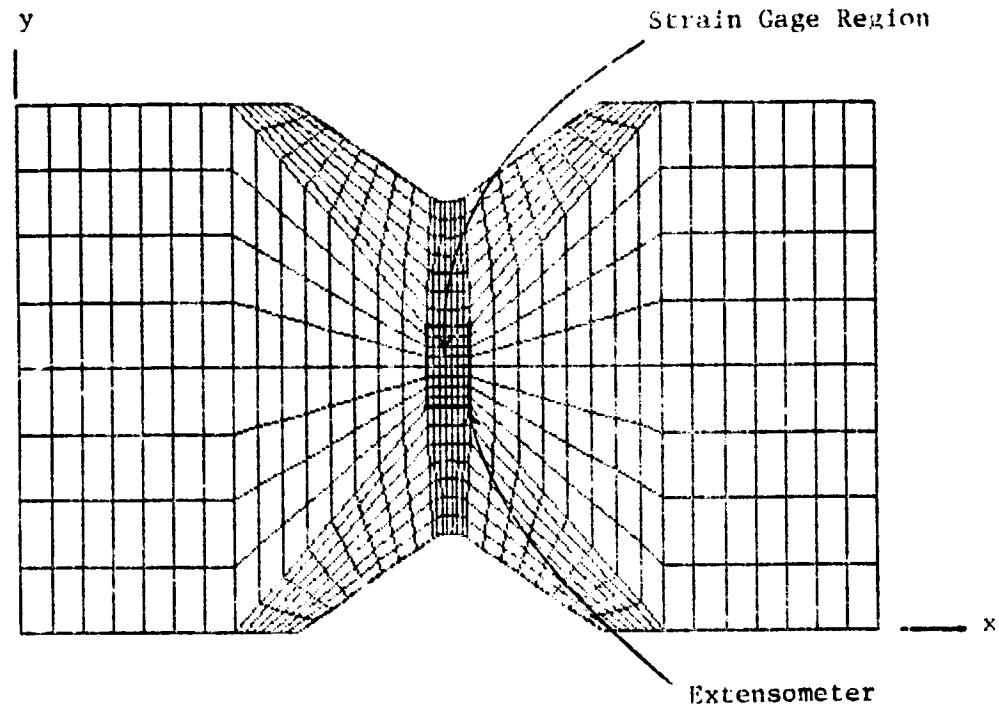

b) Central Test Region.

Figure 5. Finite Element Mesh Used to Model an Iosipescu Shear Specimen Containing 110-Degree Edge Notches.

are presented in References [5,19].

As indicated in Figures 4 and 5, loads were applied via prescribed displacements. Load point nodes on the left half of the test specimen were fixed in the y coordinate direction. Load point nodes on the right half of the test specimen were displaced in the negative y coordinate direction, reflecting the actual loading method of the test fixture. As the actual test fixture loads each point in a compressive mode, care must be taken to ensure no tensile loads develop at the loading points during the finite element simulation. No tensile forces were present at the loading points for any of the cases reported here. All shear test simulations consisted of 14 loading increments in order to model the inelastic behavior of the test specimen. All loadings were simulated at ambient (room temperature, dry) environmental conditions. The finite element program is capable of modeling nonambient environmental conditions; however this was beyond the scope of the present study.

2.5 Finite Element Stress Results

Stress versus displacement plots for the 90-degree and the 110-degree notch angle models are shown in Figure 6. The displacements indicated are the boundary displacements applied to each of the finite element models. From a testing viewpoint, these values represent the simulated displacement measurement of the testing machine, assuming a rigid test fixture and load train. The plots of Figure 6 illustrate the nonlinear response which would be observed by the testing machine operator. The applied shear stress is calculated by dividing the applied load by the specimen cross-sectional area (between notch roots). Applied loads were determined from the nodal reaction forces induced by the displacements at the boundaries.

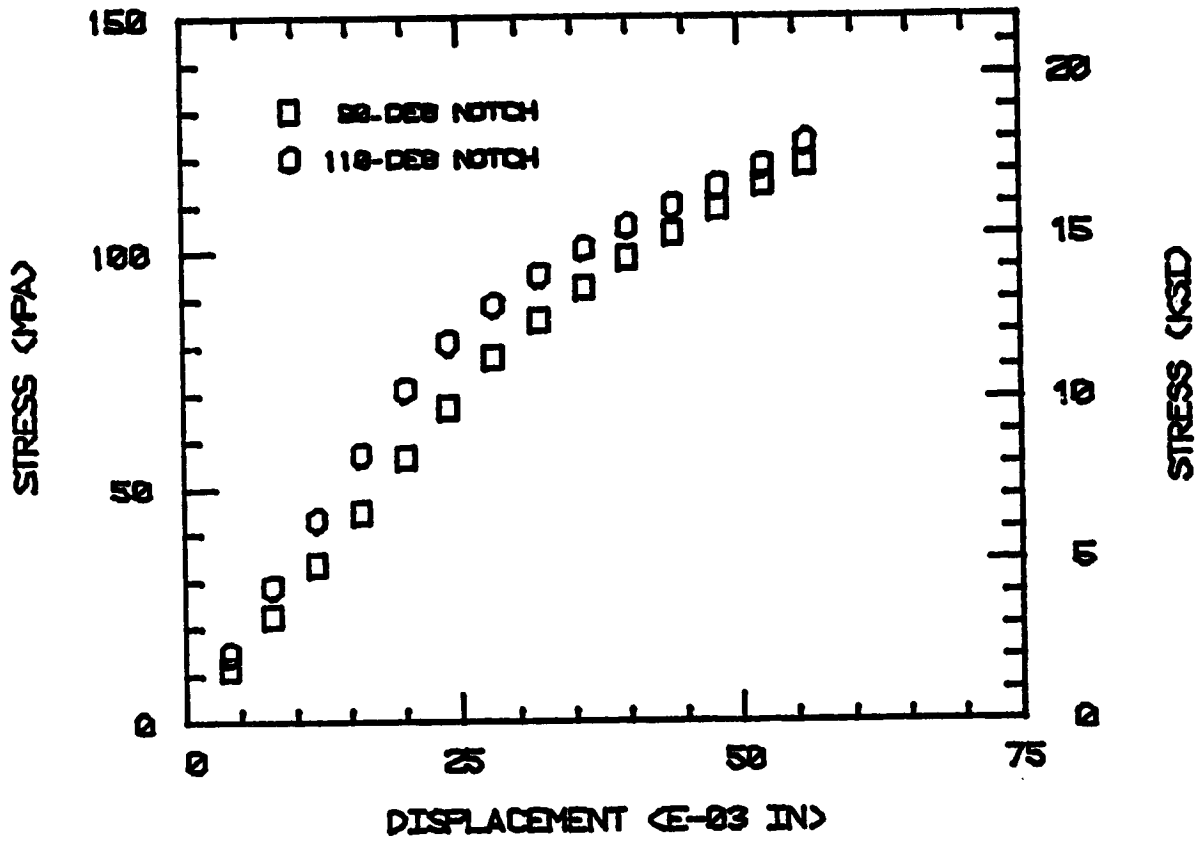

Figure 6. Predicted Average Shear Stress Versus Fixture Displacement Plots for the 90-Degree and 110-Degree Notch Angle Specimen Geometries.

Stress distribution contour plots were examined for each of the 14 increments for both finite element models. Results to be presented here have been selected from four of those loading increments, corresponding to four different regions in the load-displacement regime. Increment 1 results are shown as representing the material in the linear elastic range. These results are directly comparable with those presented by other authors using linear analyses. Stress contours and distributions from Increment 4 are presented since at this applied stress level many elements have begun to respond inelastically, yet the overall specimen response is still almost linear. Increment 8 results represent a stress level of obvious nonlinear load-displacement behavior. Finally, results are presented for Increment 12. Stresses at this level of loading are very high and the specimen is near ultimate failure.

Knowing the actual state of stress within the test region is, of course, of major importance in understanding the test method. Ideally, the stress state should be a pure shear stress τ_{xy}, with no bending-induced axial normal stress σ_x or loading point-induced transverse normal stress σ_y components. Normalized bending stress contours $\sigma_x/\bar{\tau}$ for Increments 1, 4, 8, and 12 are plotted in Figures 7 and 8 for the 90-degree and 110-degree notch models, respectively. Stress contours plotted in Figures 7 and 8 and subsequent figures have been normalized by the absolute value of the applied shear stress $\bar{\tau} = |\tau_{applied}|$. Relative to the coordinate system used, as shown previously in Figures 4 and 5, actual applied shear stresses were negative. Stress values were normalized by the absolute value of the applied shear stress in order to preserve the sign of the normal stresses, negative indicating compression.

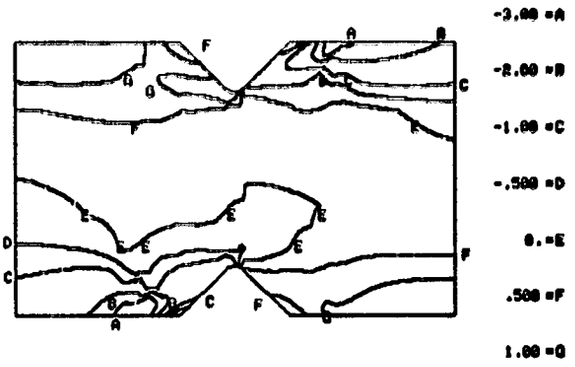

a) Increment 1, $\bar{\tau}$ = 11.7 MPa (1.70 ksi)

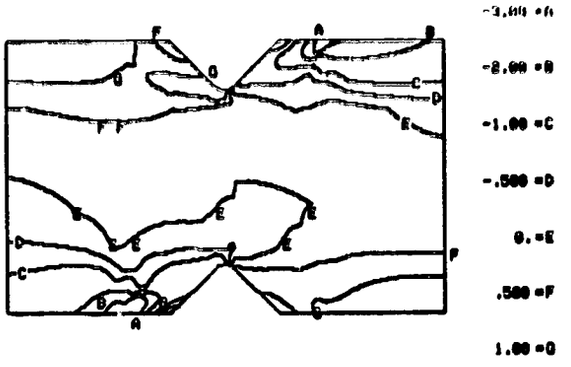

b) Increment 4, $\bar{\tau}$ = 44.9 MPa (6.51 ksi)

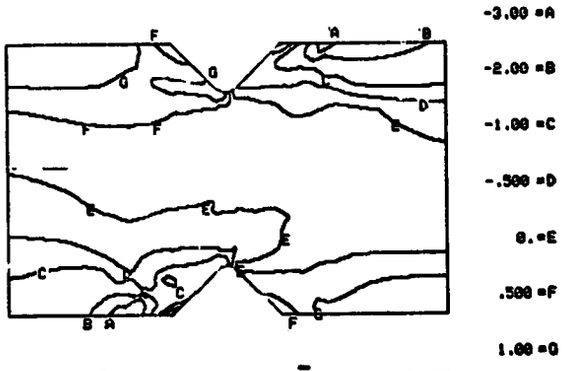

c) Increment 8, $\bar{\tau}$ = 85.1 MPa (12.34 ksi)

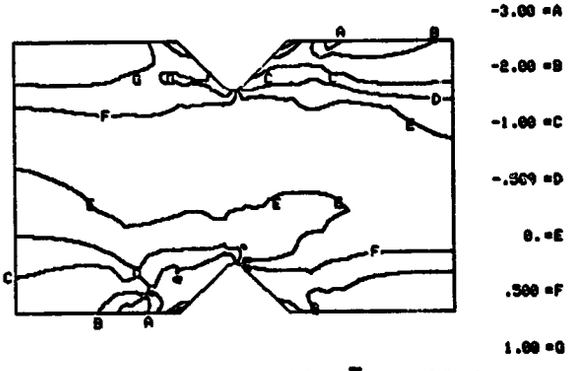

d) Increment 12, $\bar{\tau}$ = 109.2 (15.84 ksi)

Figure 7. Normalized Axial Bending Stress Contours $\sigma_x/\bar{\tau}$ for a 90-Degree Notch Iosipescu Shear Test Specimen of AS4/3501-6 Graphite/Epoxy.

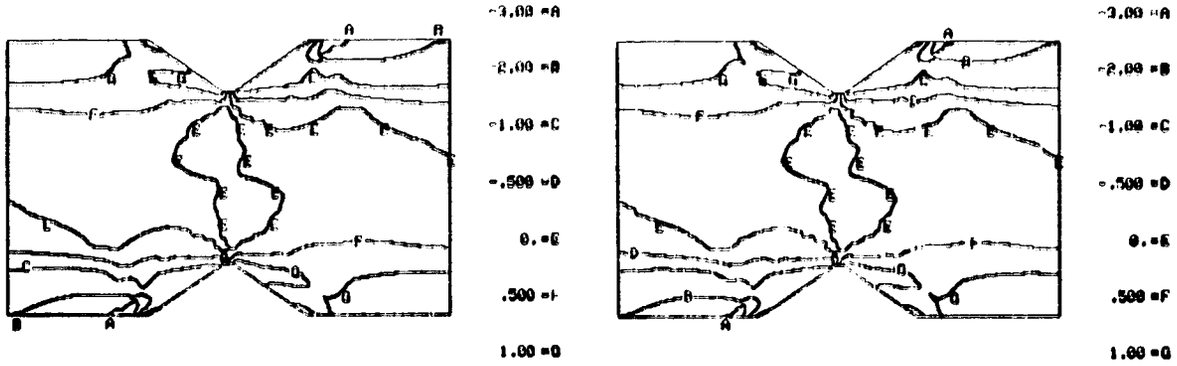

a) Increment 1, 14.5 MPa (2.11 ksi)

b) Increment 4, 57.1 MPa (8.28 ksi)

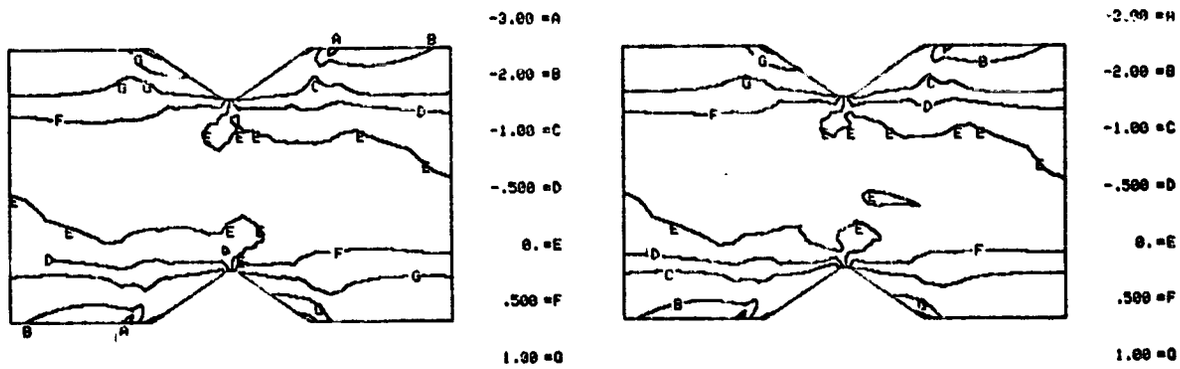

c) Increment 8, 95.0 MPa (13.78 ksi)

d) Increment 12, 114.0 MPa (16.53 ksi)

Figure 8. Normalized Axial Bending Stress Contours $\sigma_x/\bar{\tau}$ for a 110-Degree Notch Iosipescu Shear Test Specimen of AS4/3501-6 Graphite/Epoxy.

Looking first at Figure 7 for the 90-degree notch model, it can be seen that the test region of the specimen is essentially free of bending induced stresses in all increments, as indicated by the 0.0 contour labeled E in Figures 7a-7d. Bending stresses did increase at the roots of the notches, being as high as 1.0 times the applied shear stress, as indicated by the G contour at the top notch root in Figure 7b. However, it will be noted that even slightly removed from the notch root, for all four increments, bending stresses are only 0.5 times the applied shear stress or less. Also, a bending stress of 0.5 $\bar{\tau}$ in Increment 1 for example, is only 5.9 MPa (0.85 ksi), which is a negligibly low stress in the fiber direction of a graphite/epoxy composite. Even in Increment 12, the 0.5 $\bar{\tau}$ bending stresses shown in Figure 7d represent an actual stress of only 54.6 MPa (7.92 ksi), which is less than 3 percent of the longitudinal strength of this material.

Similar bending stress results can be seen in the results plotted for the 110 degree notch model shown in Figure 8. The 0.0 stress contour labeled E actually encloses the center test region in Figures 7a and 7b, which represent Increments 1 and 4. Figures 7c and 7d (for Increments 8 and 12) also show that bending stresses were negligible within the center test region.

Normalized transverse stress, $\sigma_y/\bar{\tau}$, is plotted for Increments 1, 4, 8, and 12 for the 90-degree notch model in Figure 9. One conclusion reached during the analytical study of the previous year [7] was that the inner loading points of the original version of the test fixture were too close to the center of the test specimen. Inner loading points in the latest version of the test fixture begin at a point 6.3 mm (0.25

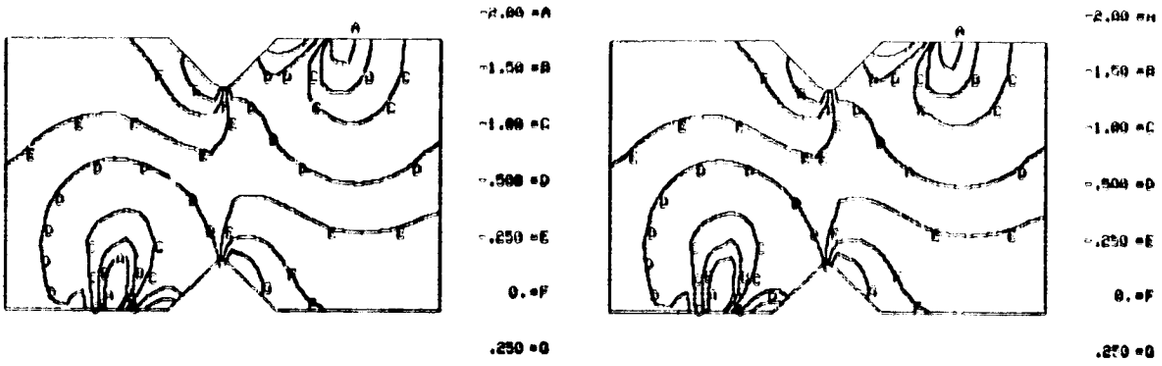

a) Increment 1, $\bar{\tau}$ = 11.7 MPa (1.70 ksi)

b) Increment 4, $\bar{\tau}$ = 44.9 Mpa (6.51 ksi)

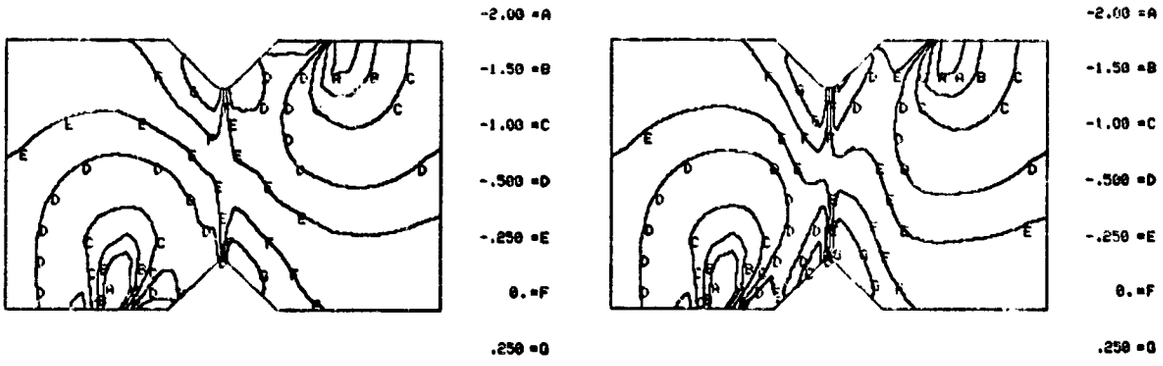

c) Increment 8, $\bar{\tau}$ = 85.1 MPa (12.34 ksi)

d) Increment 12, $\bar{\tau}$ = 109.2 (15.84 ksi)

Figure 9. Normalized Transverse Normal Stress Contours $\sigma_y/\bar{\tau}$ for a 90-Degree Notch Iosipescu Shear Test Specimen of AS4/3501-6 Graphite/Epoxy Composite.

in) away from the center of the test specimen, as opposed to the 7.5 mm (0.3 in) distance in the original fixture. This subject will be discussed in more detail later in this section. As can be seen in Figure 9, the center region of the test specimen is subjected to σ_y stresses between 0.25 $\bar{\tau}$ and 0.50 $\bar{\tau}$ (Contours D and E) for Increments 1 and 4 (see Figures 9a and 9b. The σ_y stresses are 0.25 $\bar{\tau}$ or less after Increment 4, Figures 9c and 9d. It will be remembered that Increment 4 was selected for presentation since it represents the stress state just prior to significant inelastic material behavior. The σ_y stresses are lower relative to the applied shear stress $\bar{\tau}$ in the subsequent Increments 8 and 12 due to material yielding. Repositioning the loading points appears to have improved the overall stress state in the test region as compared to the results presented in the previous year report [7]. However, some σ_y stress is still present in the test region, becoming progressively less significant when compared to the applied shear stress $\bar{\tau}$ as the test progressed. It will be noted that these transverse normal stresses are compressive, as expected, and are therefore less important in terms of inducing transverse failure than if they had been tensile. A tensile transverse stress is present near the notch root, however; the significance of this will also be discussed further in later paragraphs.

Normalized transverse stress $\sigma_y/\bar{\tau}$ contour plots for the 110-degree notch model are shown in Figure 10. As was true for the 90-degree model, σ_y transverse stresses are as high as 0.25 $\bar{\tau}$, as illustrated by contour E in Figure 10a. However, the relative importance of the σ_y stresses as compared to the applied stress $\bar{\tau}$ decreases as the test simulation proceeds. Contour E (0.25 $\bar{\tau}$) moves farther from the specimen center as the $\sigma_y/\bar{\tau}$ stress ratio decreases at the specimen center, as shown in

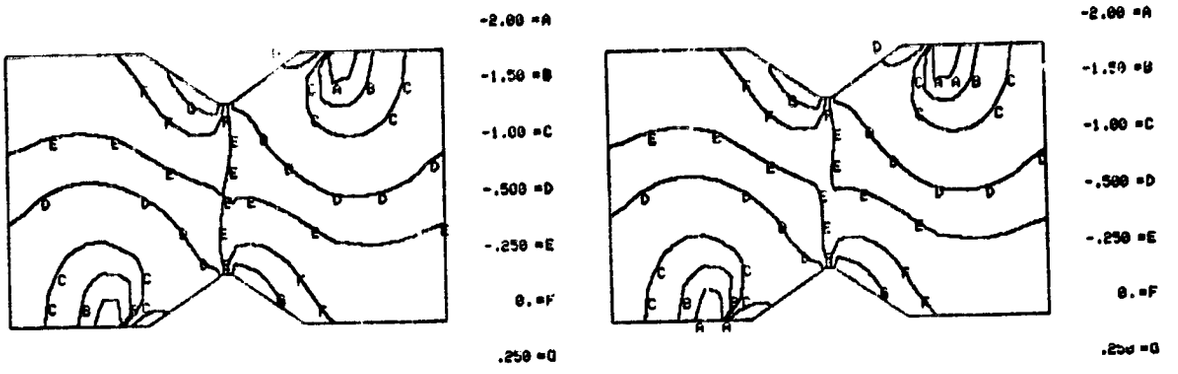

a) Increment 1, 14.5 MPa (2.11 ksi)

b) Increment 4, 57.1 MPa (8.28 ksi)

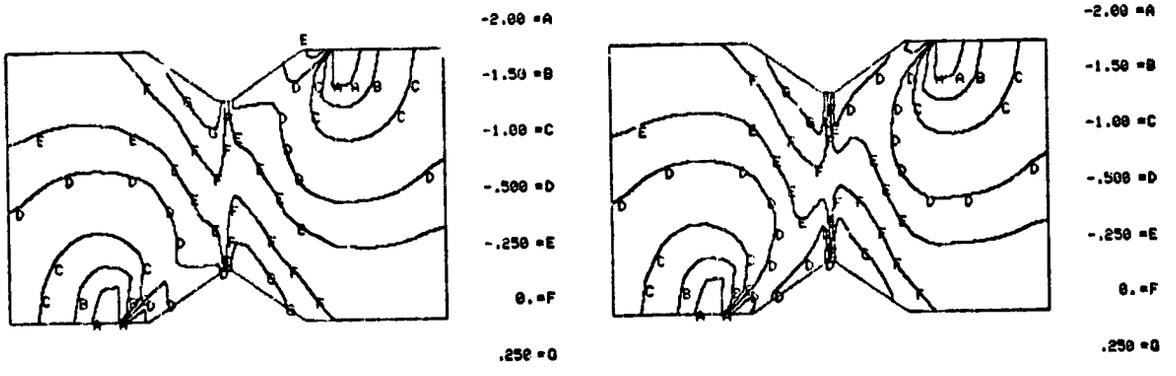

c) Increment 8, 95.0 MPa (13.78 ksi)

d) Increment 12, 114.0 MPa (16.53 ksi)

Figure 10. Normalized Transverse Stress Contours $\sigma_y/\bar{\tau}$ for a 110-Degree Notch Iosipescu Shear Test Specimen of AS4/3501-6 Graphite/Epoxy Composite.

Figures 10b, 10c, and 10d for Increments 4, 8, and 12, respectively. Again, the transverse normal σ_y stresses are primarily negative (compressive), with the exception of two locations near the notch regions illustrated by the 0.25 $\bar{\tau}$ contour labeled C in Figure 10. In comparing Figure 10 stress results to the 90-degree notch specimen transverse stress results shown in Figure 9, it would appear that the transverse stresses are less significant in the 110-degree notch test specimen for this particular orthotropic material.

The particular stress contours of interest are, of course, the shear stress contours. Normalized shear stress contours are plotted for the 90-degree notch model in Figure 11. Ideally, there should be a uniform shear stress region of contour value 1.00 throughout the center of the specimen. If so, then the actual shear stress in the test region would match the applied shear stress as measured by the testing machine. In examining Figure 11 for the 90-degree notch model, it can be seen that the center test region is being subjected to a fairly uniform shear stress. During the initial loading (see Increments 1 and 4 plotted in Figures 11a and 11b), some shear stress concentration occurs at the notch roots. This shear stress concentration is as high as -1.25 $\bar{\tau}$ (it will be remembered that the applied shear stress is negative), as shown by the contours labeled B in Figures 11a and 11b. This shear stress concentration is greatly reduced with increasing load, due to the inelastic material behavior which occurs, as shown for Increments 8 and 12 in Figures 11c and 11d. At these two applied stress levels, the shear stress is indeed reasonably uniform, at a value equal to - 1.0 $\bar{\tau}$.

Another way to illustrate the spatial stress distribution is by means of a stress profile plot at the specimen midlength. Stress profile

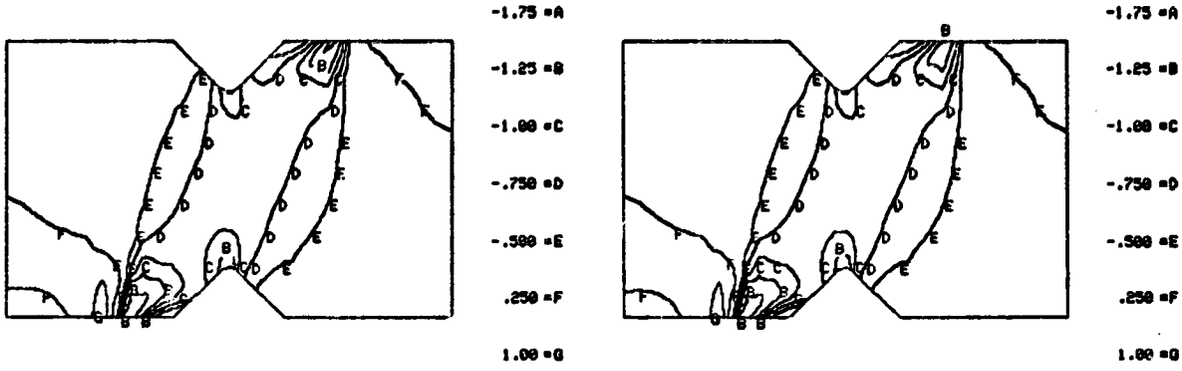

a) Increment 1, $\bar{\tau}$ = 11.7 MPa (1.70 ksi)

b) Increment 4, $\bar{\tau}$ = 44.9 MPa (6.51 ksi)

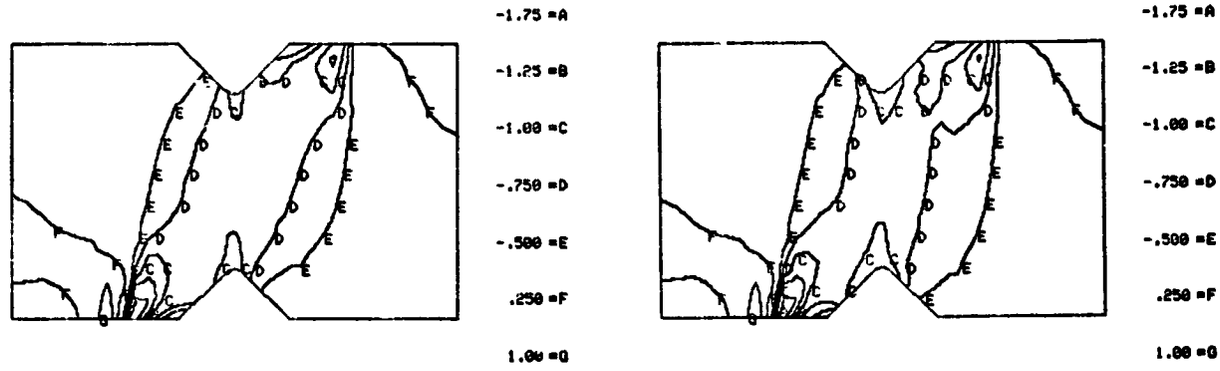

c) Increment 8, $\bar{\tau}$ = 85.1 MPa (12.34 ksi)

d) Increment 12, $\bar{\tau}$ = 109.2 MPa (15.84 ksi)

Figure 11. Normalized Shear Stress Contours $\tau_{xy}/\bar{\tau}$ for a 90-Degree Notch Iosipescu Shear Test Specimen of AS4/3501-6 Graphite/Epoxy Composite.

plots for the 90-degree notch model, using the element shear stresses in the center column of finite elements, are plotted in Figure 12. During the initial linear portion of the test simulation, Increments 1 and 4 plotted in Figures 12a and 12b, respectively, there exists a shear stress concentration at the notch root of 1.25 times the applied shear stress. Once significant inelastic material behavior occurs (Increments 8 and 12, plotted in Figures 12c and 12d, respectively), the shear stress concentration is blunted, the shear stress distribution becoming uniformly equal to 1.0, to within a few percent.

Similar stress contour and stress profile plots are shown for the 110-degree notch model in Figures 13 and 14, respectively. As in the 90-degree model, there is some shear stress concentration at the notch root in the 110-degree notch model during the initial Increments 1 and 4, as shown in Figures 14a and 14b. However, this stress concentration is not as high. Otherwise, the behavior of the 110-degree notch specimen is very similar to that of the 90-degree notch specimen. A shear stress concentration is present during the initial (linear) increments, although slightly lower than for the 90-degree notch model. As inelastic material behavior occurs, the shear stress approaches a uniform value equal to $-1.0\ \bar{\tau}$, as shown in Figures 13c, 13d, 14c and 14d.

2.6 Strain Measurement Analysis

An effort was made during the present program to study two available shear strain measurement techniques and to evaluate their possible usefulness. One easily implemented shear strain transducer is a strain gage rosette containing two strain gages oriented at ±45 degrees to the loading direction. One such strain rosette is shown mounted on an

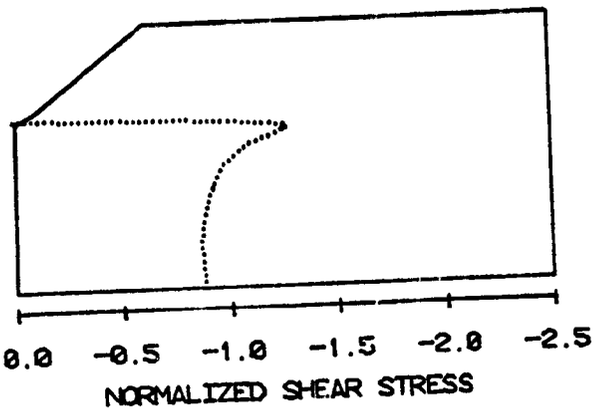

a) Increment 1, $\bar{\tau}$ = 11.7 MPa (1.70 ksi)

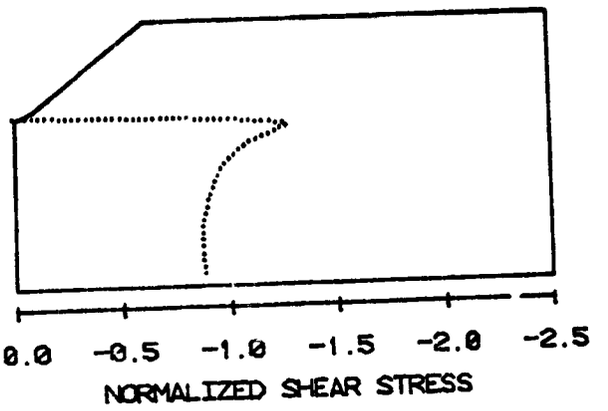

b) Increment 4, $\bar{\tau}$ = 44.9 MPa (6.51 ksi)

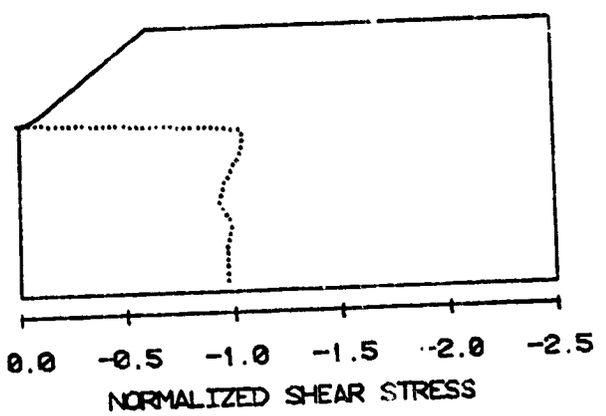

c) Increment 8, $\bar{\tau}$ = 85.1 MPa (12.34 ksi)

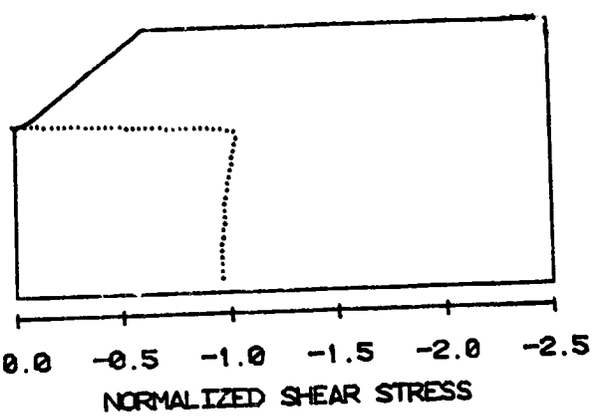

d) Increment 12, $\bar{\tau}$ = 109.2 MPa (15.84 ksi)

Figure 12. Normalized Shear Stress Profiles $\tau_{xy}/\bar{\tau}$ for a 90-Degree Notch Iosipescu Shear Test Specimen of AS4/3501-6 Graphite/Epoxy Composite.

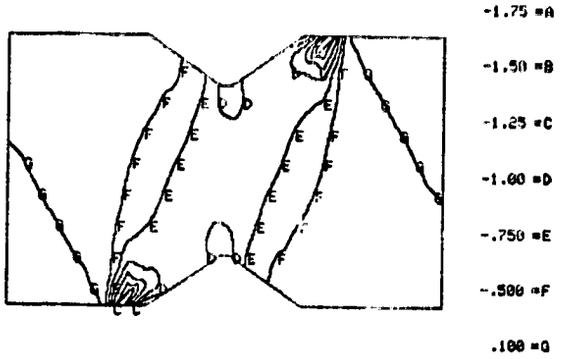

a) Increment 1, 14.5 MPa (2.11 ksi)

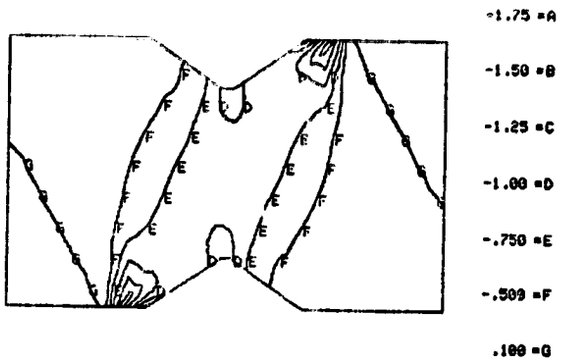

b) Increment 4, 57.1 MPa (8.28 ksi)

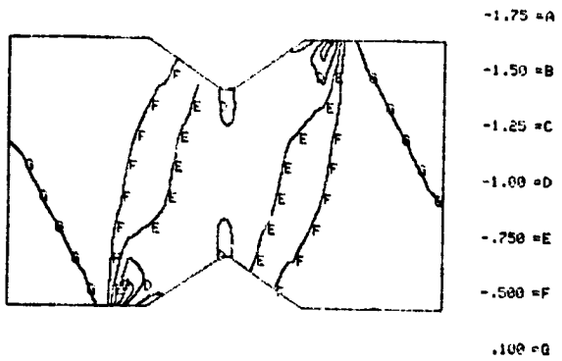

c) Increment 8, 95.0 MPa (13.78 ksi)

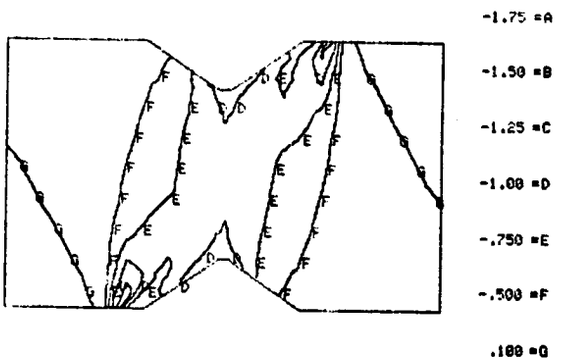

d) Increment 12, 114.0 MPa (16.53 ksi)

Figure 13. Normalized Shear Stress Contours $\tau_{xy}/\bar{\tau}$ for a 110-Degree Notch Iosipescu Shear Test Specimen of AS4/3501-6 Graphite/Epoxy Composite.

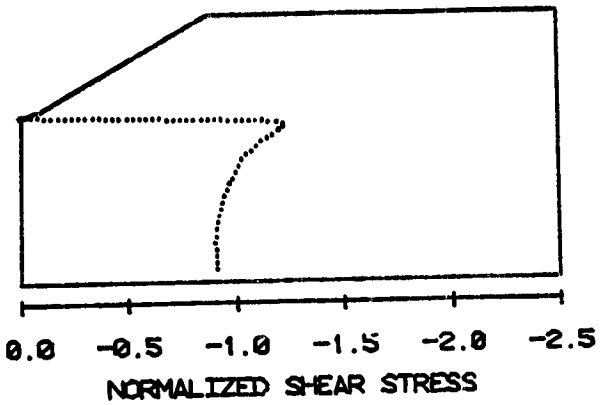

a) Increment 1, 14.5 MPa (2.11 ksi)

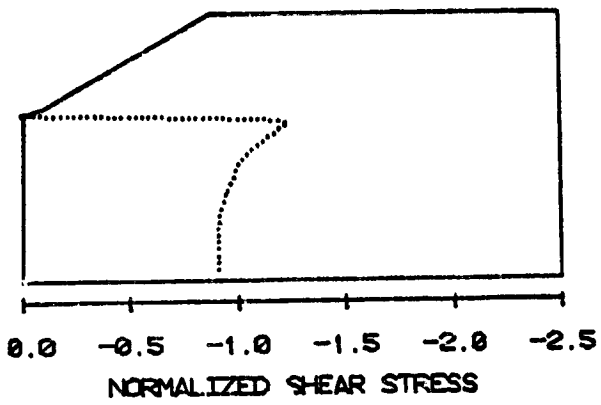

b) Increment 4, 57.1 MPa (8.28 ksi)

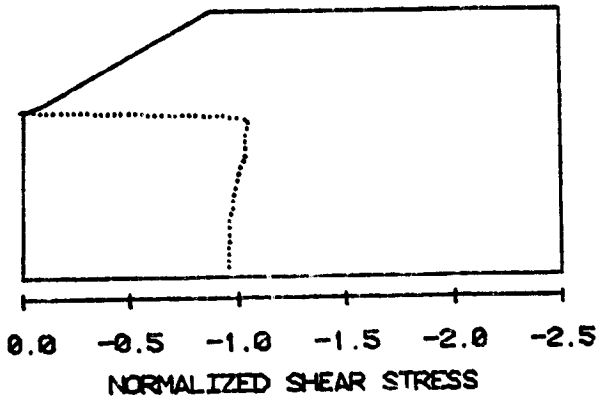

c) Increment 8, 95.0 MPa (13.78 ksi)

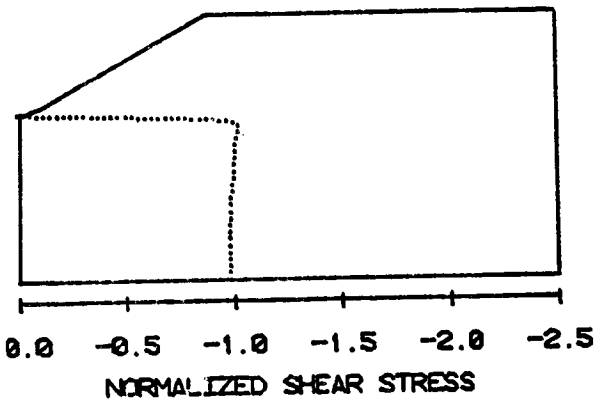

d) Increment 12, 114.0 MPa (16.53 ksi)

Figure 14. Normalized Shear Stress Profiles $\tau_{xy}/\bar{\tau}$ for a 110-Degree Notch Iosipescu Shear Test Specimen of AS4/3501-6 Graphite/Epoxy Composite.

Iosipescu shear test specimen of woven fabric T300/934 graphite/epoxy in Figure 15. This particular Micro Measurements EA-06-062TV-350 strain gage rosette covers an area 1.57 mm x 2.92 mm (0.062 in. x 0.115 in.). During construction of the finite element model, a set of elements was defined for both the 90-degree notch and the 110-degree notch models corresponding to this strain gage area. These areas were previously illustrated in Figures 4b and 5b.

The second shear strain transducer that was modeled was a modified extensometer, described previously in References [6, 8-10]. One version of this device is shown in Figure 16. The modified extensometer attaches to four points on the test specimen, as previously illustrated in Figures 4b and 5b. The four points corresponding to the corners of the strain rosette were used, thus calculating a shear strain over the same instrumented area. In the finite element models, these four points corresponded to four nodes whose displacements were monitored during a given shear test simulation.

The modified extensometer measures the displacement of the right set of two attachment points relative to the left set of attachment points. During a test, the original square defined by the four attachment points translates, rotates, and deforms, as shown in Figure 17a. Because the modified extensometer is mounted directly on the test specimen, the deflection measurement of the right side relative to the left side is entirely in coordinates relative to the extensometer and test specimen, as illustrated in Figure 17b. The shear strain is equal to the angle change, i.e.,

$$\gamma \approx \tan \gamma = \frac{\Delta y}{L_x} \text{ (for small angles)}$$

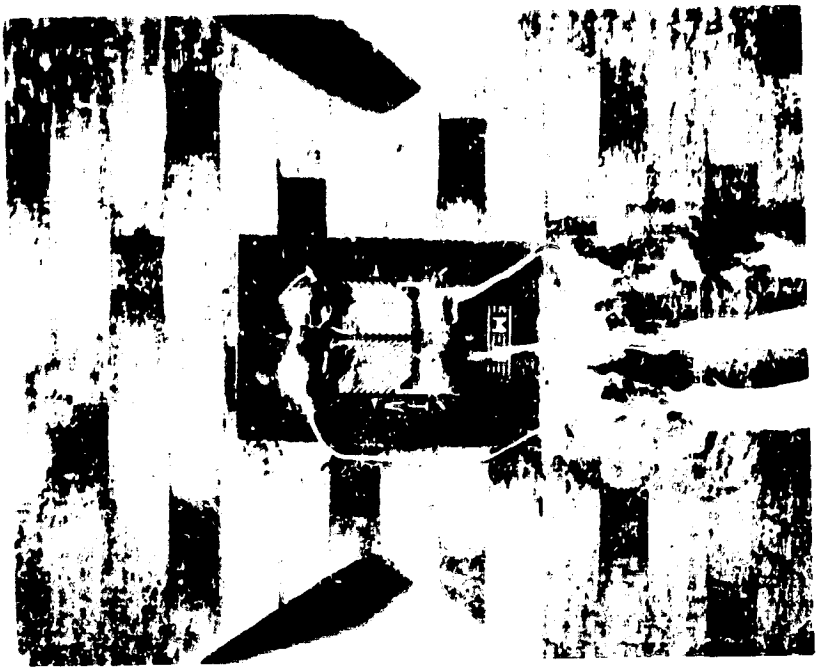

Figure 15. Shear Strain Gage Rosette Mounted on an Iosipescu Shear Test Specimen of Woven Fabric T300/934 Graphite/Epoxy.

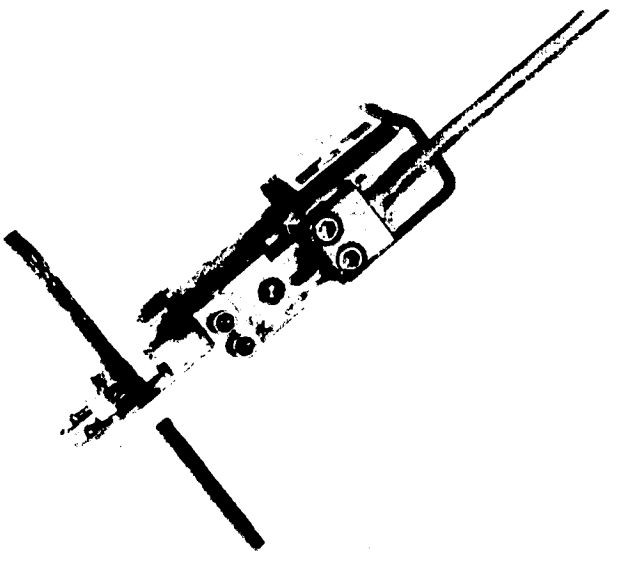

Figure 16. Modified Extensometer Used as a Shear Strain Transducer.

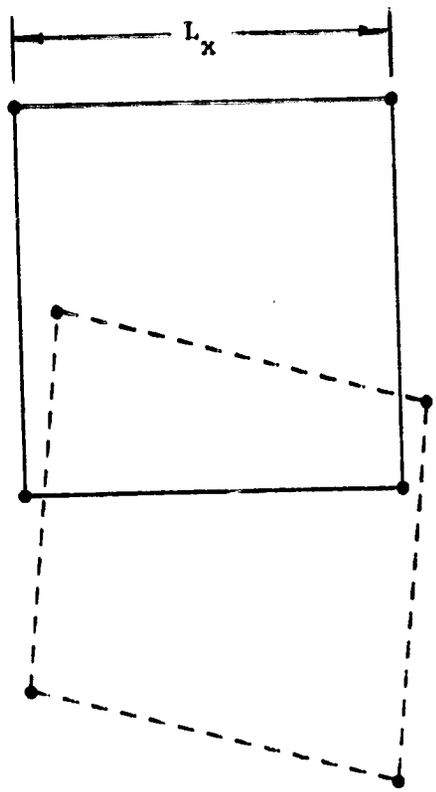

a) Actual Motion of the Modified Extensometer.

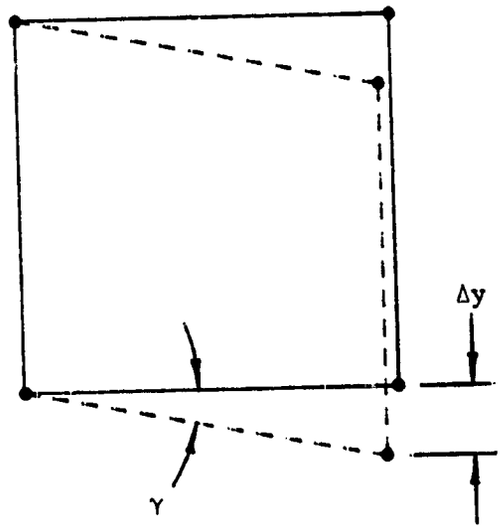

b) Shear Displacement Relative to the Extensometer Coordinate System.

Figure 17. Shear Strain Measurement with a Modified Extensometer.

where γ = shear strain

Δy = measured relative vertical displacement

L_x = horizontal spacing between extensometer attachment halves

Note that the extensometer must be free to rotate with the test region of the specimen in this application. A convenient means of attaching an extensometer for this application is currently being designed.

Shear stress-strain plots for a unidirectional AS4/3501-6 graphite/epoxy composite as simulated by what could be measured with a testing machine, strain gages, and modified extensometer are shown for the 90-degree notch model in Figure 18. Also plotted in Figure 18 (solid line) is the shear stress-strain behavior used as input to the analysis. The strain gage rosette and the modified extensometer obviously produced essentially the same response throughout this simulated test. In actual practice, however, the strain rosette itself would have failed at approximately 6% shear strain as the individual strain gages have a maximum range of 3%. The two strain gages of the rosette are wired in a half bridge configuration such that the recorded strain for the bridge is the difference between the two individual strain gage responses. As one gage will measure positive strain and one gage will measure negative strain, the net measured strain is the sum of the absolute values for each individual strain gage. (Thus the full shear strain range is 3% + 3% = 6%.) The full-scale range of this strain gage rosette is more limited than that of the modified extensometer. The overall simulated test performance does deviate from the input material response. Obviously, the ideal simulated test would exactly track the input material properties. The simulated tests plotted in Figure 18 measured

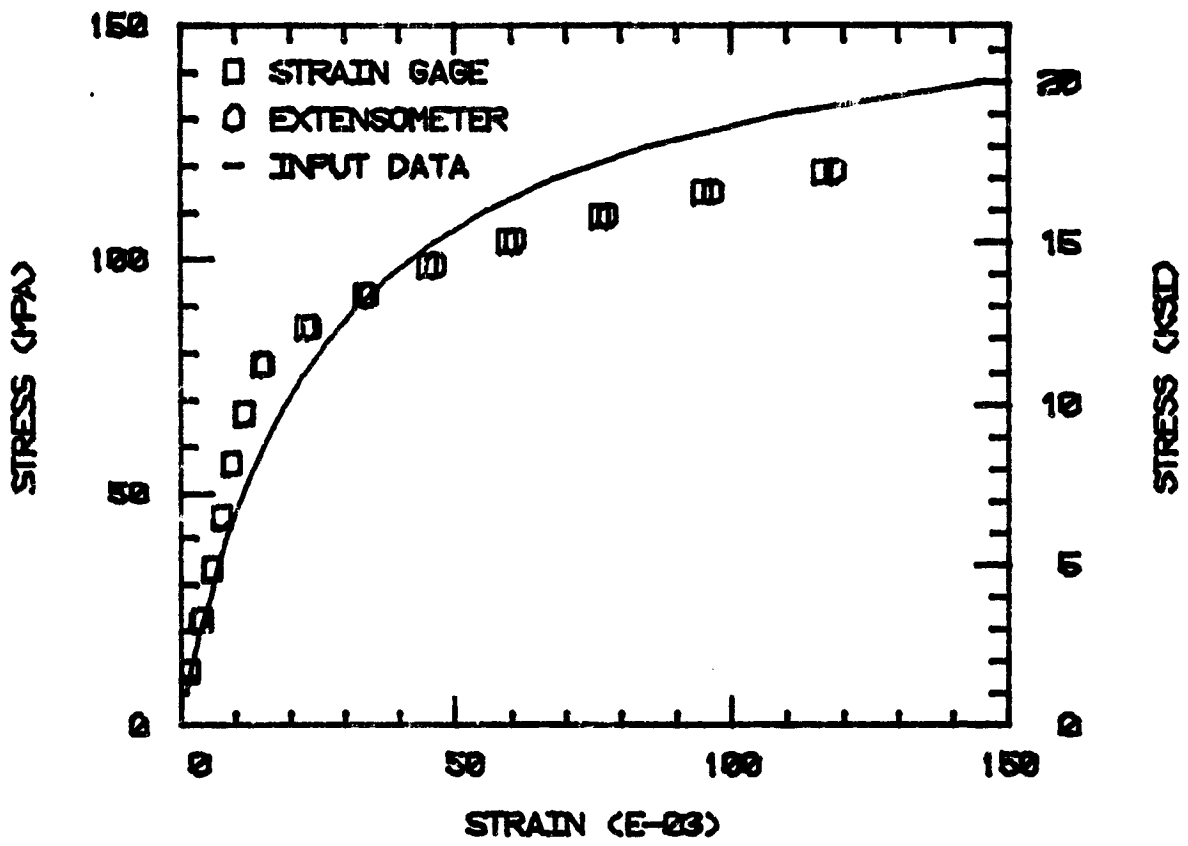

Figure 18. Simulated Shear Stress-Strain Plots for an AS4/3501-6 Graphite/Epoxy Composite Using a Modified Extensometer and a Strain Gage Rosette on the 90-Degree Notch Iosipescu Model.

shear modulus greater than the input initial shear modulus of 5.17 GPa (0.750 Msi). The modified extensometer calculated initial shear modulus was 5.95 GPa (0.863 Msi), an error of 15.1 percent. The strain gage rosette calculated shear modulus was 5.87 GPA (0.851 Msi), an error of 13.5 percent. It will be noted that these are analytical (finite element) predictions, subject to the inaccuracies of the model and boundary conditions.

Simulated stress-strain plots and input material response are plotted for the 110-degree model in Figure 19. Again, the calculated response of the strain rosette and the modified extensometer differ only slightly. However, there is some deviation from input material response. The modified extensometer calculations of initial shear modulus were greater than the input 5.17 GPa (0.750 Msi) shear modulus, producing a shear modulus of 5.73 GPa (0.832 Msi); an error of 10.9 percent. The strain gage rosette simulation produced a shear modulus of 5.68 GPa (0.824 Msi), an error of 9.9 percent.

One-increment (linear elastic) calculations were also performed using material properties for 6061-T651 aluminum alloy as input. These input elastic constants were listed previously in Table 2. Simulated modified extensometer calculations for the 90-degree notch model produced a shear modulus of 23.8 GPa (3.45 Msi) as compared to the input 25.9 GPa (3.76 Msi), an error of -6.1 percent relative to the input properties. The simulated strain gage calculations showed a modulus of 24.3 GPa (3.45 Msi), an error of -8.2 percent. Shear modulus calculations for the 110-degree notch model produced a simulated modified extensometer shear modulus of 24.3 GPa (3.45 Msi), an error of -8.2 percent. The simulated strain gage rosette measured a shear modulus

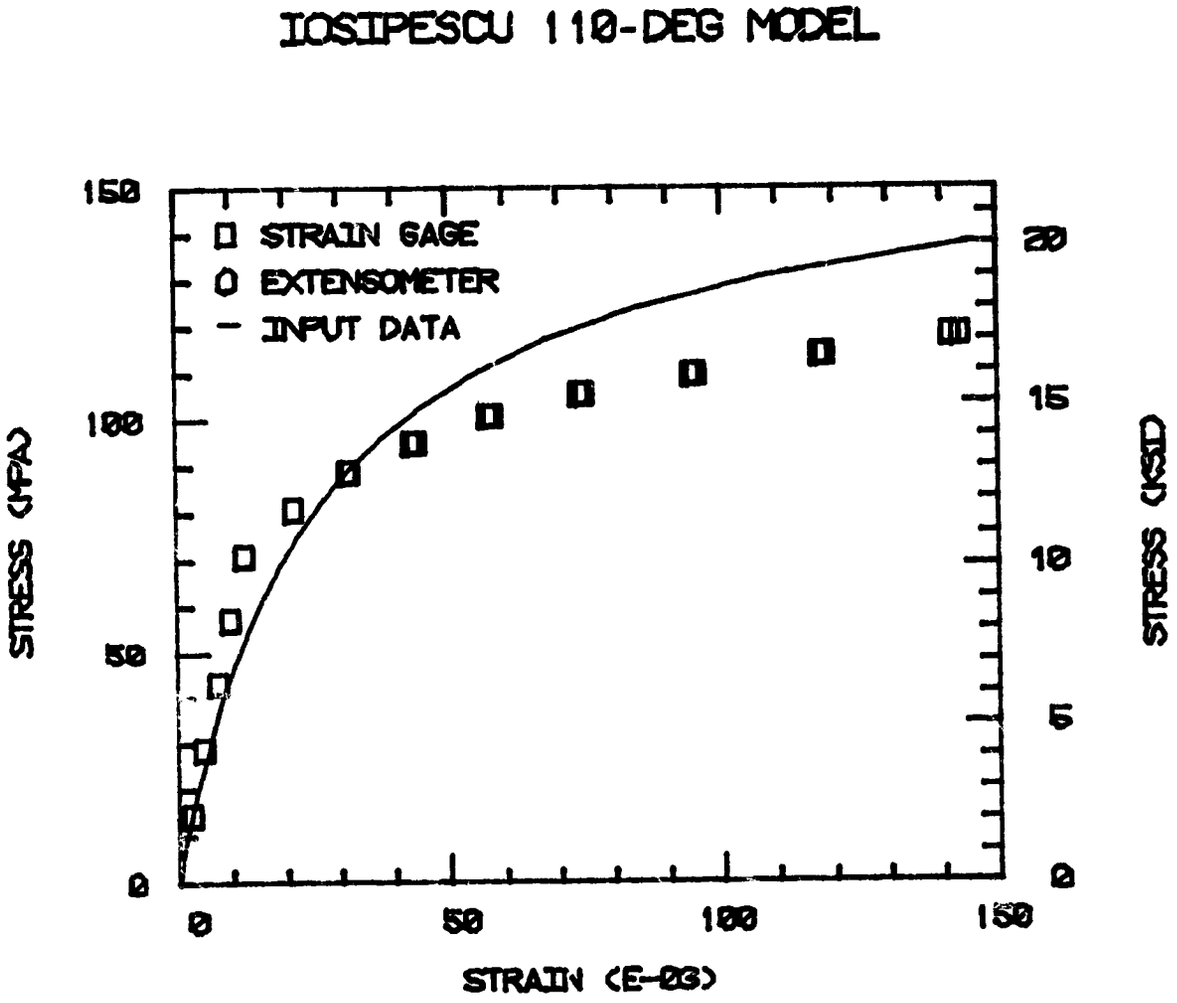

Figure 19. Simulated Shear Stress-Strain Plots for an AS4/3501-6 Graphite/Epoxy Composite Using a Modified Extensometer and a Strain Gage Rosette on the 110-Degree Notch Iosipescu Model.

of 23.6 GPa (3.43 Msi), an error of -8.8 percent.

It should be emphasized that the errors in shear modulus measurement discussed above are analytical predictions, subject not only to possible errors in the model used to simulate actual test procedures, but also to errors introduced by the analysis itself. The analysis uses an incremental loading procedure and the tangent modulus method to establish the constitutive behavior for a given element [12]. A possible source of disagreement between input and output shear stress-strain behavior, as depicted in Figures 18 and 19, is failure of the analysis to properly track the constitutive behavior for each element. This particular topic of research is currently being studied as part of separate programs. Verification experiments were performed on AS4/3501-6 unidirectional composite Iosipescu shear specimens as well as on 6061-T651 aluminum alloy Iosipescu shear specimens, indicating far less error than predicted by the analysis. These correlations are presented in the next subsection.

To summarize the analytical results presented to this point, two different notch angles have been modeled. Stress contours indicate that the shear stresses in the test regions of both specimens were reasonably uniform and free of bending-induced longitudinal normal stresses. Transverse normal stresses induced at the load points did slightly intrude into the test regions of each geometry. Output results were examined to determine how a modified extensometer or a strain gage rosette would perform in measuring shear strains. Shear moduli values were calculated from these strains and from the applied loads (stresses), for comparison with the input data. Overall, the 110-degree notch Iosipescu shear specimen appears to be slightly better than the

90-degree notch specimen in terms of uniformity of shear stress and better accuracy of modulus measurement for an orthotropic composite. The 90-degree notch specimen produced less theoretical error in modulus measurement for an isotropic (aluminum) specimen, as would be expected [4].

2.7 Experimental Verification

A series of Iosipescu shear tests were performed on 6061-T651 aluminum alloy and unidirectional AS4/3501-6 graphite/epoxy composite specimens in order to verify some of the analytical results obtained. Test specimens were 7.62 cm (3.0 in) long, 1.91 cm (0.75 in) wide. Aluminum specimens were 0.95 cm (0.375 in) thick; the graphite/epoxy specimens were 1 mm (0.04 in) thick. Notches were machined with a root radius of 0.13 cm (0.05 in) to a depth of 0.38 cm (0.15 in). This notch depth was therefore 20 percent of the specimen width. All specimens were instrumented with strain gage rosettes as previously shown in Figure 15. The modified extensometer was not used for these tests as the specimens could not accommodate both types of instrumentation simultaneously. The finite element analyses predicted little difference between strain rosette and modified extensometer shear strain measurements. Experimental verification of the modified extensometer is planned as part of a continuing effort.

Ten Iosipescu shear specimens of aluminum alloy were tested, five with 90-degree notches and five with 110-degree notches. The 90-degree notch specimen is the preferred specimen for testing isotropic materials in shear [4]. Specimens incorporating the 110-degree notch were tested to verify that the analysis correctly predicted shear property measurement trends. Averages for the five Iosipescu shear tests on the

aluminum alloy specimens of each notch angle are presented in Table 3. As expected, the 90-degree notch specimen results were closest to literature values. The average measured shear modulus (using strain rosettes) was 25.5 GPa (3.70 Msi), a difference from the literature (calculated) value of Table 2 of only -2.6 percent. The average measured shear strength for the 90-degree notch specimens was 219 MPa (31.7 ksi), a difference of 5.7 percent from the literature value of 207 MPa (30.0 ksi). These results obviously compare quite well.

Measured shear properties for the 110-degree notch aluminum alloy specimens are also presented in Table 3. The average measured shear modulus was 22.3 GPa (3.23 ksi), which is 14 percent lower than the literature value. The average measured shear strength using the 110-degree notch specimen was 221 GPa (32.1 ksi), which is 7 percent higher than the literature value. Stress-strain plots as well as tabulated results for the individual aluminum specimens are shown in Appendix B.

Comparing theoretical and experimental results, the finite element analysis predicted a shear modulus error (using strain rosettes) of -8.2 percent. The actual experimental difference from published literature modulus values was -2.6 percent. For the 110-degree notch specimen, the analysis predicted a shear modulus measurement error of -8.8 percent (again with strain rosettes). The actual experimental shear modulus difference was -14 percent. Thus the 90-degree notch specimen actually performed better experimentally than the analysis predicted. The analysis also underpredicted the error in using the 110-degree notch specimen for testing aluminum. However, the analysis did correctly predict the error trends with notch angle, even though there was some difference between actual and predicted error.

TABLE 3

MEASURED SHEAR PROPERTIES OF 6061-T651 ALUMINUM ALLOY

Notch Angle (Degrees)	Shear Strength* (MPa)	(ksi)	Shear Modulus* (GPa)	(Msi)
90	219	31.7	25.5	3.70
110	221	32.1	22.3	3.23
Literature Values [20]	207	30.0	25.9	3.76

*Average of five tests

Failed aluminum shear specimens are shown in Figures 20 and 21, for the 90-degree and 110-degree notch configurations, respectively. The failure region is obviously very narrow, extending between notch roots. These failed specimens are very representative of all 10 aluminum specimens tested.

Five Iosipescu shear specimens of unidirectional $[0]_{8T}$ AS4/3501-6 graphite/epoxy composite were then tested, using the 110-degree notch configuration. These specimens were of the same overall dimensions as the aluminum specimens, except that their thickness was only 0.1 cm (0.04 in). A complete tabulation of results of these tests is presented in Appendix B, along with the measured shear stress-strain plots for all five specimens. The average measured shear modulus was 5.9 GPa (0.85 Msi) and the average shear strength was 108 MPa (15.6 ksi). These values are comparable to published shear modulus results of 5.9 GPa (0.85 Msi) [21] and 6.1 GPa (0.88 Msi) [22], and shear strength results of 117 GPa (17 ksi) [23], using other test methods. Two of these unidirectional specimens failed due to crushing at the inner load points. All five specimens first cracked at the notch roots, but continued to load to eventual catastrophic failure. An example of this initial crack is shown in Figure 22. As can be seen in the photograph, a crack has opened near the notch root, propagating parallel to the fibers, away from the inner loading point. A similar crack was present at the bottom notch, although not shown in Figure 22.

Initial failure of the material in this mode is understandable (although undesirable) in view of the stress state present at the notch root. Re-examining Figures 9 and 10, i.e., the contour plots of transverse normal stress, and noting the contour labeled G, it can be

Figure 20. Failed Iosipescu Shear Specimen of 6061-T651 Aluminum, 90 Degree Notch Configuration.

Figure 21. Failed Iosipescu Shear Specimen of 606.-T651 Aluminum, 110 Degree Notch Configuration.

Figure 22. Initial Cracking in a Unidirectional $[0]_{8T}$ AS4/3501-6 Graphite/Epoxy Iosipescu Shear Test Specimen.

seen that significant transverse normal tensile stresses are present to the left of the top notch root and to the right of the bottom notch root for both the 90-degree and 110-degree specimen configurations. This stress is probably inherent in the test method and cannot be totally eliminated. Therefore, an effort was made to understand the effect of cracking upon the stress state within the test specimen.

Finite element models were generated which contained "cracks" to the left of the top notch and to the right of the bottom notch, as shown in Figure 23 and 24. Cracks were modeled by using elements of very low material properties, viz., stiffnesses six orders of magnitude less than stiffnesses of "uncracked" elements. Stiffnesses equal to zero cannot be used as this will result in zero values on the principal diagonal of the stiffness matrix, making the problem numerically unsolvable. No attempt was made to rigorously model stresses near the crack roots, nor to model crack propagation. These two models were merely simple attempts to understand the effect on test region stresses caused by the geometric influence of the crack.

Normalized stress contour plots for the 90-degree notch cracked model are plotted in Figure 25. Normalized axial bending stresses $\sigma_x/\bar{\tau}$ are plotted in Figure 25a. Comparing Figure 25a to Figure 7a for the uncracked 90-degree notch model, it is apparent that the presence of the cracks did not significantly alter the bending stress contours. The only apparent influence of the crack was to move the stress contours slightly away from the notch roots. This is probably an artifact of the model, however, as the "crack" is two elements in height at that point (see Figure 23) rather than the very narrow crack present in the test specimen (see Figure 22). The finite element mesh was not sufficiently

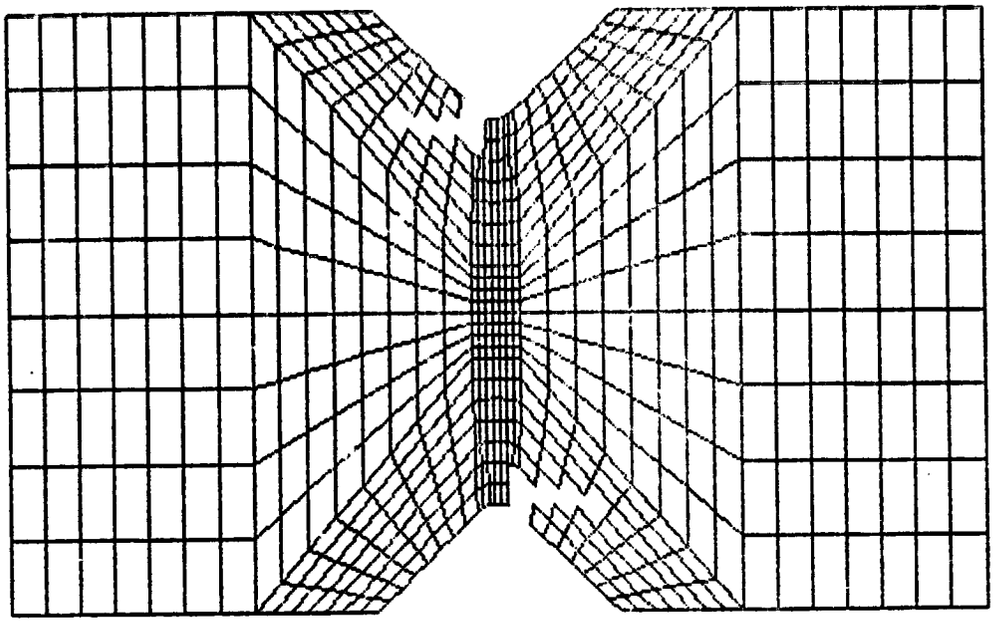

Figure 23. Cracked Iosipescu 90-Degree Notch Model.

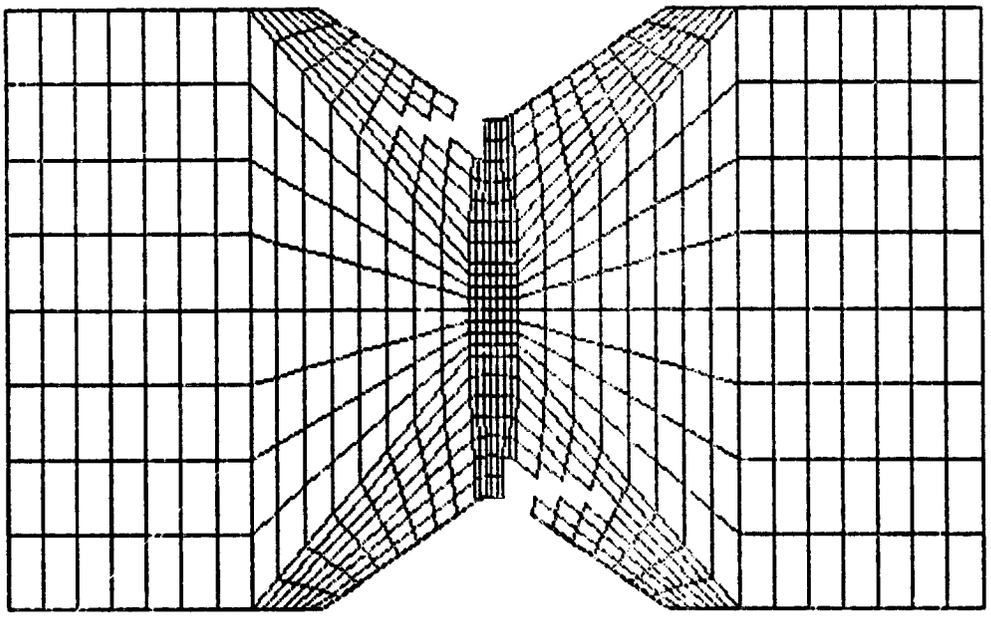

Figure 24. Cracked Iosipescu 110-Degree Notch Model.

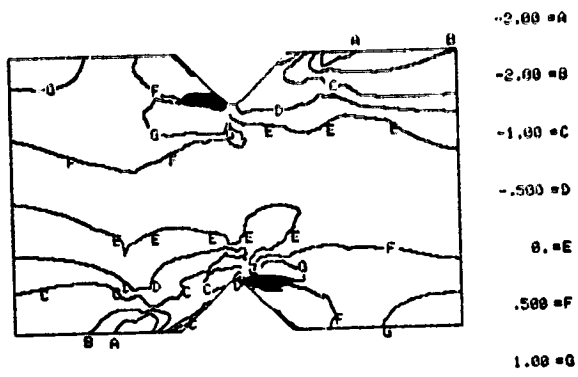

a) Normalized Axial Bending Stress, $\sigma_x/\bar{\tau}$

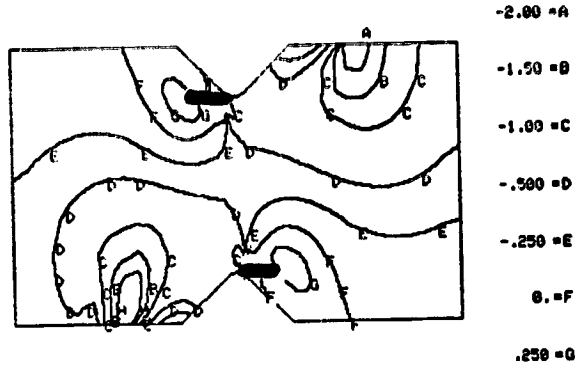

b) Normalized Transverse Normal Stress, $\sigma_y/\bar{\tau}$

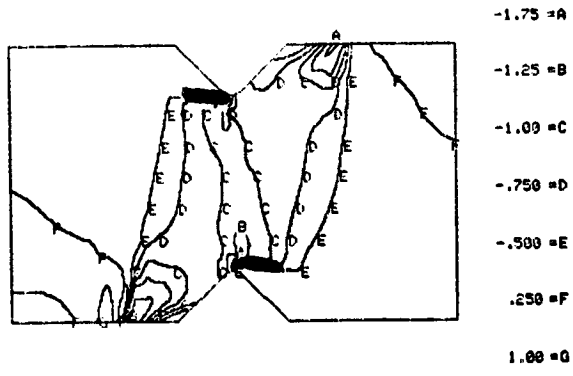

c) Normalized Shear Stress, $\tau_{xy}/\bar{\tau}$

Figure 25. Normalized Stress Contours for a 90-Degree Notch Cracked Iosipescu Shear Test Specimen of AS4/3501-6 Graphite/Epoxy Composite, $\bar{\tau}$ = 11.4 MPa (1.65 ksi).

refined to obtain more than qualitative results.

The presence of the crack appears to merely shift the positions of certain stress contours, rather than significantly altering the stress profiles. This is seen to be true when comparing the normalized transverse stresses plotted in Figure 25b for the cracked model to the comparable plot for the uncracked model shown in Figure 9a. The transverse normal tensile stress contour labeled G has moved out to the end of the crack, which it probably caused. Thus the influence of the crack was to move the undesireable transverse normal tensile stress further from the test region.

Normalized shear stress contours for the 90-degree notch cracked model are plotted in Figure 25c; the comparable uncracked results are plotted in Figure 11a. Again, the crack merely influenced the positions of the stress contours, without drastically altering the stress state within the test region. Shear stresses were, if anything, somewhat more uniform in the cracked model than in the uncracked model. This was also indicated in the shear distribution plot for the 90-degree notch cracked model shown in Figure 26. The shear stress concentration at the root of the notch was blunted somewhat by the presence of the crack, as compared to the 90-degree notch uncracked model shear profile, shown previously in Figure 12a.

The presence of a crack had very similar effects in the 110-degree notch model, as can be seen in the stress contours plotted in Figure 27. Normalized bending stresses $\sigma_x/\bar{\tau}$ were still small in the test region, as shown in Figure 27a, just as they were in the uncracked model results, Figure 8a. Normalized transverse normal stresses $\sigma_y/\bar{\tau}$ were still present in the cracked 110-degree notch model, Figure 27b, but did not appear

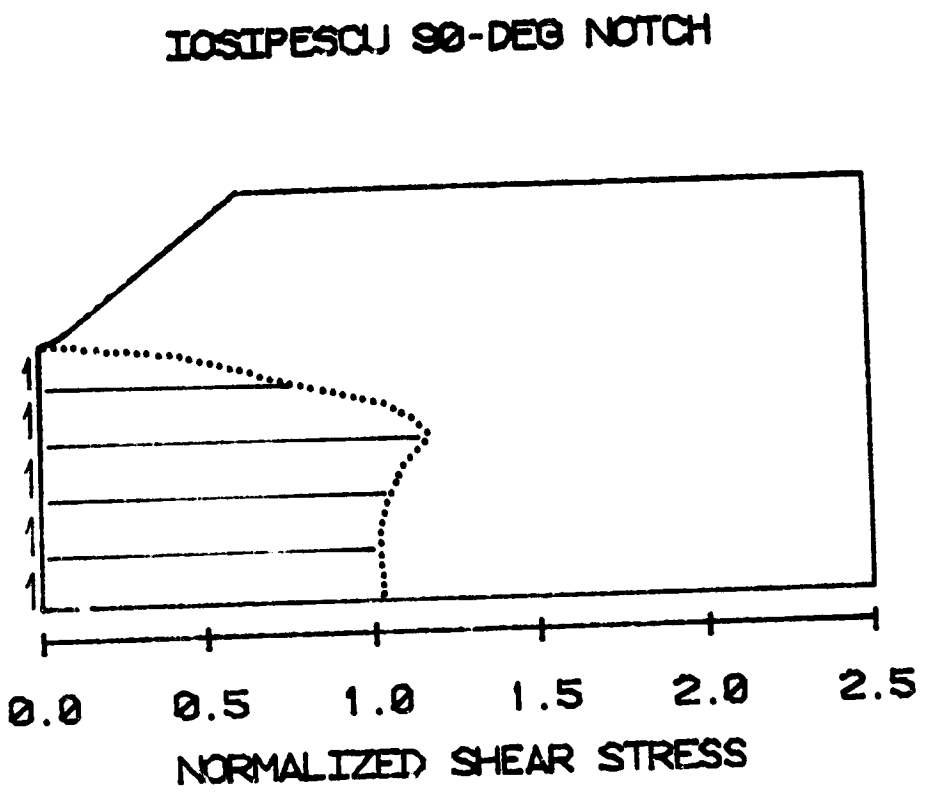

Figure 26. Normalized Shear Stress Profile $\tau_{xy}/\bar{\tau}$ for a 90-Degree Notch Cracked Iosipescu Shear Test Specimen of AS4/3501-6 Graphite/Epoxy, $\bar{\tau}$ = 11.4 MPa (1.65 ksi).

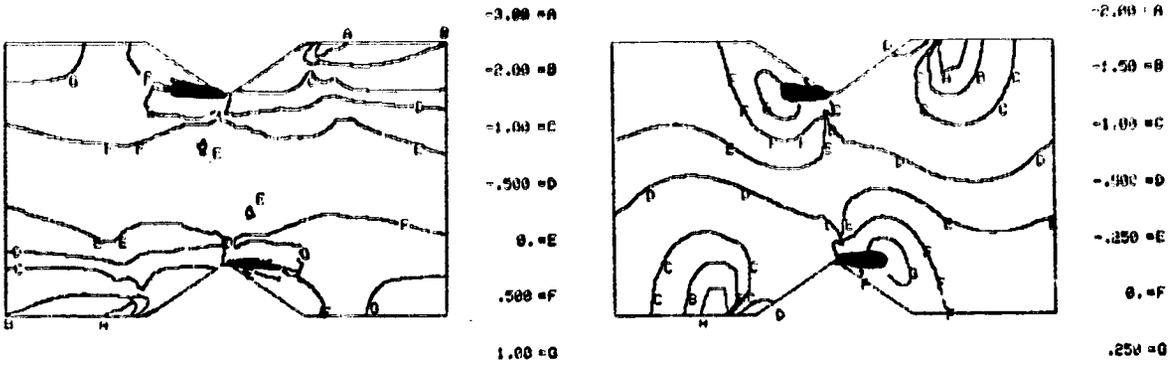

a) Normalized Axial Bending Stress, $\sigma_x/\bar{\tau}$

b) Normalized Transverse Normal Stress, $\sigma_y/\bar{\tau}$

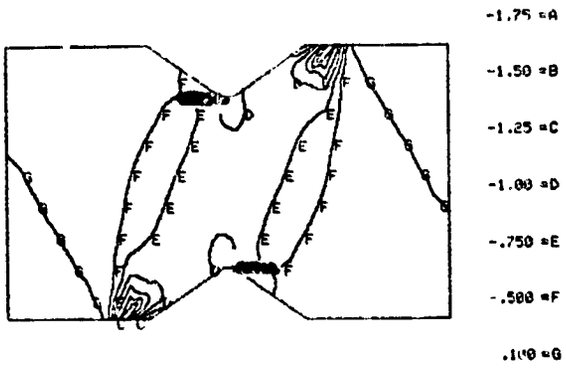

c) Normalized Shear Stress, $\tau_{xy}/\bar{\tau}$

Figure 27. Normalized Stress Contours for a 110-Degree Notch Cracked Iosipescu Shear Test Specimen of AS4/3501-6 Graphite/Epoxy, Composite, $\bar{\tau}$ = 14.0 MPa (2.03 ksi).

any more detrimental than for the uncracked transverse stress results plotted in Figure 10a. Normalized shear stresses, plotted in Figure 27c, were also relatively unchanged as compared to the uncracked results of Figure 13a. However, there were still shear stress concentrations present at the notch root, shifted to the tip of the modeled crack. The normalized shear stress profile for the 110-degree notch cracked specimen is shown in Figure 28. Comparing this plot to the corresponding uncracked results shown in Figure 14a, it can be seen that the shear stress concentration has been reduced.

These crack models, admittedly simple preliminary attempts, indicate that the initial cracking at the notch roots, while disturbing, is not necessarily detrimental in determining composite shear strength accurately. Failed unidirectional Iosipescu shear test specimens exhibit many smaller cracks throughout the test region, as shown in the dye-enhanced X-radiograph of Figure 29, indicating failures occur away from the notch roots. The two major stress relieving cracks beginning at the left of the top notch and to the right of the bottom notch are quite obvious. These cracks occurred early in the tests, resulting in momentary load drops. These are the cause, for example, of the small discontinuities in the shear stress-displacement plots shown in Figure B3 in Appendix B. The specimens continued to load, however, eventually reaching a final ultimate, catastrophic failure point, failing in shear.

Two of these specimens failed due to crushing at the inner loading points. Some damage is also apparent at the top edge of the specimen shown in Figure 29. This crushing is due to an unfavorable load distribution at the inner loading surface, resulting in very high compressive forces directly at the edge of the loading surface. This was

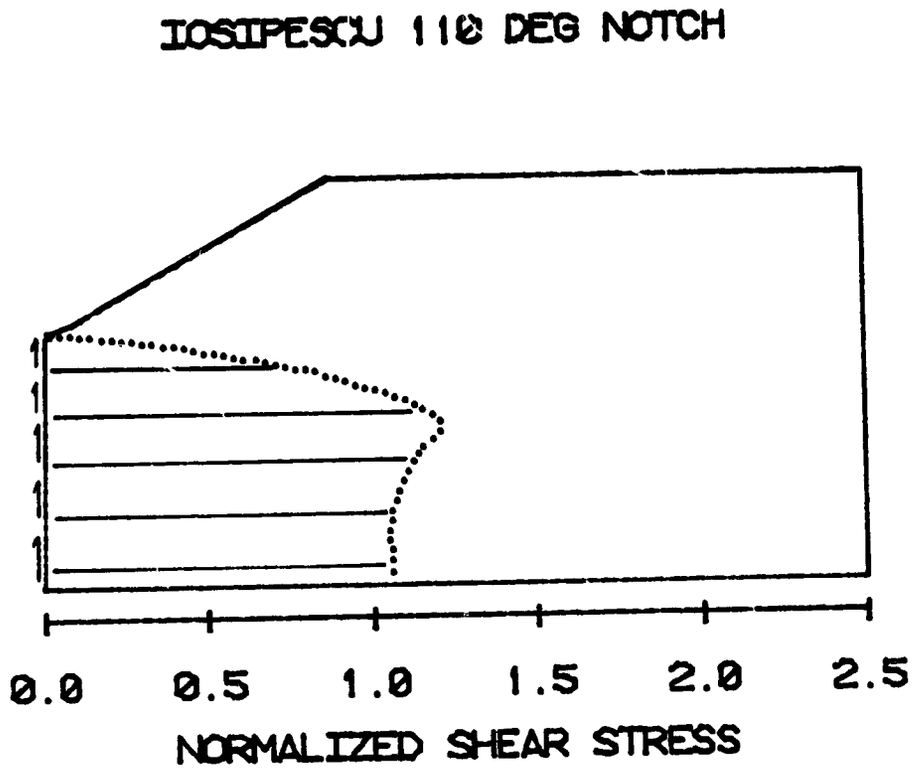

Figure 28. Normalized Shear Stress Profile $\tau_{xy}/\bar{\tau}$ for a 110-Degree Notch Cracked Iosipescu Shear Test Specimen of AS4/3501-6 Graphite/Epoxy, $\bar{\tau}$ = 14.0 MPa (2.03 ksi).

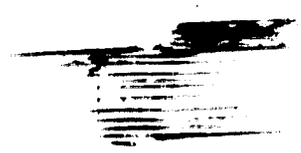

Figure 29. Dye-Enhanced X-Radiograph of a Failed Iosipescu Shear Specimen of $[0]_{8T}$ AS4/3501-6 Graphite/Epoxy Composite, 110-Degree Notch Configuration.

shown analytically by plotting the nodal resultant forces P_n at the center load surface for each of the two notch angle models. These plots are shown in Figure 30. The nodal forces have been normalized by the total force P as applied by a testing machine. Ideally, the distribution would be constant rather than concentrated as indicated in Figure 30.

Referring back to Figure 1, the total force applied at the inner loading surface is equal to

$$P_{inner} = \frac{Pa}{a - b}$$

where P_{inner} = total force applied at the inner load surface

a = distance between outer loading points

b = distance between inner loading points

Edge crushing had been only a minimal problem with the original test fixture analyzed in the previous study [7]. One of the tasks of the present effort included redesigning the test fixture to move the inner loading points farther from the specimen midline, that is, to increase b. In the original fixture,

$$a = 5.1 \text{ cm } (2 \text{ in})$$

$$b = 0.51 \text{ cm } (0.2 \text{ in})$$

Therefore,

$$P_{inner} = 1.11 \bar{P}$$

In the redesigned fixture,

$$a = 7.6 \text{ cm } (3 \text{ in})$$

$$b = 1.3 \text{ cm } (0.5 \text{ in})$$

Therefore,

$$P_{inner} = 1.20 \bar{P}$$

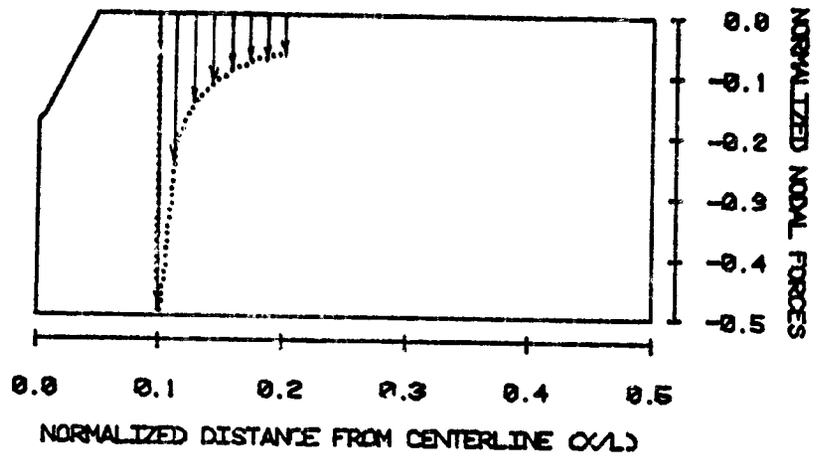

a) 90-Degree Notch Model, P = 180 N (40.8 lb)

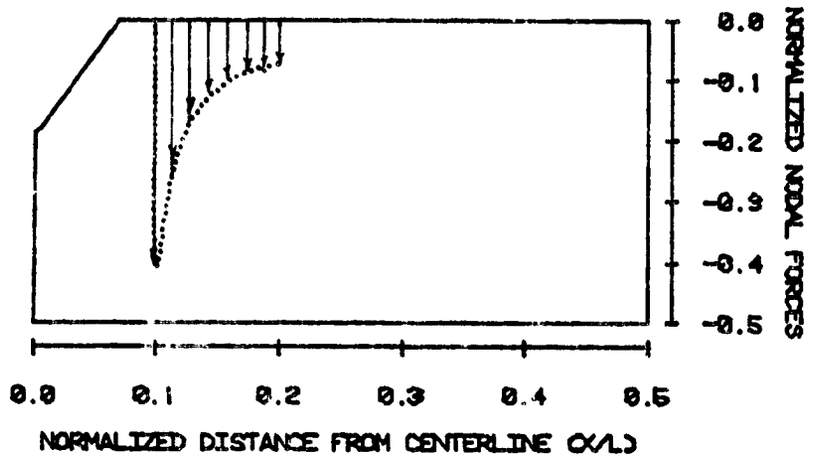

b) 110-Degree Notch Model, P = 220 N (49.4 lb)

Figure 30. Normalized Nodal Force Distributions P_n/P at the Inner Load Surfaces of an AS4/350-6 Graphite/Epoxy Iosipescu Shear Specimen.

Presumably the slight increase in the applied inner load was not the only factor causing the crushing problems in testing unidirectional graphite/epoxy coposite specimens. In rounding the notch root, the depth of the notch was decreased slightly, to less than 20 percent of the width. The combination of slightly increased inner load and slightly increased test width (due to decreased notch depth) may have been enough to cause the crushing failures. It should be noted here that no such problems were encountered in testing the fabric specimens, as will be discussed in Section 3.

Several possible solutions exist to alleviate the edge crushing problem. First, the most obvious solution to the crushing problem is to increase the notch depth, thus decreasing the specimen width in the test section. This will result in lower applied loads for a given shear strength. The previous recommended notch depth was 20 percent of the overall specimen width or height resulting in a test section width equal to 60 percent of the overall specimen width. Iosipescu recommended a notch depth of 22.5 percent of the overall width as being optimum [4]. Notch depths up to 25 percent of the overall width will work as well, at the same time decreasing the applied inner load.

Second, the ends of the specimens could be tabbed or otherwise reinforced, to permit them to better withstand the compressive loading forces. Tabbed specimens are commonly used to measure tensile properties; therefore no new specimen fabrication techniques need be developed. However, this solution results in higher testing costs on a per specimen basis due to higher specimen preparation costs. One of the principal advantages of the Iosipescu shear test is its simplicity of

use; tabbed specimens add additional complications.

A third solution, again involving a change in the test specimen, would be to test $[0/90]_{ns}$ layup materials rather than unidirectional materials. This would theoretically not alter the shear response of the material, but would greatly increase the specimen's resistance to compressive edge loads. One demonstration of this is given by the shear test results for woven graphite/epoxy presented in Section 3 of this report. However, using special layups to measure shear properties with the Iosipescu shear test is no more attractive than having to make special laminates for any other shear test, e.g., using $[\pm 45]_{ns}$ laminates for off-angle shear tests. Again, one major prime advantage of the Iosipescu shear test is the ability to cut a specimen from the same unidirectional panel used to measure the longitudinal or transverse normal properties.

A fourth possibility to prevent crushing of the edges of unidirectional test specimens is to alter the test fixture to help distribute the inner load to keep compressive stresses below the critical level. Ideally, the concentrated load distribution currently present (see Figure 29) should be altered to a constant distribution. The load distribution can be altered by changing the fixture loading surface shape, e.g., using a large radius or a sloped profile. This was modeled analytically and found to be feasible. Practically, however, the dimensional changes required to properly contour the loading surfaces were found to be of the order of 13 μm (0.0005 in). Tolerances on rotation of the moving fixture half are of this order. One other fixture change would be to move the inner load points back towards the midlength of the specimen as in the original design. However, this would

again allow the load-induced compressive stresses to intrude into the test region as was shown previously [7]. Further lengthening of the specimen also provides only minimal relief. A more practical solution is to use a less stiff material at the inner loading surfaces. Deformation of this material would help redistribute the surface loads on the specimen and reduce the likelihood of crushing prior to actual shear failure. Brass inserts 0.05 mm (0.002 in) thick were placed on the inner loading surfaces for the five tests of unidirectional composite to achieve the shear failures represented by Figure 29. Further development of test techniques for measuring unidirectional composite shear properties will continue as part of future work.

To summarize the results discussed in this section, two different notch angles were modeled for isotropic and orthotropic Iosipescu shear test specimens. While notch angle did affect both simulated and actual test results, the differences were not great. It would appear from the finite element analyses that the 110-degree notch Iosipescu shear specimen was better than the 90-degree notch specimen for shear testing orthotropic materials. The 90-degree notch specimen is more accurate for testing isotropic materials, as theory predicts [4]. This was confirmed here in the 6061-T651 aluminum alloy also.

Cracks emanating from the notch roots were evident in the unidirectional graphite/epoxy composite specimens tested. A preliminary analysis of the geometric effect of these cracks indicates that they do not drastically alter the stress state within the test region of the specimen. If anything, these cracks appear to make the shear stress distribution more uniform within the test section.

Finally, an analysis was conducted to define and improve the inner

loading point load distribution. Several possibilities are suggested for eliminating this edge crushing, the most promising being an increase in the notch depth.

SECTION 3

SHEAR PROPERTIES OF WOVEN COMPOSITES

3.1 Test Matrix

The modified Iosipescu shear test fixture was used to measure the in-plane and through-the-thickness (interlaminar) shear properties of three woven fabric T300/934 graphite/epoxy composites. Material coordinates were defined, with the 1-coordinate direction being parallel to the warp direction, the 2-coordinate direction being parallel to the fill direction, and the 3-coordinate direction being perpendicular to the plane of the plate. Shear stresses were defined in the conventional manner, i.e., that is shear stress is applied perpendicular to the first noted coordinate direction, parallel to the second coordinate direction. Thus, a τ_{12} shear test was performed with the shearing load perpendicular to the 1 or warp direction, parallel to the 2 or fill direction. All three fabrics were tested in both of the in-plane shear directions and in two of the possible four interlaminar directions. A matrix of the tests performed on these three fabric composites is presented in Table 4.

The three fabric composites consisted of three different weave patterns as listed in Table 4, viz., an Oxford weave, a 5-harness satin weave, and an 8-harness satin weave. All three laminates were fabricated of Union Carbide T300 graphite fiber and Fiberite 934 epoxy resin. NASA-Langley fabricated the laminates and performed the fiber volume measurements listed in Table 4.

Test specimens were machined by the CMRG at the University of Wyoming using procedures described in Appendix A. In-plane (12 and 21) shear specimens were 7.6 cm (3.0 in) long, 1.91 cm (0.75 in) wide, and

TABLE 4
IOSIPESCU SHEAR TEST MATRIX FOR THREE T300/934
GRAPHITE/EPOXY FABRIC COMPOSITES
(110-DEGREE NOTCH ANGLE SPECIMENS)

Weave Pattern	Fiber Volume (%)	Shear Test Orientation	No. of Shear Tests
Oxford	55.7	12	4
		21	5
		13	5
		23	6
5-Harness Satin	54.8	12	5
		21	6
		13	5
		23	5
8-Harness Satin	56.7	12	5
		21	4
		13	5
		23	5

of as-received thickness, nominally 0.25 cm (0.10 in). Interlaminar Iosipescu shear specimens were 7.6 cm (3.0 in) long, 1.3 cm (0.5 in) wide, and nominally 0.328 cm (0.13 in) thick. The interlaminar specimen width was achieved by stacking layers of the 0.25 cm (0.10 in) thick laminates, bonded together with an epoxy adhesive, as described in Appendix A.

The 110-degree notch angle was used in testing these specimens, machined to a depth equal to 20 percent of the overall width. The analysis indicated that notch angle did not significantly affect test results; the 90-degree notch is the preferred geometry. The 20 percent notch depth was also sufficient; no edge crushing was observed in any of these test specimens.

Each of the woven fabric shear test specimens was instrumented with a Micro Measurements EA-06-062TV-350 strain gage rosette for shear strain measurement. These rosettes measure 1.57 mm x 2.92 mm (0.062 in x 0.115 in) and contain two 350-Ohm strain gages oriented at ±45 degrees. These strain gages were wired in a half-bridge configuration. One instrumented test specimen was shown previously in Figure 15. Testing was performed according to the procedures described in Appendix A.

3.2 Test Results

Averaged shear strengths and shear moduli for the three graphite fabric/epoxy composites are plotted in Figures 31 and 32, respectively, and tabulated in Table 5. Complete results for each individual test specimen are included in Appendix C, including tables of strengths and moduli as well as the shear stress-strain and shear stress-displacement plots.

As shown in Figure 31, the in-plane 12 and 21 shear strengths for

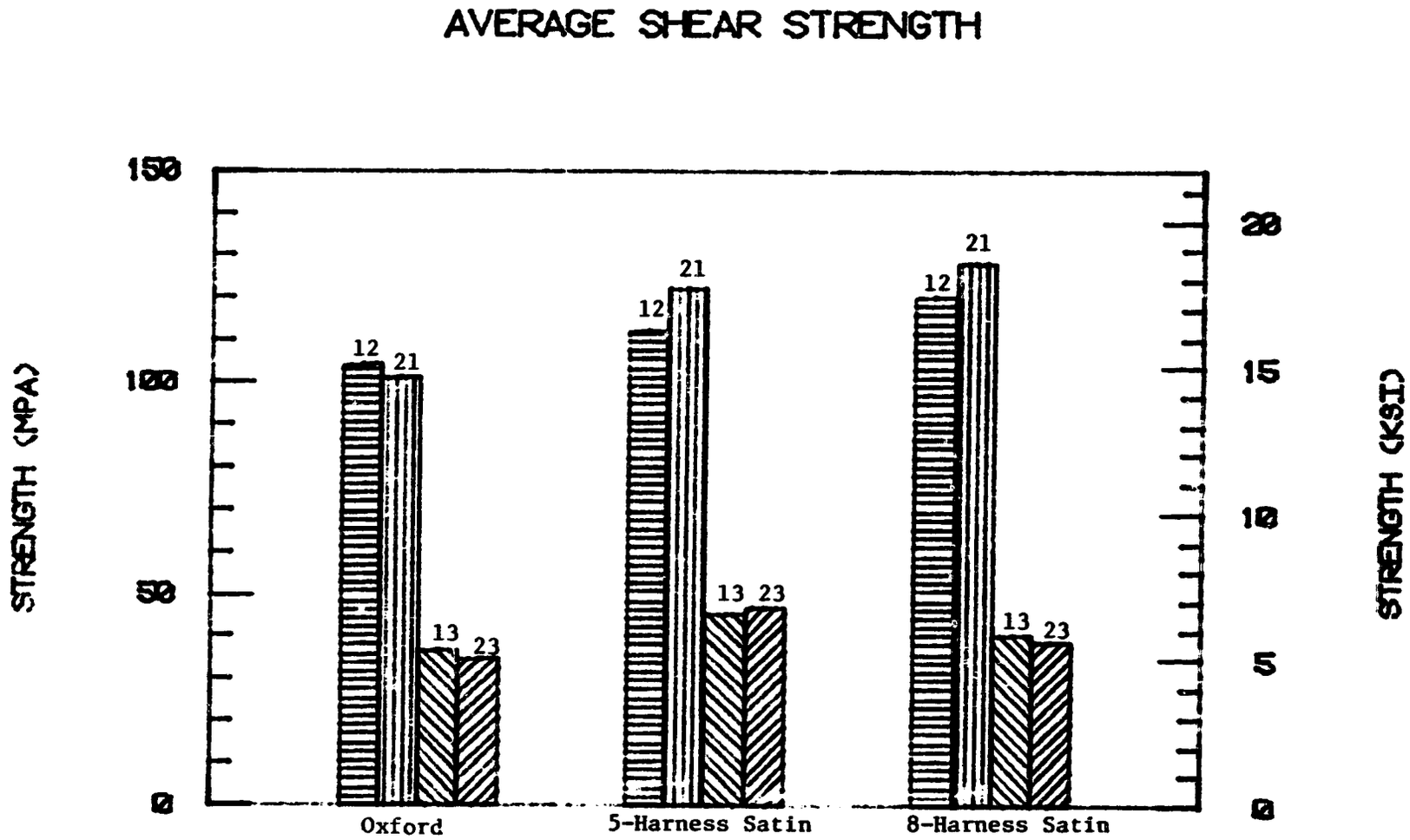

Figure 31. Average In-plane and Interlaminar Shear Strengths for Three T300/934 Graphite/Epoxy Fabric Composites.

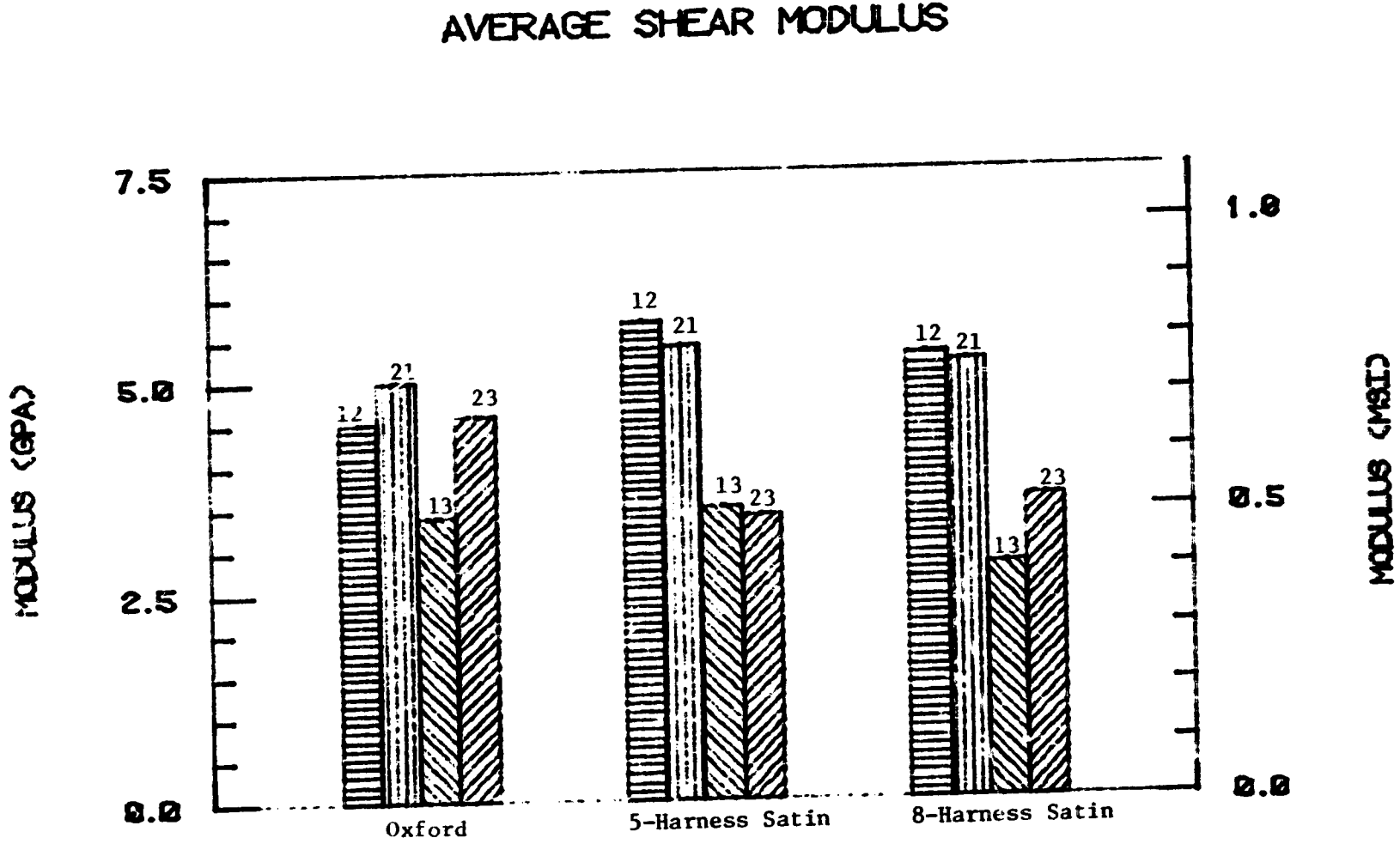

Figure 32. Average In-plane and Interlaminar Shear Moduli for Three T300/934 Graphite/Epoxy Fabric Composites.

TABLE 5
AVERAGE IOSIPESCU SHEAR STRENGTHS AND SHEAR MODULI FOR
T300/934 WOVEN GRAPHITE/EPOXY COMPOSITES

Weave Pattern	Test Orientation	Strength (MPa)	Strength (ksi)	Modulus (GPa)	Modulus (Msi)
Oxford	12	104	15.1	4.5	0.65
	21	101	14.7	5.0	0.72
	13	37	5.31	3.4	0.49
	23	35	5.1	4.6	0.67
5-Harness	12	112	16.2	5.7	0.83
	21	122	17.7	5.4	0.78
	13	46	6.6	3.5	0.51
	23	47	6.8	3.4	0.49
8-Harness	12	120	17.4	5.3	0.77
	21	128	18.6	5.2	0.76
	13	40	5.8	2.8	0.40
	23	39	5.6	3.6	0.52

the Oxford weave material were virtually the same, as would be expected due to stress symmetry considerations. This same consistency was true for the 5-harness and 8-harness weave materials as well. The interlaminar strengths were considerably lower than the in-plane strengths for each material, but again were virtually the same when comparing the 13 and 23 strengths for each material.

Similar results were obtained for the average shear moduli plotted in Figure 32, although there was somewhat more scatter in the data. In-plane (12 and 21) shear moduli were virtually the same for each material. There does at first appear to be some difference between interlaminar (13 and 23) shear moduli for the Oxford and 8-harness weave materials. However, these differences were within the data scatter. Interlaminar (13 and 23) shear moduli for the 5-harness weave material were also virtually identical.

In comparing the three materials to each other, it would appear that there was little difference in interlaminar (13 and 23) shear strength between the three weave patterns, as shown in Figure 31. There does seem to have been a gradual increase in the in-plane shear strengths in going from the Oxford to the 5-harness satin to the 8-harness satin weave materials. The improvement is slight, but apparent, with the 8-harness weave material approaching or equaling the 117 MPa (17 ksi) in-plane shear strength of many unidirectional graphite/epoxy composites [23]. Average shear moduli for the various shear directions were approximately equal among the three different materials, within data scatter.

Shear moduli were calculated in the conventional manner, i.e., as the initial slope of the shear stress-strain curve. However, the

determination of the shear strengths was subject to some interpretation. The major problem involves the definition of shear failure. In fiber-reinforced composite materials, a local shear failure may occur, followed by a local reorientation of the fibers which then begin to load in a tensile mode. These fibers, loading in a tensile mode, prevent ultimate fracture in the test specimen, even though the material has failed locally due to shear stresses.

This type of behavior, i.e., local shear failure followed by fiber reorientation, was evident in the shear stress-strain and shear stress-displacement plots for the three graphite fabric/epoxy composites tested during this program. Representative in-plane shear stress-strain and shear stress-displacement plots are shown in Figure 33 for one of the Oxford-weave test specimens. Similar plots for all of the tested specimens are presented in Appendix C.

The shear stress-strain plots (a typical example being given in Figure 33a), exhibited linear response in only a small initial portion of the test. The shear stress-strain curve was smoothly curved, exhibiting no clearly defined yield point. Strains continued to increase to a value of 6 percent, at which level the maximum shear strain measuring capability of the strain rosette was reached. Stress continued to increase, as indicated by the vertical portion of the stress-strain plot of Figure 33a, until the specimen reached a maximum value and stress dropped.

In studying the shear stress-displacement plot of Figure 33b, it can be seen that the shear stress initially increased smoothly with increasing displacement or crosshead travel of the testing machine. However, beyond approximately 100 MPa (15 ksi) the shear stress remained

NAP124

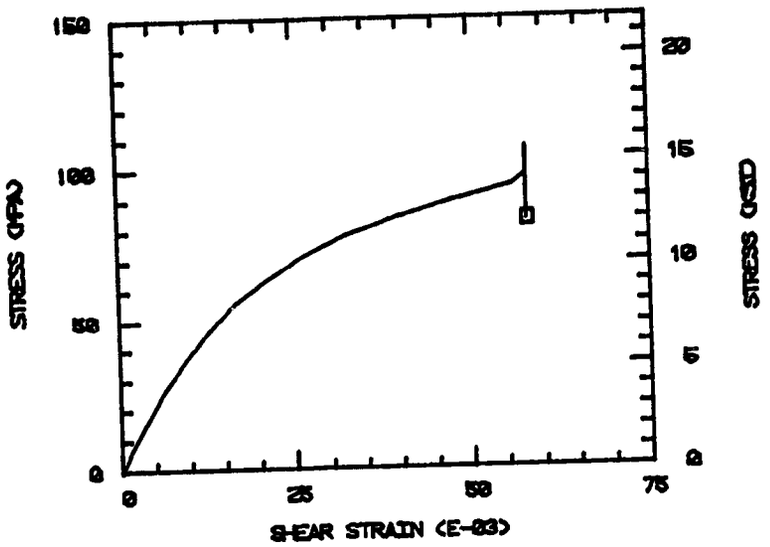

a) Shear Stress-Strain

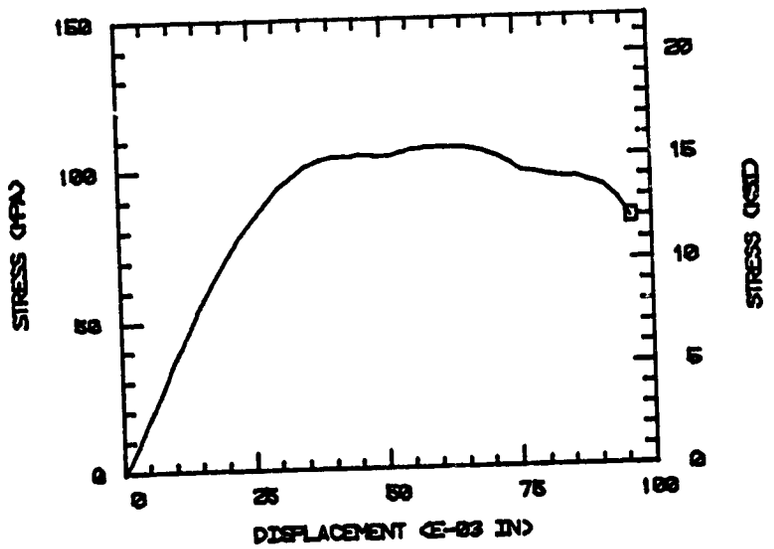

b) Shear Stress-Displacement

Figure 33. Typical In-plane (12) Iosipescu Shear Results for an Oxford Weave T300/934 Graphite/Epoxy Composite, Specimen Number NAP124.

practically constant with increasing displacement for a considerable portion of the curve. Shear stress then began to increase again, reached a maximum, then dropped. The actual shear failure of this material was at the first flattened portion of the shear stress-displacement plot. During that portion of the test the fibers went through some local reorientation, at which time they began to carry a portion of the load in a local tensile stress mode. Overall specimen stress then continued to increase with continued displacement until gross specimen failure occurred. The difference between the interpreted shear failure and the ultimate stress calculated based on the maximum load attained was small for this particular test specimen. However, a much greater difference was encountered when testing interlaminar shear specimens. A similar shear strength definition problem has also been encountered in shear testing glass-reinforced sheet molding compounds, as described in References [9,10]. Strengths reported here for the graphite fabric/epoxy laminates were based on the initial shear stress value prior to fiber reorientation rather than the maximum load attained.

Representative failures for in-plane and interlaminar test specimens are shown for the 8-harness satin-weave material in Figures 34 and 35, respectively. The in-plane (12 and 21) shear failures shown in Figure 34 occurred along a path between the notch roots. Failure in both instances appeared to be on the 21 shear plane, as indicated by the horizontal cracks shown in Figure 34a and the vertical cracks shown in Figure 34b. Failures in the interlaminar (13 and 23) specimens, such as shown in Figure 35, occurred between the notch roots and consisted of cracks perpendicular to the direction of shear loading, marked by arrows in Figure 35. Some cracks also occurred in the bond lines between

a) In-Plane (12) Shear Orientation

b) In-Plane (21) Shear Orientation

Figure 34. Typical Failures for In-Plane Iosipescu Shear Test Specimens of 8-Harness Satin-Weave T300/934 Graphite/Epoxy Composite.

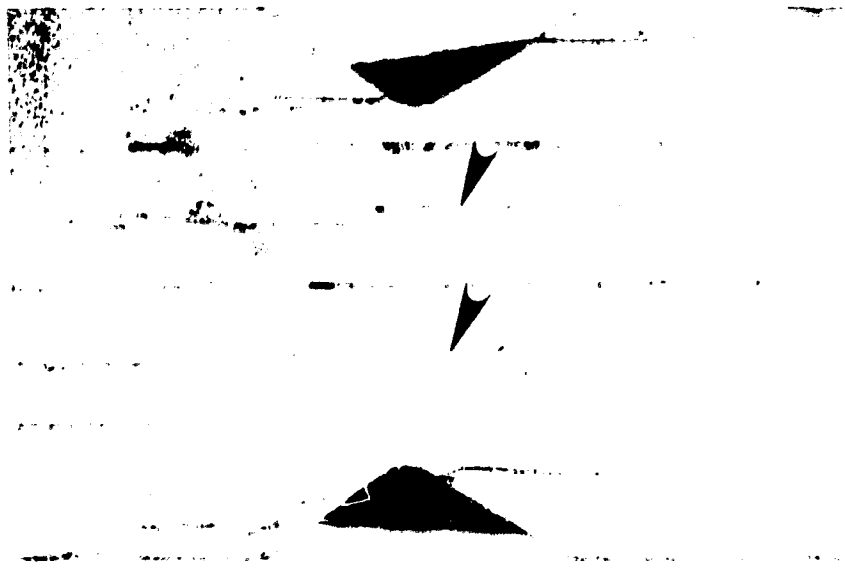

a) Interlaminar (13) Shear Orientation

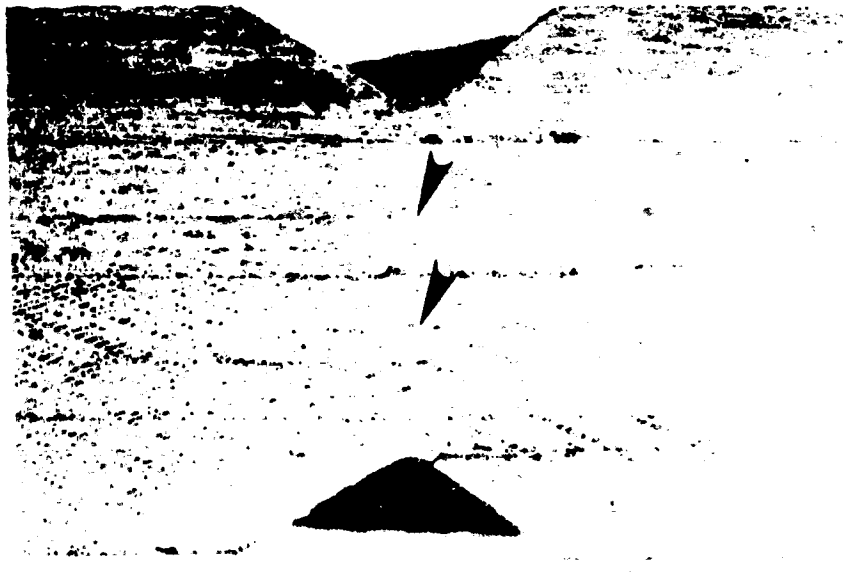

b) Interlaminar (23) Shear Orientation

Figure 35. Failed Interlaminar Iosipescu Shear Test Specimens of 8-Harness Satin-Weave T300/934 Graphite/Epoxy Composite.

various laminate layers. It will be recalled that layers were stacked to achieve the desired specimen width for the interlaminar shear specimens. In future work, particularly for 3-D weave patterns, the stacking of layers to achieve a desired interlaminar shear specimen thickness will probably not be practical. Laminates will have to be fabricated to the desired thickness (laminate thickness being interlaminar shear specimen width). The newer Iosipescu shear fixture will accommodate specimens of various widths, as described in Appendix A.

Overall, a representative and consistent set of shear properties, including both in-plane and interlaminar properties, was obtained for each of the three different weave patterns. The different weave geometries did not appear to greatly alter the shear properties of the material, although slight differences in in-plane shear strength were observed.

The Iosipescu shear test method performed very well in measuring the in-plane shear properties of the three materials, and reasonably well in measuring the interlaminar properties. In future test work, it would be desirable to cut interlaminar Iosipescu shear specimens of woven composites from thicker laminates rather than from bonded, stacked sheets of thinner laminates.

SECTION 4

CONCLUSIONS

Overall, most project objectives were achieved during this second-year research effort. The Iosipescu shear test fixture was completely redesigned, incorporating some of the following features:

a) Inner loading surfaces were moved farther from the test region.

b) Test specimen size was increased by 50 percent to provide more room for shear strain measurement instrumentation.

c) A clamping mechanism was incorporated to remove the necessity for strict tolerances on specimen width, resulting in less expensive specimen fabrication.

d) The test fixture now will accommodate a range of specimen widths.

Fixture drawings, specimen fabrication methods, and testing procedures are all included in Appendix A.

A finite element analysis was performed to determine the stress state within two different Iosipescu shear test specimen geometries. These specimens were also analyzed to determine the feasibility and potential accuracy of using gages or a modified extensometer for shear strain measurement. It was found that the notch angle does affect the stress state within the test region, as would be expected. Results

indicated that a 90-degree notch is the most suitable angle for testing isotropic materials, but a 110-degree notch may be more suitable for shear testing of highly orthotropic unidirectional composite materials. However, the difference is small.

Both a modified extensometer and strain gage rosettes were found, analytically, to be suitable for measuring shear strain in the Iosipescu specimen. Strain gage rosettes have proven very usable in past work, and were used extensively in this present program as well. However, they lack sufficient shear strain measurement range for highly nonlinear shear behavior, as in shear testing at elevated temperatures. Work is proceeding to design a suitable attachment mechanism for the modified extensometer to take advantage of its greater shear measurement range.

Some preliminary work was done to model the effect of cracks at the notch roots, observed in tests of unidirectional graphite/epoxy laminates. It was found that the cracks did not significantly alter the shear stress distribution within the test region of the specimen; if anything the shear stress distribution was improved. This cracking is apparent only in shear testing of unidirectional composites and was not a factor in tests of the woven fabric materials.

In-plane and interlaminar shear properties were measured for three fabric-reinforced graphite/epoxy composites. The three different weave geometries performed essentially the same in shear. However, the 5-harness and 8-harness satin-weave materials did exhibit slightly higher in-plane shear strengths then the Oxford weave material.

Work to be accomplished in the third year of this program includes shear properties measurement for a wider variety of weave patterns. In a

parallel task, development will continue on the modified extensometer as a shear strain transducer. Although little further analytical work is planned, analyses do exist for modeling these woven composite materials to study the effects of weave geometry on the various material properties. The same 3-D finite element program and associated plotting software used in the present study to model the Iosipescu shear test specimen could also be used to perform micromechanics studies of woven fabric composites. These analytical efforts may be further explored as time permits.

REFERENCES

1. Arcan, M. and Goldenberg, N., "On a Basic Criterion for Selecting a Shear Testing Standard for Plastic Materials," (In French) ISO/TC 61-WG 2 SP. 171, Burgenstock-Switzerland, 1957.

2. Goldenberg, N., Arcan, M. and Nicolau, E., "On the Most Suitable Specimen Shape for Testing Shear Strength of Plastics," International Symposium on Plastics Testing and Standardization, ASTM STP 247; American Society for Testing and Materials, 1958, pp. 115-121.

3. Arcan, M., Hashin, Z. and Voloshin, A., "A Method to Produce Uniform Plane-stress States with Applications to Fiber-reinforced Materials," Experimental Mechanics, Vol. 18, No. 4, 1978, pp. 141-146.

4. Iosipescu, N., "New Accurate Procedure for Single Shear Testing of Metals," Journal of Materials, Vol. 2, No. 3, September 1967, pp. 537-666.

5. Slepetz, J. M., Zagaeski, T. F. and Novello, R. F., "In-plane Shear Test for Composite Materials," Report No. AMMRC TR 78-30, Army Materials and Mechanics Research Center, Watertown, Massachusetts, July 1978.

6. Walrath, D. E. and Adams, D. F., "The Iosipescu Shear Test as Applied to Composite Materials," Experimental Mechanics, Vol. 23, No. 1, March 1983, pp. 105-110.

7. Walrath, D. E. and Adams, D. F., "Analysis of the Stress State in an Iosipescu Shear Test Specimen," Report UWME-DR-301-102-1, Department of Mechanical Engineering, University of Wyoming, Laramie, Wyoming, June 1983.

8. Adams, D. F. and Walrath, D. E., "Iosipescu Shear Properties of SMC Composite Materials", Composite Materials: Testing and Design (Sixth Conference), ASTM STP 787, 1982, pp. 19-33.

9. Walrath, D. E. and Adams, D. F., "Shear Strength and Modulus of SMC-R50 and XMC-3 Composite Materials," Report UWME-DR-004-105-1, Department of Mechanical Engineering, University of Wyoming, Laramie, Wyoming, March 1980.

10. Walrath, D. E., and Adams, D. F., "Static and Dynamic Shear Testing of SMC Composite Materials," Report UWME-DR-004-103-1, Department of Mechanical Engineering, University of Wyoming, Laramie, Wyoming, May 1980.

11. Walrath, D. E. and Adams, D. F., "Damage Mechanisms/Failure Mechanics of Carbon-Carbon Composite Materials," Report UWME-DR-904-101-1, Department of Mechanical Engineering, University of Wyoming, Laramie, Wyoming, September, 1979.

12. Monib, M. M. and Adams, D. F., "Three-Dimensional Elastoplastic Finite Element Analysis of Laminated Composites," Report UWME-DR-001-102-1, University of Wyoming, Department of Mechanical Engineering, November 1980.

13. Grimes, G. C., Adams, D. F. and Dusablon, E. G., "The Effects of Discontinuities on Compression Fatigue Properties of Advanced Composites," Northrop Technical Report NOR 80-158, Naval Air Systems Command, Contracts N00019-79-C-0275 and N00019-79-C-0276, October 1980.

14. Ramkumar, R. L., Grimes, G. C., Adams, D. F. and Dusablon, E. G., Effects of Materials and Processes Defects on the Compression Properties of Advanced Composites," Northrop Technical Report NOR 82-103, Naval Air Systems Command, Contracts N00019-80-C-0484 and N00019-80-C-0490, May 1982.

15. Adams, D. F., Ramkumar, R. L. and Walrath, D. E., "Analysis of Porous Laminates in the Presence of Ply Drop-offs and Fastener Holes," Northrop Technical Report NOR 84-113, Naval Air Systems Command Contracts N00019-82-C-0156 and N00019-82-C-0063, May 1984.

16. Bergner, Jr. H. W., Davis, Jr. J. G. and Herakovich, C. T., "Analysis of Shear Test Method for Composite Laminates," Report VPI-E-77-14, Virginia Polytechnic Institute and State University, Blacksburg, Virginia, April 1977.

17. Herakovich, C. T. and Bergner, Jr. H. W., "Finite Element Stress Analysis of a Notched Coupon Specimen for In-plane Shear Behavior of Composites," Composites, July 1980, pp. 149-154.

18. Wang, S. S., Goetz, D. P. and Corten, H. T., "Shear Fatigue Degradation and Fracture of Random Short-Fiber SMC Composite," Journal of Composite Materials, Vol. 18, January 1984, pp. 2-20.

19. Marloff, R. H., "Finite Element Analysis of Biaxial Stress Test Specimen for Graphite/Epoxy and Glass Fabric/Epoxy Composites," Composite Materials: Testing and Design (Sixth Conference), ASTM STP 787, 1982, pp. 34-49.

20. Metals Handbook, Volume 2 - Properties and Selection: Nonferrous Alloys and Pure Metals, Ninth Edition, American Society for Metals, 1979.

21. Renton, W. J. and Ho, T., "The Effect of Environment on the Mechanical Behavior of AS/3501-6 Graphite/Epoxy Material," Final Phase I Report, NASC Contract No. N00019-77-C-0369, June 1978.

22. Knight, M., "The Determination of Interlaminar Moduli of Graphite/Epoxy Composites," 5th Mechanics of Composites Review, Dayton, Ohio, 1981.

23. Grimes, G. C. and Adams, D. F., "Investigation of Compression Fatigue Properties of Advanced Composites," Northrop Technical Report NOR-79-17, Naval Air Systems Command Contracts N00019-77-C-0518 and N00019-77-C-0519, October 1979.

APPENDICES

APPENDIX A

IOSIPESCU SHEAR TEST PROCEDURES

A.1. Test Fixture

The Iosipescu shear test fixture is designed to test flat specimens nominally 7.62 cm (3 in) long, nominally 1.91 cm (0.75 in) wide, and up to 1.27 cm (0.5 in) thick. A test fixture is shown in Figure A1. This test fixture is designed to be used in a testing machine set up in a compression mode. The fixture can be inserted between two flat compression plattens. However, it is usually more convenient to attach the right fixture half to the upper testing machine load surface using the center hole provided in the fixture. This fixture has been loaded to 22 kN (5000 lbs) applied force without damage to the fixture.

Machine drawings of this test fixture are included as Figures A2 through A6. All parts are fabricated from low carbon cold rolled steel with the exception of the linear bushing and post. These items are manufactured by Thompson Industries, Manhasset, New York, and may be purchased from any of their distributors.

The fixture as shown in Figure A1 is designed to test specimens nominally 1.91 cm (0.75 in) in width. The wedge clamp blocks allow approximately 1 mm (0.04 in) variation on that width. Only light clamping is required, to ensure that no specimen rotation takes place during the test. Narrower specimens may be tested by using thicker wedges, changing the height dimension of the wedge in Figure A3.

A.2. Test Specimen Fabrication

Iosipescu shear specimens for use with the present test fixture are

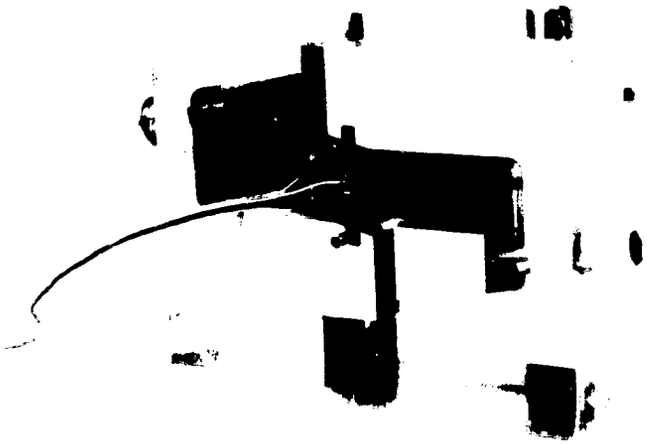

Figure A1. Iosipescu Shear Test Fixture

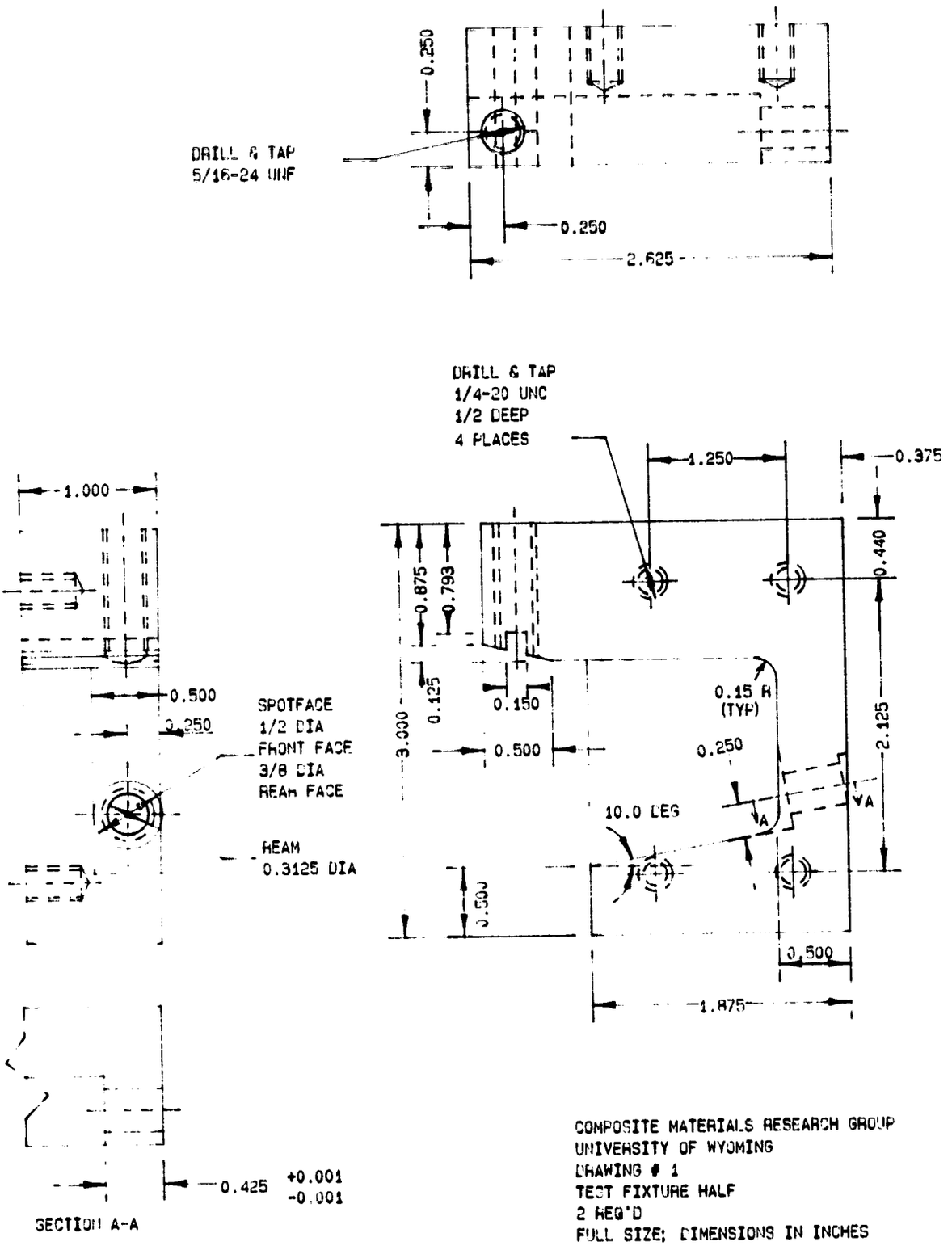

Figure A2. Iosipescu Shear Test Fixture Half

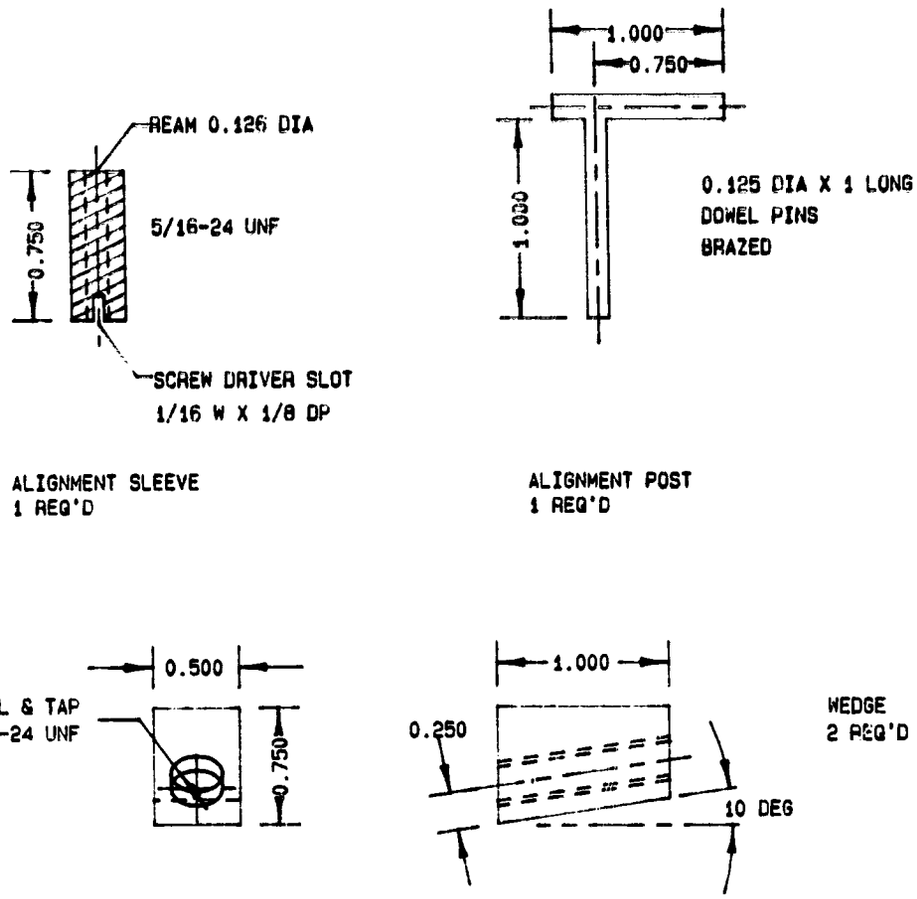

Figure A3. Iosipescu Shear Test Fixture Alignment Tool Assembly and Clamp Assembly.

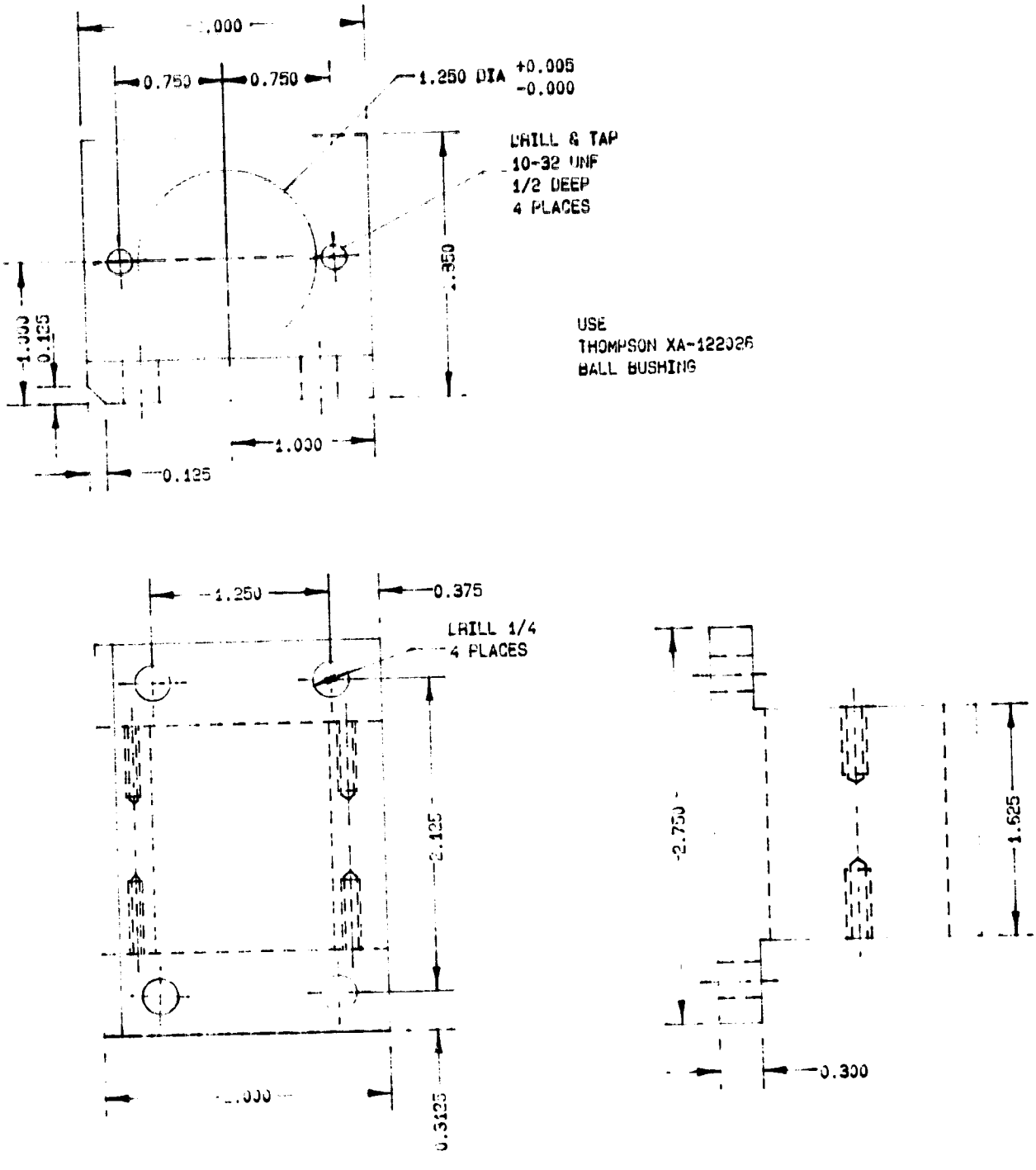

COMPOSITE MATERIALS RESEARCH GROUP
UNIVERSITY OF WYOMING
DRAWING # 3
RIGHT SIDE SUPPORT ASSEMBLY
1 REQ'D
FULL SIZE; DIMENSIONS IN INCHES

Figure A4. Iosipescu Shear Test Fixture Bearing Mounting Assembly.

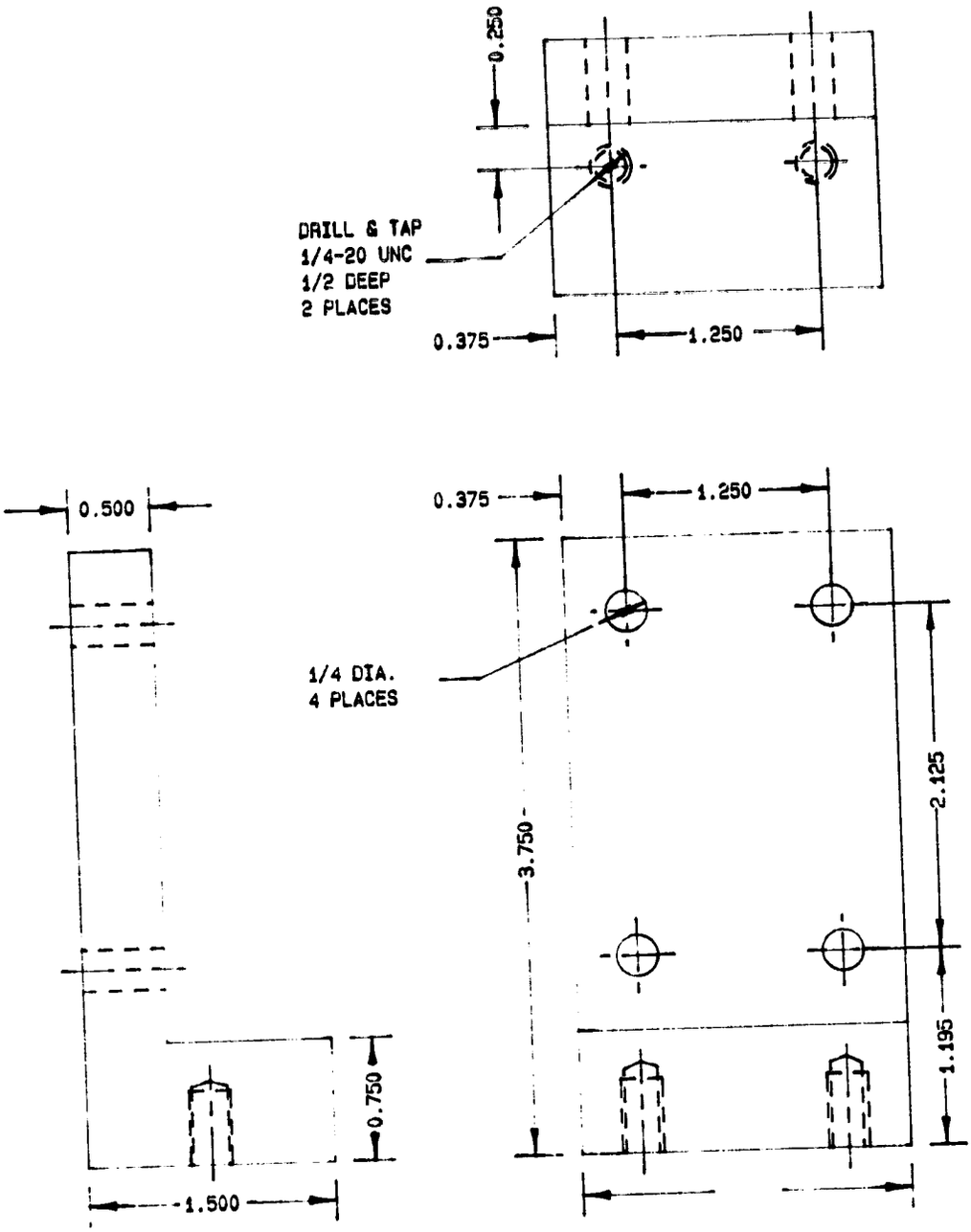

Figure A5. Iosipescu Shear Test Fixture Fixed Half Mounting Bracket.

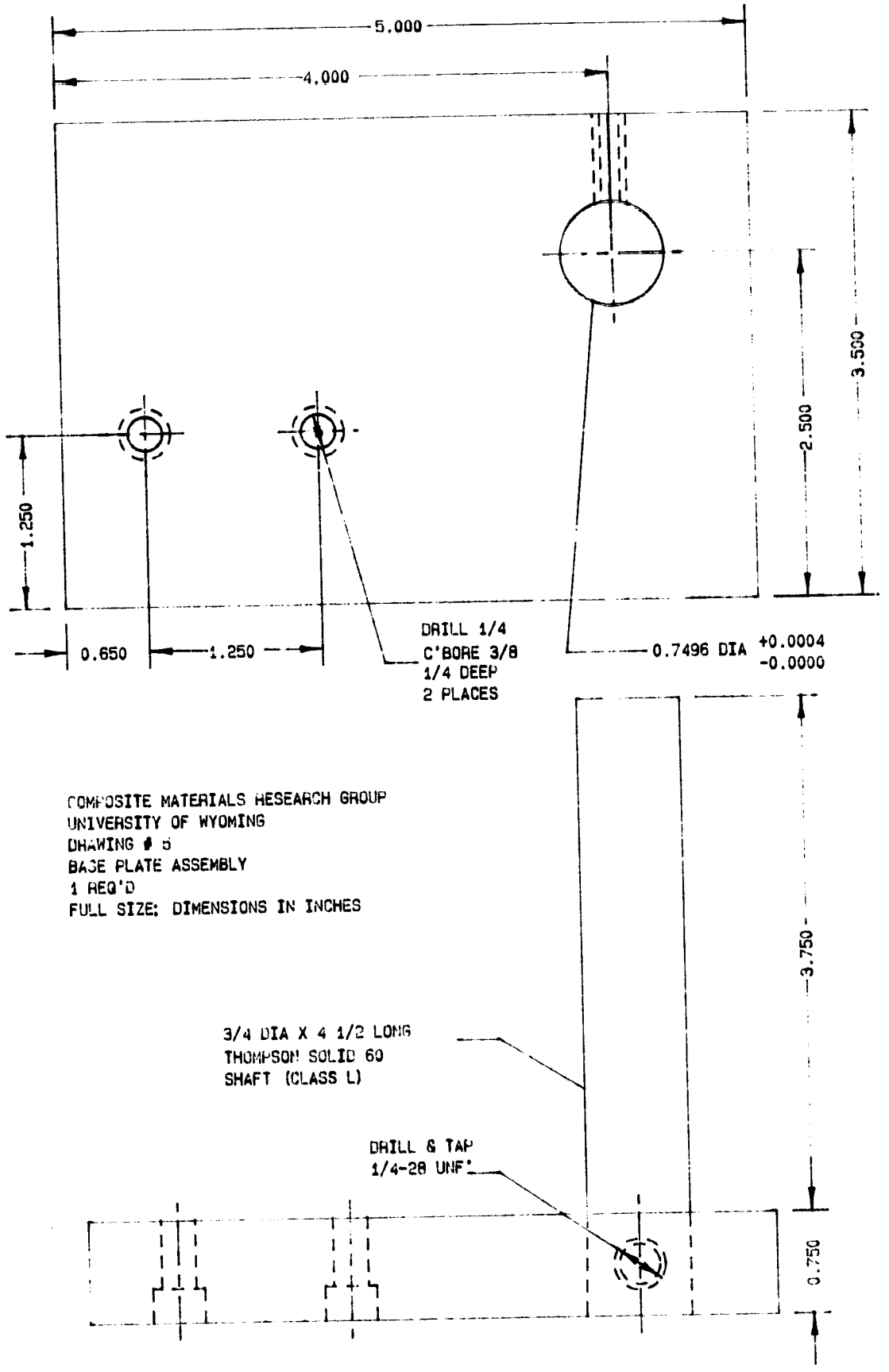

Figure A6. Iosipescu Shear Test Fixture Base and Post Assembly

7.62 cm (3 in) long, 1.91 cm (0.75 in) wide, and of any thickness up to 1.27 cm (0.5 in) thick, as shown in Figure A7. Very thin specimens may be tested, but care must be taken to ensure compressive buckling does not occur. This can be done with bonded tabs or backup plates.

Composite specimens are typically cut with diamond abrasive tooling; metal specimens are typically prepared using conventional metalworking tools. Notches are ground in the composite specimens using a 60-grit abrasive wheel in a standard surface or tool grinder. This wheel is dressed to grind the prescribed notch angle and root radius shown in Figure A7. Care must be taken to avoid delaminating specimens. Stacking and clamping specimens has been found to be effective. Notches are usually cut in metal specimens with a 90° milling cutter with proper root radius ground onto the cutter if possible.

Shear tests may be performed with the Iosipescu shear fixture in any of the six material shear coordinate planes. It is conventional to define a material coordinate system where the 1-coordinate is parallel to the principal in-plane material direction, the 2-coordinate is the other in-plane axis, and the 3-coordinate is perpendicular to the plane of the plate. The shear stress is then defined as being applied perpendicular to the first coordinate, parallel to the second. Therefore 12 and 21 are the in-plane shear components while the interlaminar shear components are denoted 13, 31, 23, and 32. Specimens to impose any one of these six shear components can be fabricated from thin laminates by stacking and bonding sufficient layers of the laminated plate to obtain the desired specimen width, as indicated in Figure A8. An in-plane 12 or 21 specimen is simply cut from the plate, as shown in Figure A8a. Interlaminar shear specimens 13, 31, 23, or 32 are cut from thick plates

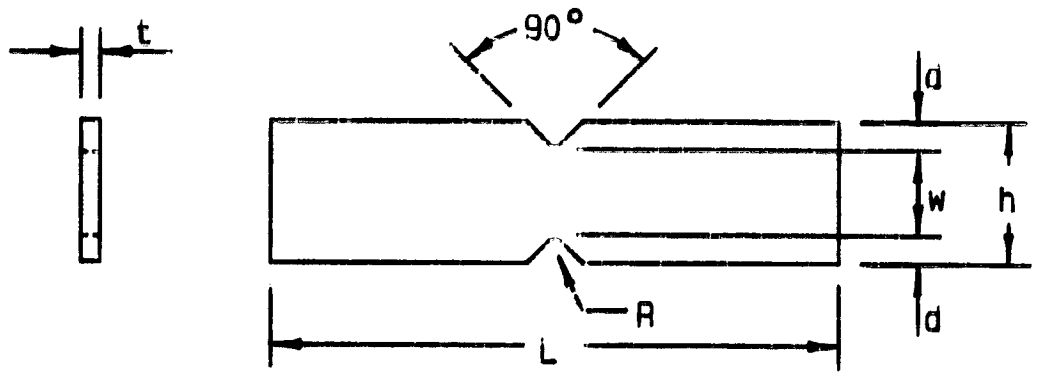

Figure A7. Iosipescu Shear Test Specimen

t = 1.27 cm (0.5 in)
h = 1.91 cm (0.75 in)
d = 0.38 cm (0.15 in)
L = 7.62 cm (3.0 in)
r = 0.13 cm (0.05 in)

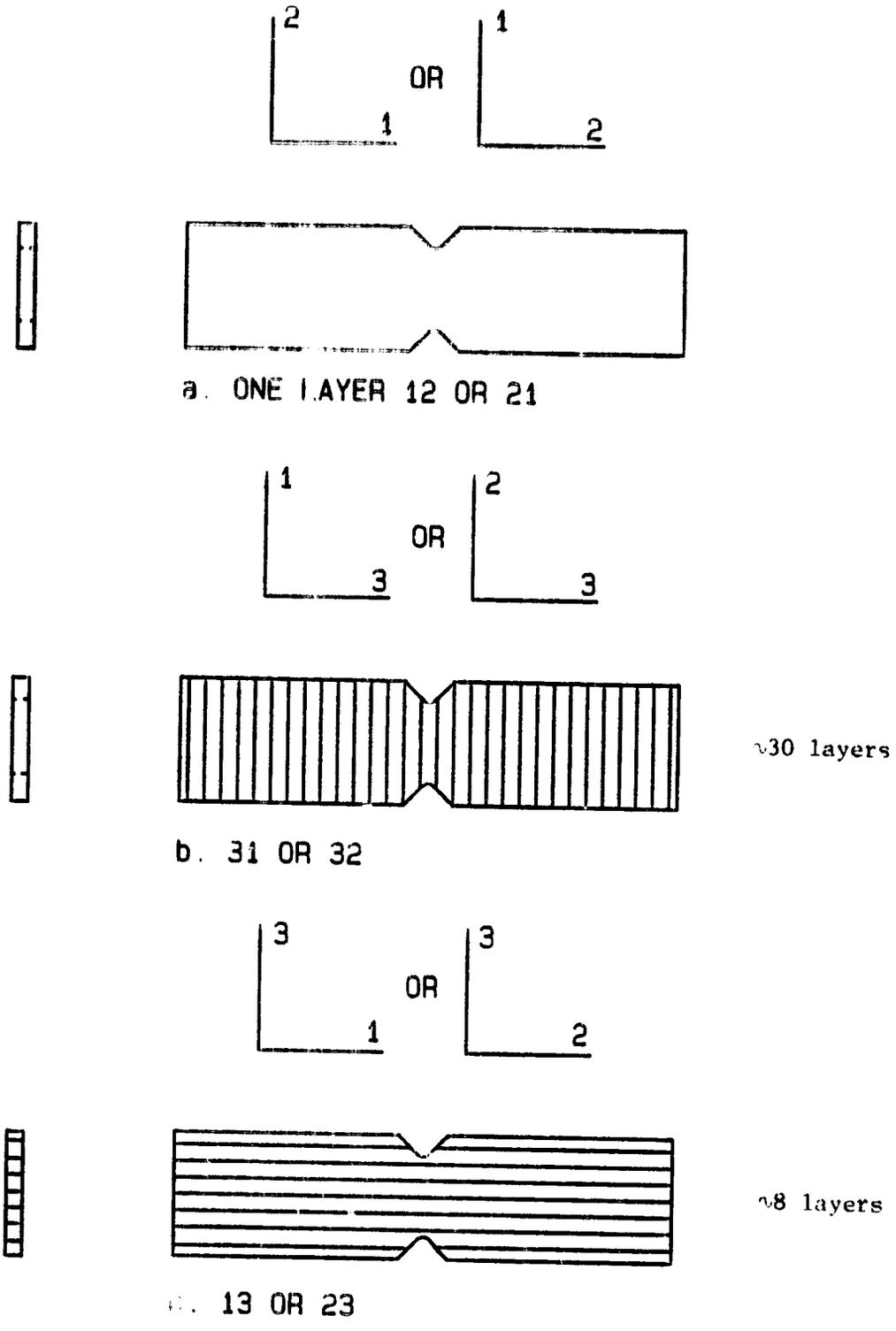

Figure A8. Iosipescu Shear Test Specimen Configurations Assuming t = 2.5 mm (0.1 in)

formed by stacking and bonding sufficient layers of the thinner plates to obtain the desired thickness, as shown in Figures A8b and A8c. However, the specimen type depicted in Figure A8b has been shown to be very fragile [9,10], producing poor results, and is therefore not recommended. The specimen type of Figure A8c is preferred.

Specimens may be instrumented with strain gages, as shown in Figure 9, or a modified extensometer may be used, as shown in Figure A10. Further discussion of these shear strain methods may be found in Reference [7]. A more convenient mechanism for attaching an extensometer to measure shear strains in the Iosipescu shear test specimen is currently being designed.

Test Procedures

Specimens should be centered in the test fixture using the lift-up alignment tool to index on the lower specimen notch. The wedge clamps are then tightened to hold the specimen firmly in place. These clamps need only be tightened "finger tight". The objective is to prevent the specimen from rotating during the test. Over tightening the wedge clamps may result in excessive transverse compression loading of the specimen.

Tests may be performed at any desired loading rate. A convenient quasi-static rate is 1 mm/min (0.04 in/min). Cyclic loading is also possible by making appropriate provisions for attaching the fixture in the test machine.

Shear stresses are calculated by dividing the applied load P by the cross-sectional area between the notch tips, i.e.,

$$\tau = \frac{P}{wt}$$

Ultimate shear strength is not necessarily related to the maximum force reached, as discussed in References [7,9,10]. During and after actual

shear failure, the reinforcing fibers in a composite material may reorient, subsequently bearing some portion of the applied force in a tensile mode. The point at which this happens can usually be determined from a load (stress) versus displacement plot, examples of which are shown in Figure 33. The point at which the stress-displacement plot abruptly changes slope is the point at which shear failure occurs. Fiber reorientation does not necessarily occur in all composites; ultimate stress may be the actual shear strength in some cases. Test results should be carefully interpreted.

APPENDIX B

ALUMINUM ALLOY AND UNIDIRECTIONAL GRAPHITE/EPOXY COMPOSITE IOSIPESCU SHEAR TEST DATA

TABLE B1
SHEAR STRENGTH AND SHEAR MODULUS FOR 6061-T651
ALUMINUM ALLOY IOSIPESCU SHEAR SPECIMENS

Specimen No.	Notch Angle (Degrees)	Strength (MPa)	Strength (ksi)	Modulus (GPa)	Modulus (Msi)
1	90	221	32.0	25.5	3.70
2		213	30.9	25.0	3.62
3		217	31.5	25.5	3.70
4		221	32.1	27.2	3.95
5		220	32.0	24.4	3.54
Avg.		219	31.7	25.5	3.70
Std. Dev.		3	0.5	1.1	0.15
1	110	225	32.6	23.3	3.38
2		219	31.8	22.1	3.20
3		218	31.6	22.9	3.32
4		220	32.0	21.7	3.15
5		223	32.3	21.5	3.12
Avg.		221	32.1	22.3	3.23
Std. Dev.		3	0.4	0.8	0.11

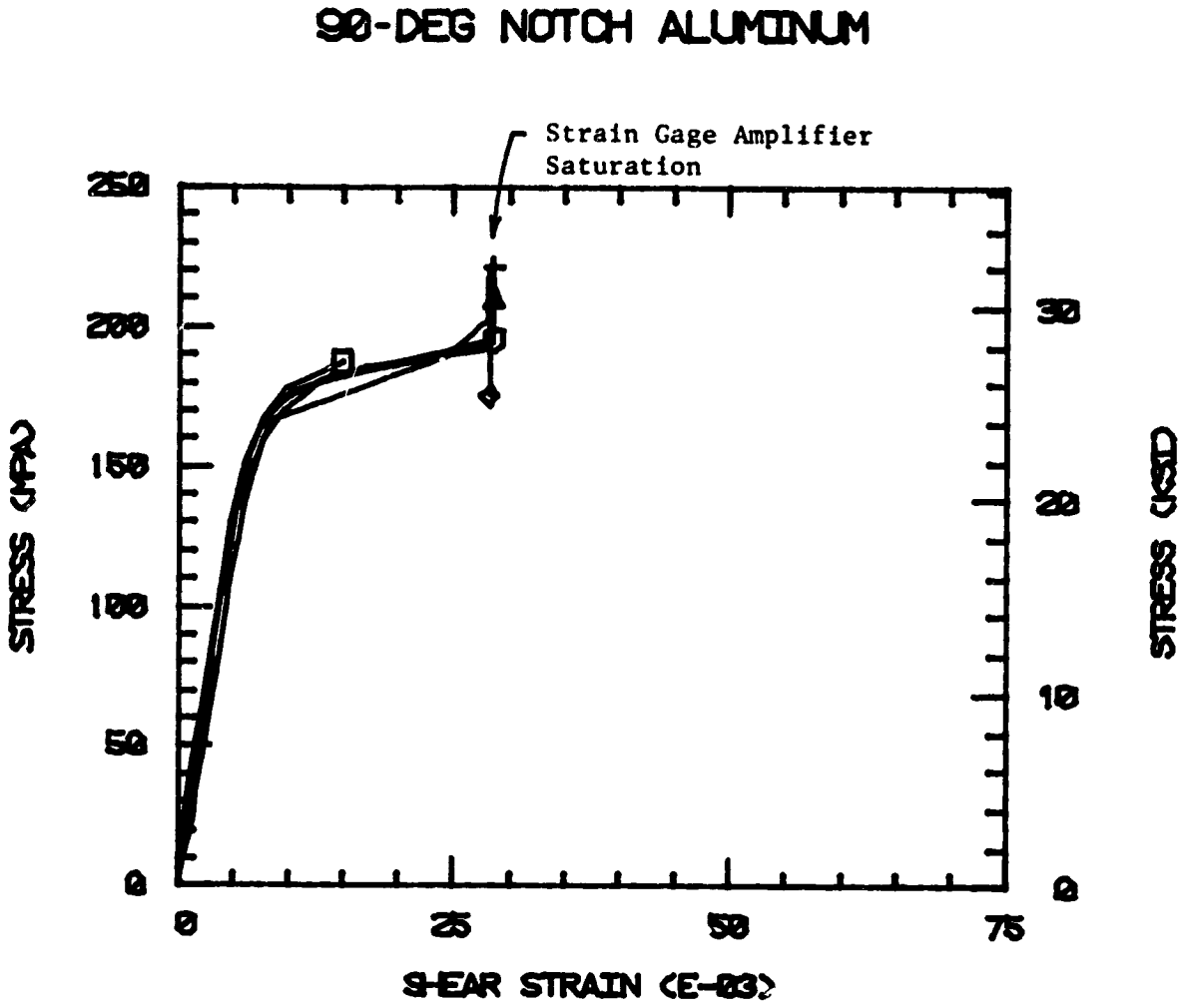

Figure B1. Iosipescu Shear Stress-Strain Results for 6061-T651 Aluminum Using a 90-Degree Notch Specimen.

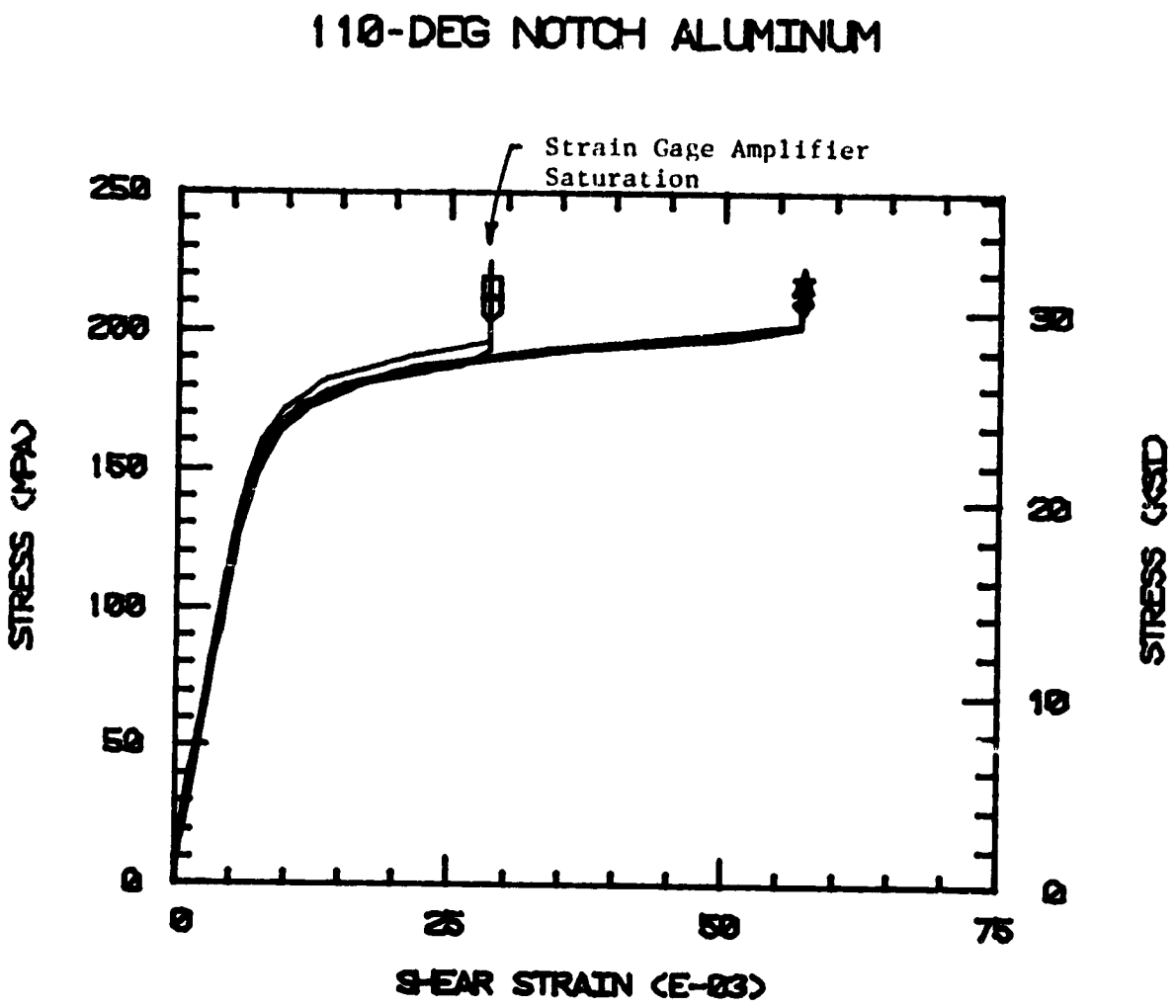

Figure B2. Iosipescu Shear Stress-Strain Results for 6061-T651 Aluminum Using a 110-Degree Notch Specimen.

TABLE B2
SHEAR STRENGTH AND SHEAR MODULUS FOR $[0]_{8T}$
AS4/3501-6 GRAPHITE/EPOXY COMPOSITE

Orientation	Specimen No.	Strength (MPa)	Strength (ksi)	Modulus (GPa)	Modulus (Msi)
12	1	101	14.6	6.5	0.95
	2	112	16.3	6.0	0.87
	3	108	15.6	5.8	0.84
	4	114	16.5	8.1*	1.17*
	5	104	15.1	5.3	0.77
	Avg.	108	15.6	5.9	0.85
	Std. Dev.	6	0.8	0.5	0.07

*not included in average

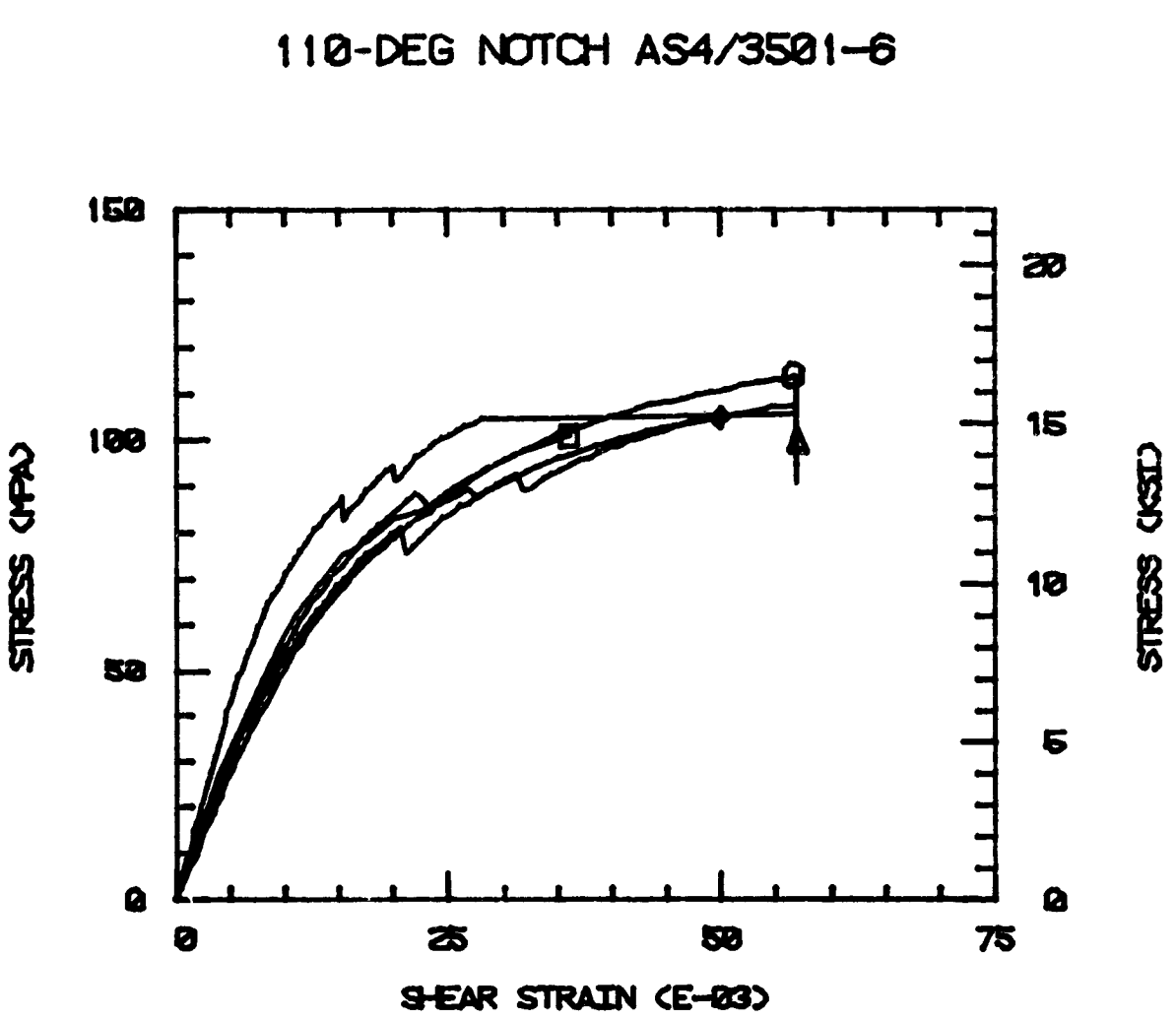

Figure B3. Iosipescu Shear Stress-Strain Results for $[0]_{8T}$ AS4/3501-6 Graphite/Epoxy. Composite Using a 110-Degree Notch Specimen.

APPENDIX C

GRAPHITE FABRIC/EPOXY COMPOSITE

IOSIPESCU SHEAR TEST DATA

TABLE C1
SHEAR STRENGTH AND SHEAR MODULUS FOR OXFORD-WEAVE
T300/934 GRAPHITE/EPOXY COMPOSITE

Test Orientation	Specimen No.	Strength (MPa)	Strength (ksi)	Modulus (MPa)	Modulus (Msi)
12	2	103	15.0	4.3	0.63
	3	106	15.3	4.7	0.68
	4	105	15.2	4.8	0.69
	5	104	15.1	4.2	0.62
	Avg.	104	15.1	4.5	0.65
	Std. Dev.	1	0.1	0.3	0.04
21	1	100	14.5	4.6	0.67
	2	100	14.5	4.7	0.68
	3	98	14.2	5.4	0.78
	4	103	15.0	5.2	0.75
	5	104	15.1	5.0	0.72
	Avg.	101	14.7	5.0	0.72
	Std. Dev.	3	0.4	0.3	0.05
13	1	40.4	5.86	3.7	0.54
	2	35.3	5.12	3.3	0.48
	3	39.0	5.66	3.0	0.44
	4	36.1	5.24	3.0	0.44
	5	33.0	4.78	3.7	0.54
	Avg.	36.8	5.33	3.4	0.49
	Std. Dev.	3.0	0.43	0.3	0.05
23	1	31.2	4.53	3.2*	0.46*
	2	31.3	4.54	4.2	0.61
	3	35.4	5.13	4.8	0.69
	4	35.2	5.10	4.7	0.68
	6	36.1	5.23	4.7	0.68
	7	40.2	5.83	3.4*	0.49*
	Avg.	34.9	5.06	4.6	0.67
	Std. Dev.	3.4	0.49	0.3	0.04

*not included in average

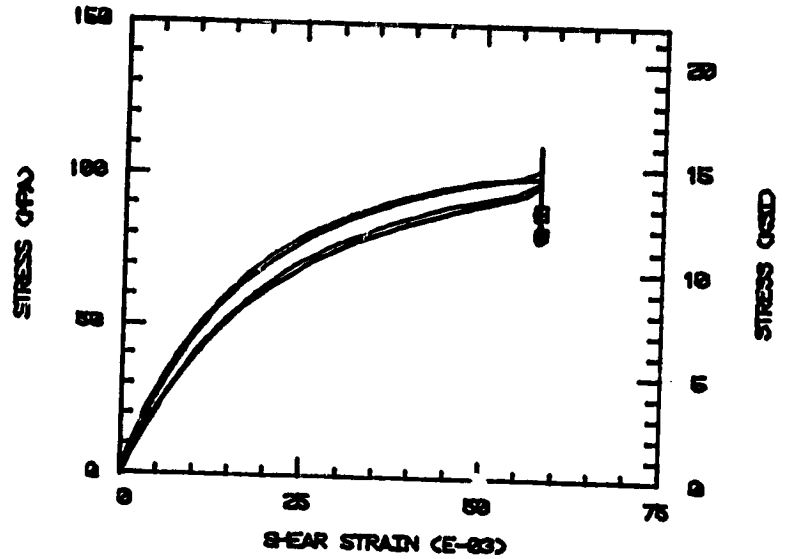

a) Stress-Strain

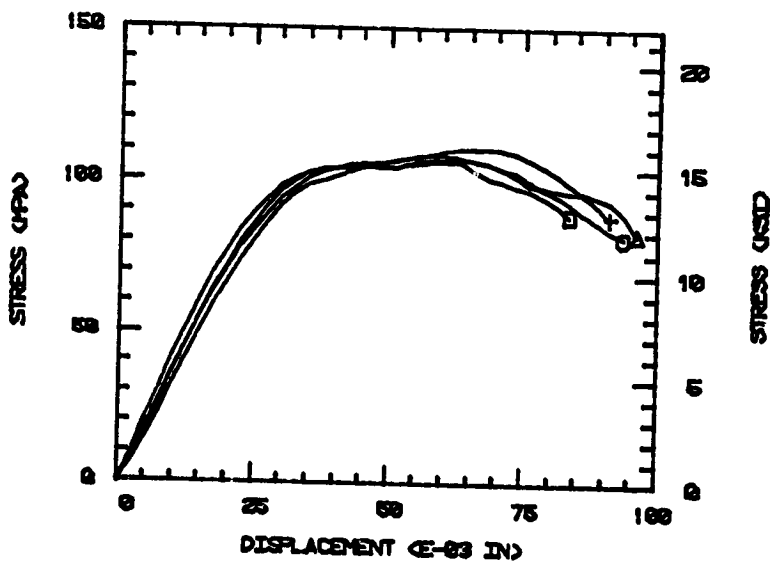

b) Stress-Displacement

Figure C1. In-plane (12) Iosipescu Shear Results for Oxford-Weave T300/934 Graphite/Epoxy Composite.

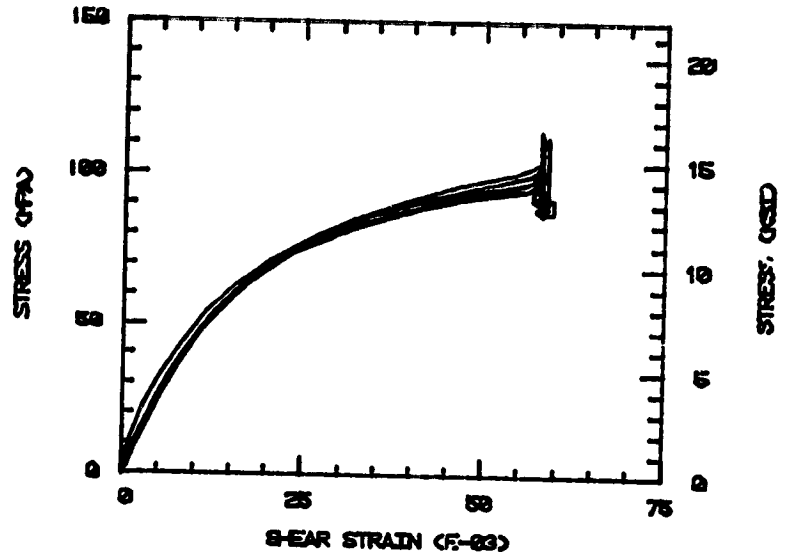

a) Stress-Strain

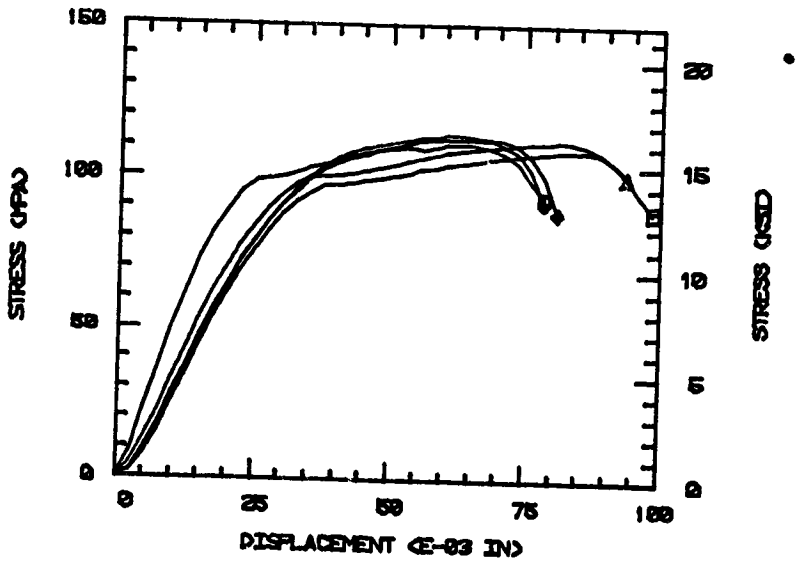

b) Stress-Displacement

Figure C2. In-plane (21) Iosipescu Shear Results for Oxford-Weave T300/934 Graphite/Epoxy Composite.

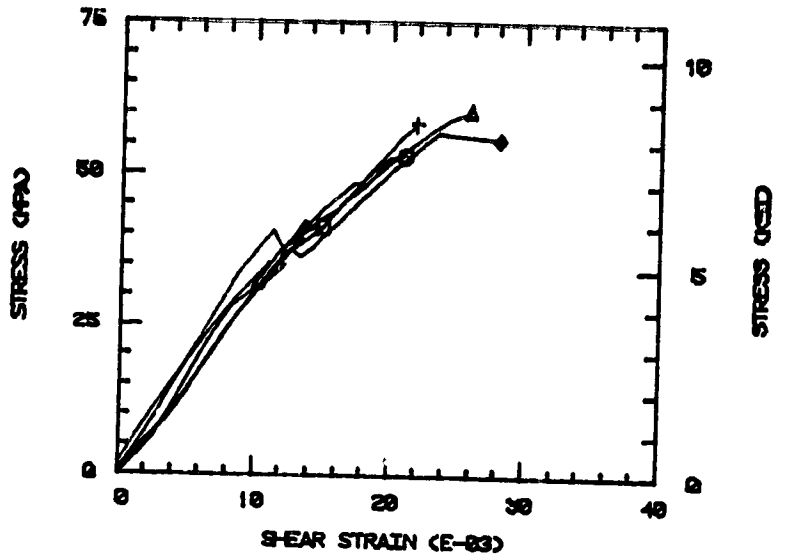

a) Stress-Strain

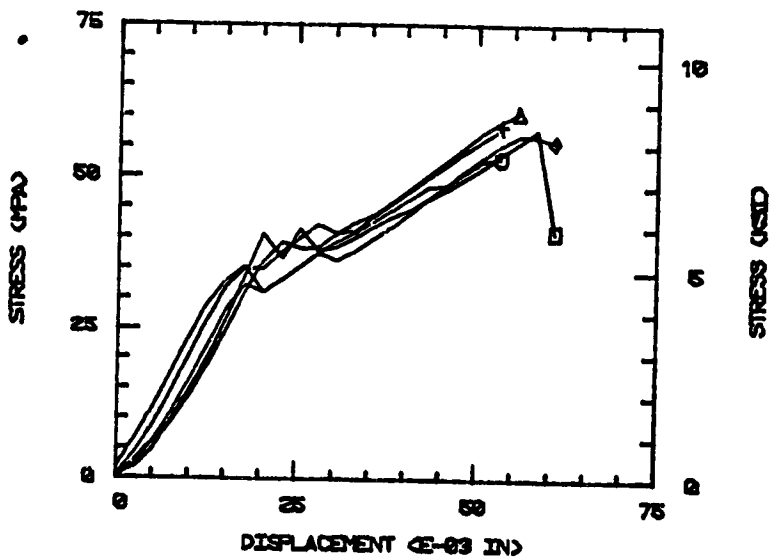

b) Stress-Displacement

Figure C3. Interlaminar (13) Iosipescu Shear Results for Oxford-Weave T300/934 Graphite/Epoxy.

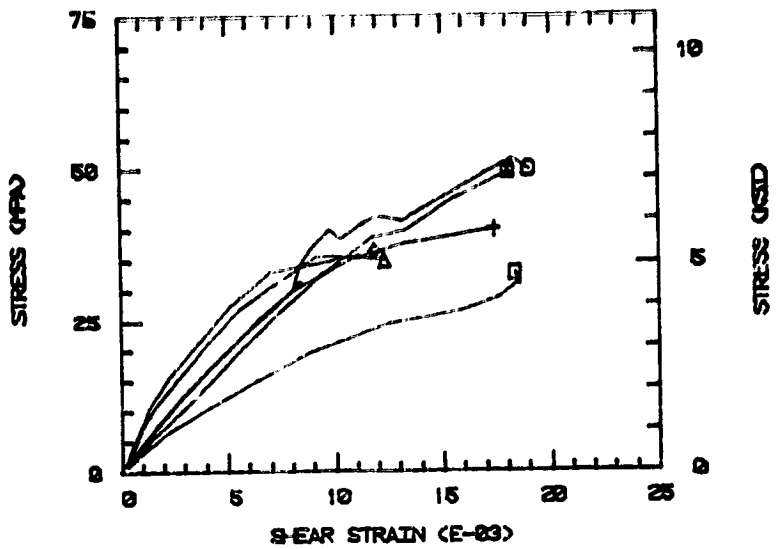

a) Stress-Strain

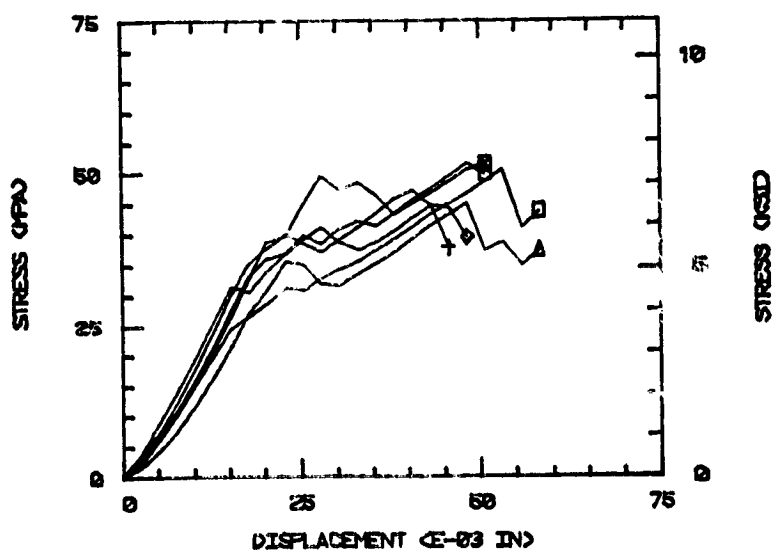

b) Stress-Displacement

Figure C4. Interlaminar (23) Iosipescu Shear Results for Oxford-WeaveT300/934 Graphite/Epoxy.

TABLE C2
SHEAR STRENGTH AND SHEAR MODULUS FOR 5-HARNESS
SATIN-WEAVE T300/934 GRAPHITE/EPOXY COMPOSITE

Test Orientation	Specimen No.	Strength (MPa)	Strength (ksi)	Modulus (GPa)	Modulus (Msi)
12	1	107	15.5	5.2	0.76
	2	115	16.7	5.8	0.84
	3	112	16.2	5.9	0.86
	4	115	16.7	5.7	0.83
	5	111	16.1	6.0	0.87
	Avg.	112	16.2	5.7	0.83
	Std. Dev.	3	0.5	0.3	0.04
21	1	119	17.3	5.5	0.80
	2	129	18.7	5.2	0.75
	3	125	18.1	5.7	0.82
	4	125	18.1	4.8	0.70
	5	116	16.8	6.1	0.88
	6	119	17.2	4.9	0.71
	Avg.	122	17.7	5.4	0.78
	Std. Dev.	5	0.7	0.5	0.07
13	1	36.1*	5.23*	3.0	0.44
	2	45.9	6.65	2.9*	0.43*
	3	51.6*	7.49*	3.9*	0.57*
	5	46.3	6.72	3.6	0.52
	6	43.6	6.33	3.9	0.56
	Avg.	45.3	6.57	3.5	0.51
	Std. Dev.	1.4	0.21	0.4	0.06
23	1	47.6	6.90	2.9	0.42
	2	41.2	5.97	3.2	0.47
	3	49.0	7.11	3.8	0.55
	4	50.4	7.31	3.2	0.46
	5	45.8	6.64	3.7	0.54
	Avg.	46.8	6.79	3.4	0.49
	Std. Dev.	3.6	0.52	0.4	0.06

*not included in average

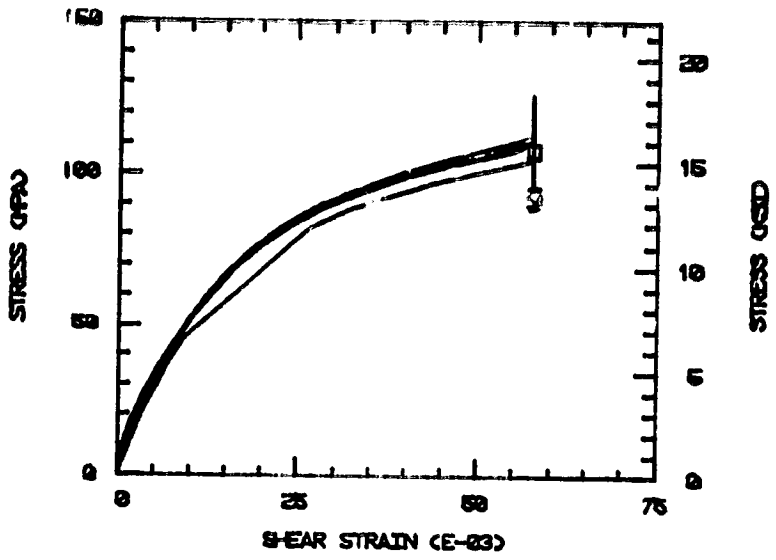

a) Stress-Strain

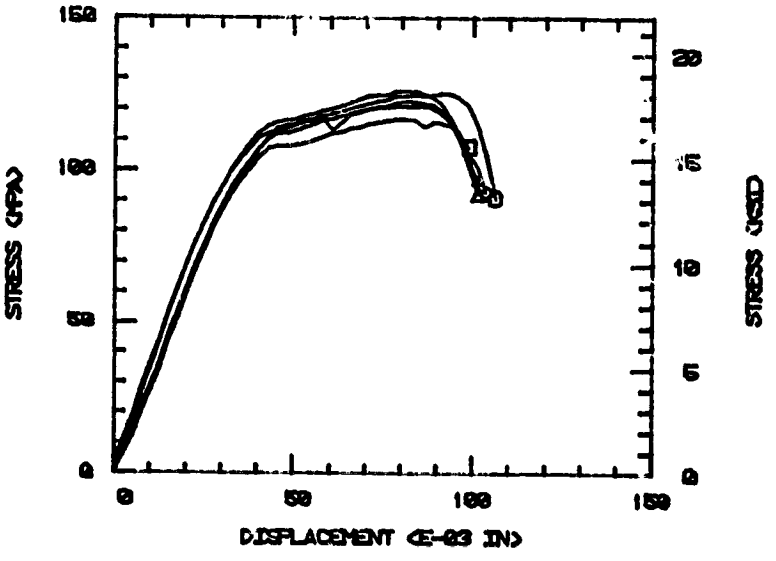

b) Stress-Displacement

Figure C5. In-plane (12) Iosipescu Shear Results for 5-Harness Satin-Weave T300/934 Graphite/Epoxy Composite.

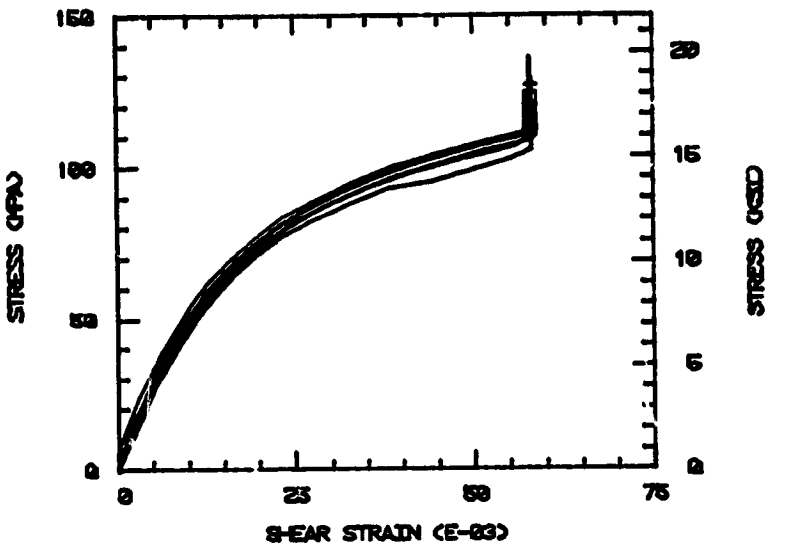

a) Stress-Strain

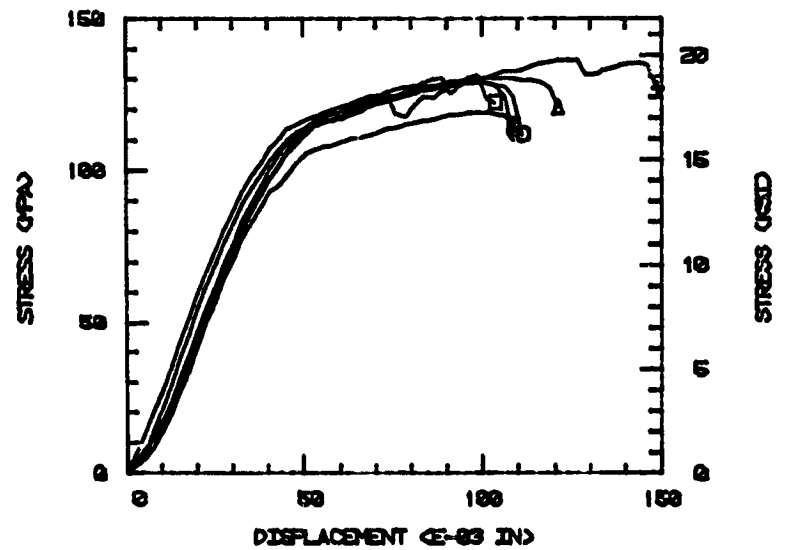

b) Stress-Displacement

Figure C6. In-plane (21) Iosipescu Shear Results for 5-Harness Satin-Weave T300/934 Graphite/Epoxy Composite.

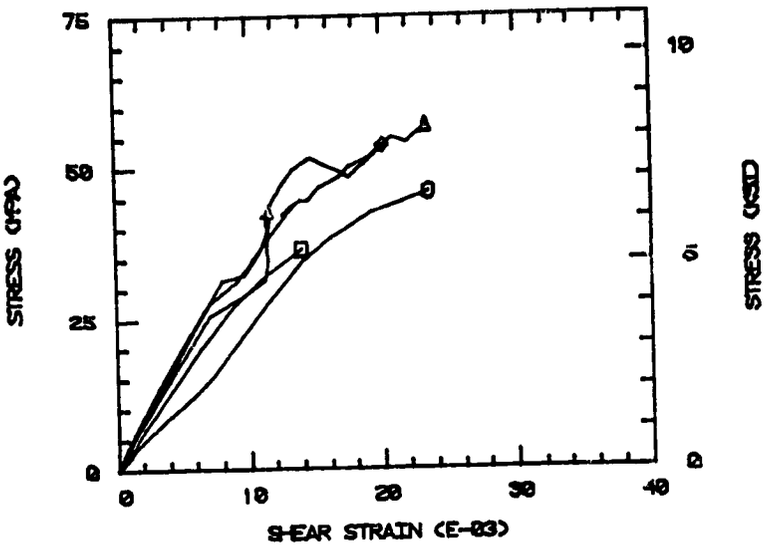

a) Stress-Strain

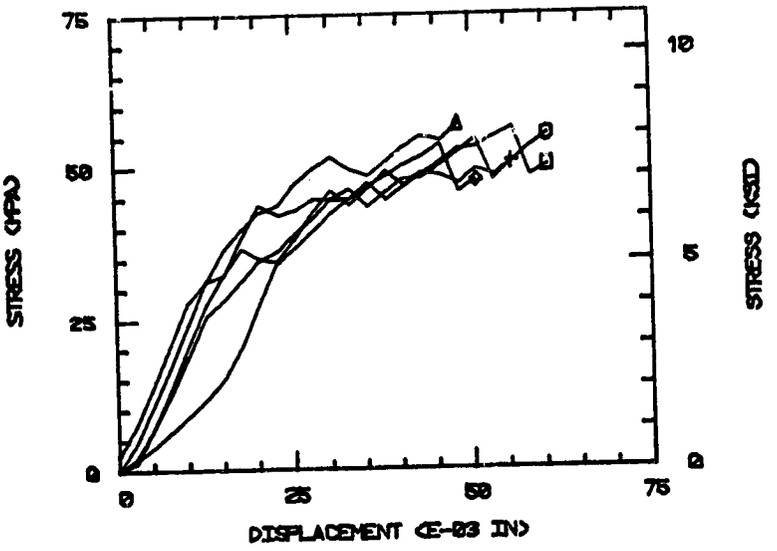

b) Stress-Displacement

Figure C7. Interlaminar (13) Iosipescu Shear Results for 5-Harness Satin-Weave T300/934 Graphite/Epoxy Composite.

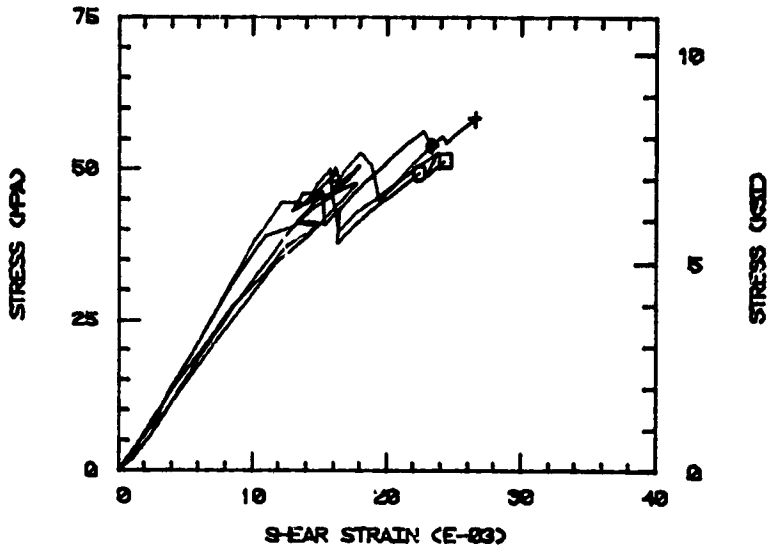

a) Stress-Strain

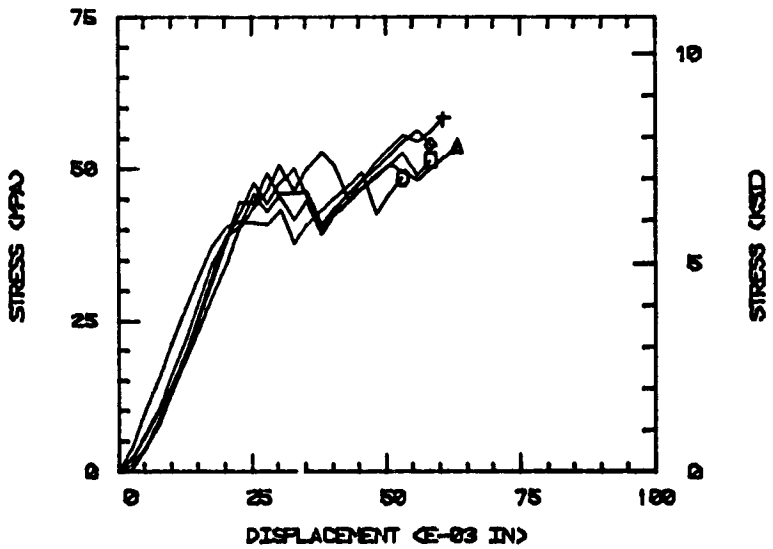

b) Stress-Displacement

Figure C8. Interlaminar (23) Iosipescu Shear Results for 5-Harness Satin-Weave T300/934 Graphite/Epoxy Composite.

TABLE C3
SHEAR STRENGTH AND SHEAR MODULUS FOR 8-HARNESS
SATIN-WEAVE T300/934 GRAPHITE/EPOXY COMPOSITE

Test Orientation	Specimen No.	Strength (MPa)	Strength (ksi)	Modulus (GPa)	Modulus (Msi)
12	1	120	17.5	6.0	0.87
	2	121	17.6	5.6	0.81
	3	120	17.5	5.1	0.74
	4	122	17.7	5.0	0.73
	5	114	16.5	4.8	0.70
	Avg.	120	17.4	5.3	0.77
	Std. Dev.	3	0.5	0.5	0.07
21	2	107	15.5	5.2	0.76
	3	108	15.7	5.1	0.75
	4	150	21.8	5.7	0.82
	5	148	21.5	4.8	0.70
	Avg.	128	18.6	5.2	0.76
	Std. Dev.	24	3.5	0.3	0.05
13	1	35.7	5.18	2.8	0.40
	2	41.4	6.00	2.5	0.36
	3	44.6	6.47	3.1	0.45
	4	36.2	5.25	3.7*	0.54*
	5	42.3	6.13	2.3*	0.33*
	Avg.	40.1	5.81	2.8	0.40
	Std. Dev.	3.9	0.57	0.3	0.05
23	1	36.2	5.25	3.0	0.43
	2	28.4*	4.12*	3.7	0.53
	3	37.3	5.41	3.8	0.56
	4	42.0	6.09	3.9	0.57
	5	47.0*	6.82*	2.8*	0.41*
	Avg.	38.5	5.58	3.6	0.52
	Std. Dev.	3.1	0.45	0.4	0.06

*not included in average

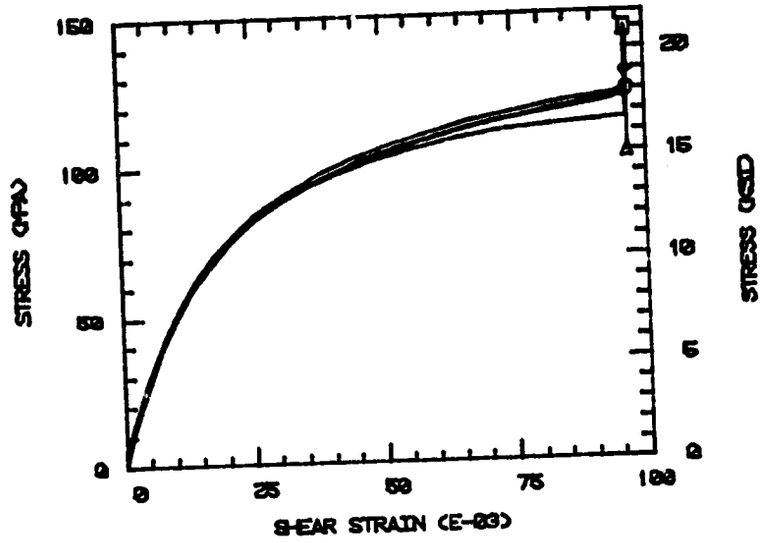

a) Stress-Strain

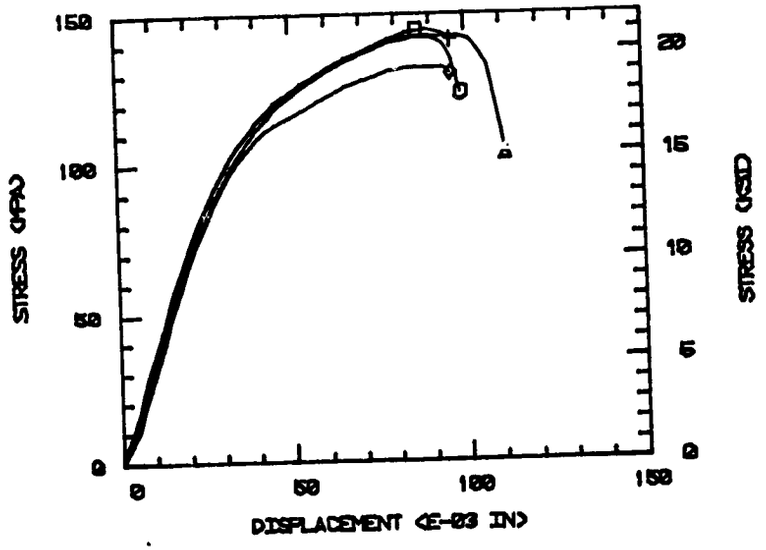

b) Stress-Displacement

Figure C9. In-plane (12) Iosipescu Shear Results for 8-Harness Satin-Weave T300/934 Graphite/Epoxy Composite.

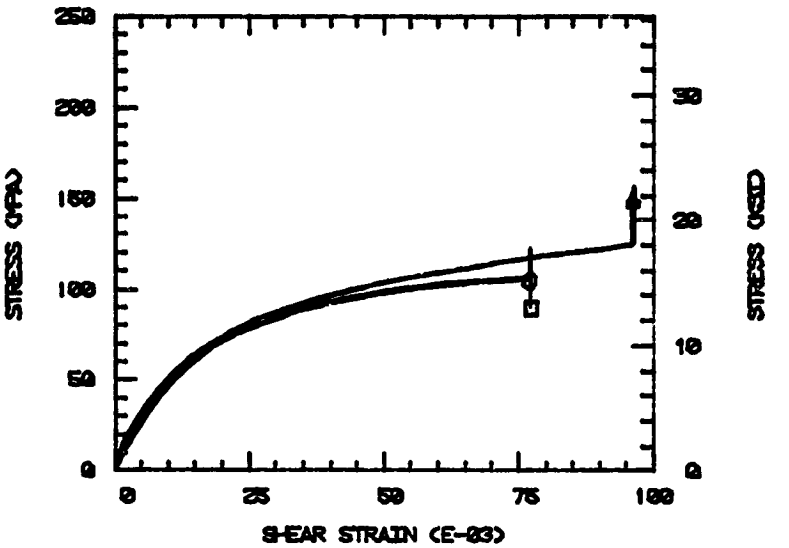

a) Stress-Strain

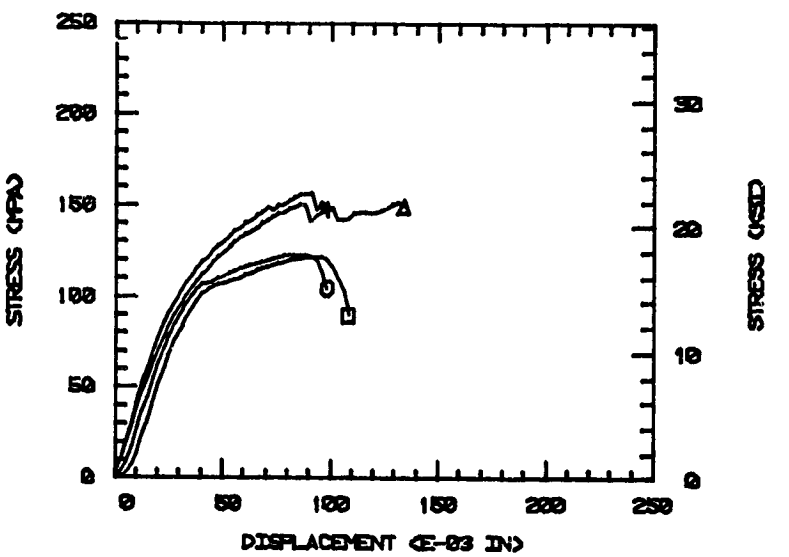

b) Stress-Displacement

Figure C10. In-plane (21) Iosipescu Shear Results for 8-Harness Satin-Weave T300/934 Graphite/Epoxy Composite.

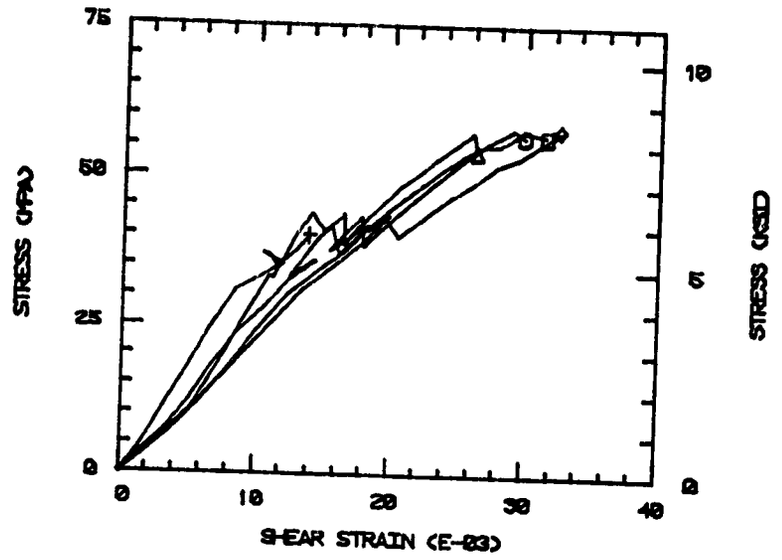

a) Stress-Strain

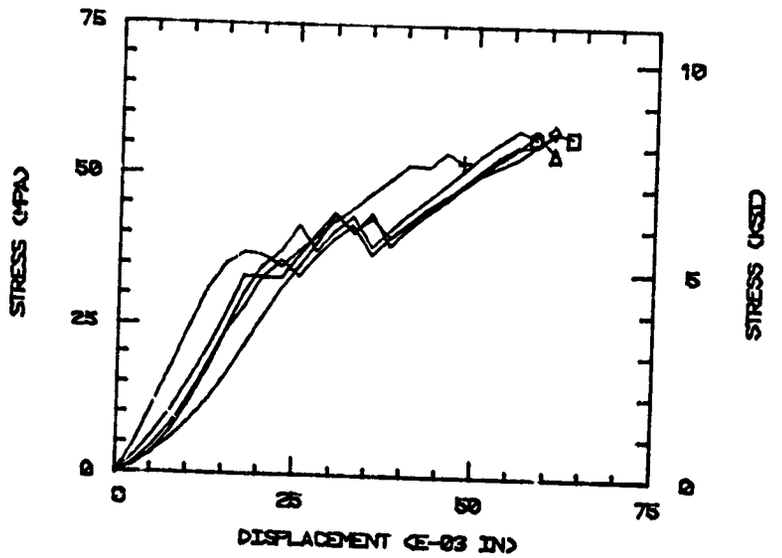

b) Stress-Displacement

Figure C11. Interlaminar (13) Iosipescu Shear Results for 8-Harness Satin-Weave T300/934 Graphite/Epoxy Composite.

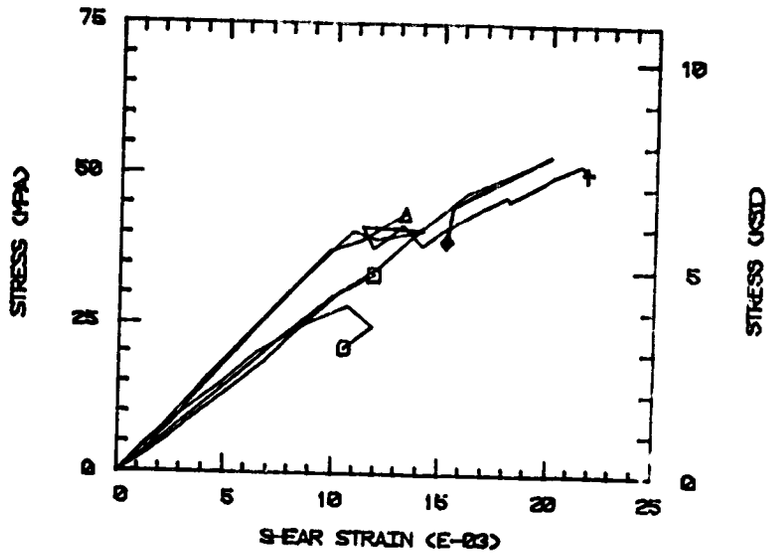

a) Stress-Strain

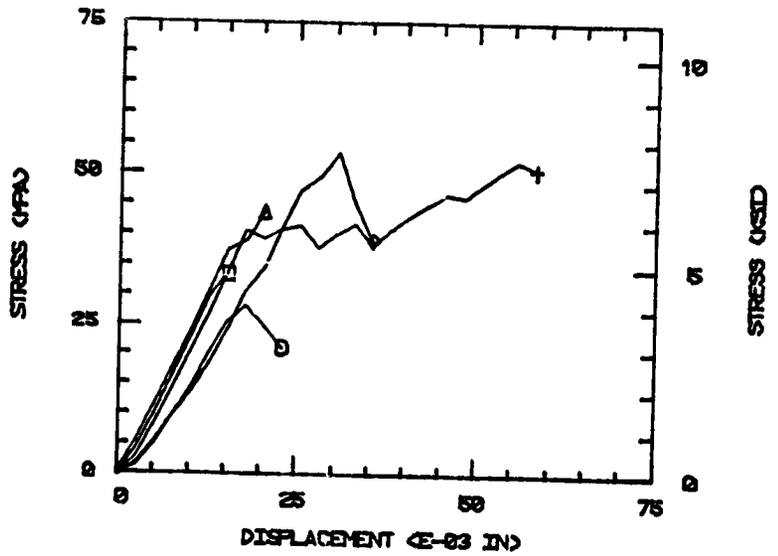

b) Stress-Displacement

Figure C12. Interlaminar (23) Iosipescu Shear Results for 8-Harness Satin-Weave T300/934 Graphite/ Epoxy Composite.